THE UNIVERSITY OF CALGARY

Expression of the *hmc* Operon of *Desulfovibrio vulgaris* Hildenborough and Molecular Characterization of its Components

by

Richard G. Keon

A THESIS

SUBMITTED TO THE FACULTY OF GRADUATE STUDIES

IN PARTIAL FULFILMENT OF THE REQUIREMENTS FOR THE

DEGREE OF MASTER OF SCIENCE

DEPARTMENT OF BIOLOGICAL SCIENCES

CALGARY, ALBERTA

SEPTEMBER, 1995

THE UNIVERSITY OF CALGARY

FACULTY OF GRADUATE STUDIES

The undersigned certify that they have read, and recommend to the Faculty of Graduate Studies for acceptance, a thesis entitled "Expression of the *hmc* Operon of *Desulfovibrio vulgaris* Hildenborough and Molecular Characterization of its Components" submitted by Richard G. Keon in partial fulfilment of the requirements for the degree of Master of Science.

G. Voordouw

Supervisor, Dr. G. Voordouw
Dept. of Biological Sciences

R. G. Huber

Dr. R. E. Huber
Dept. of Biological Sciences

Dr. M. F. Hynes
Dept. of Biological Sciences

Dr. A. Schryvers
Dept. of Microbiology and
Infectious Diseases

September 22, 1995

Date

Abstract

Desulfovibrio vulgaris Hildenborough can grow chemolithotrophically using hydrogen as sole electron donor. This metabolic ability necessitates the presence of a transmembrane redox protein complex which allows electrons evolved during periplasmic hydrogen oxidation to participate in cytoplasmic sulfate reduction. Such a complex is potentially formed by the *hmc* operon of this bacterium. The operon encodes the redox complex subunits Hmc and Orf2 to Orf6, as well as the putative regulatory proteins Rrf1 and Rrf2.

Expression of the *hmc* operon was examined during growth on different electron donors and found to be positively dependent on the presence of hydrogen. By *orf2-phoA* fusion expression, the membrane topology of Orf2 was determined to be unique among a large family of similar bacterial proteins. Western analysis indicated the membrane asssociation of Orf6. Deletion of genes *rrf1,2* resulted in de-repression of the *hmc* operon and enhanced chemolithotrophic growth of the resulting mutant.

Acknowledgements

Admittedly, it was never my plan to enter grad school. The long and winding road of my undergraduate career kept any notions of continuing my education far from conscious consideration. It was not until I approached Gerrit Voordouw for a summer research position that the idea of doing a Master's degree was first suggested to me. It is for this and numerous other reasons that I should initially thank the man who has played an integral role in bringing me to this point in my scientific career. In the truest sense, Dr. Voordouw has been my mentor offering support when I doubted my abilities, presenting objective criticism to keep me on my toes and always teaching me how to be a good scientist.

While working in the "Voordouw lab", I have met many people from all over the world but several stand out in my mind as being special. Two colleagues, in particular, have become dear friends whom I will treasure for many years to come. I thank Harm and Anita for their companionship which has made work a delightful experience (not without the help of our other friends: Coffee and Beer; Mmmm, beer). I thank my pal, Jill, for helping me stay in shape, physically, while I performed this exercise for my brain. Thanks to Jill, I'm a bigger man. I thank Hansje for the lively chats that broke up Western blotting monotony and for her impeccable technical services. I thank Rongdian for his invaluable advice and precious help on countless occasions. I thank Yin for her smiles and cheerful morning greetings. I am also indebted to my family: Mom, Dad, Jacki, Jeff and Christian who form a support structure of love and understanding on which I can always rely.

Lastly, and most of all, I extend my gratitude to the two loves of my life. Lynsey, my dolly angel, brings me immense joy before and after every work day and helps me forget my worries. Lorrie, by best friend, is always there to enjoy the good times with me and help me brave the tough times. I thank you, Lorrie, for putting up with my uneasy metamorphosis into a scientist. You both made it all worthwhile.

To Dad,
with memories of our
many scientific discussions...

Who's yawning now?

Table of Contents

Section	Page
Approval page	ii
Abstract	iii
Acknowledgements	iv
Dedication	v
Table of Contents	vi
List of Tables	ix
List of Figures	x
Abbreviations and Symbols	xii
1. Introduction	1
1.1 *Desulfovibrio vulgaris* metabolism	1
1.2 The *hmc* operon	5
1.3 Analogous operons	13
1.3.1 The *hyc* operon of *E. coli*	13
1.3.2 The *hya* operon of *E. coli*	14
1.3.3 The *dms* operon of *E. coli*	16
1.3.4 The *fdh* operon of *W. succinogenes*	16
1.3.5 The *fdn* operon of *E. coli*	17
2. Objectives	19
2.1 Overexpression of selected *hmc* operon genes in *E. coli*	19
2.2 Determination of the membrane topology of Orf2	19
2.3 Expression analysis of the *hmc* operon	20
2.4 Functional analysis of proteins Rrf1 and Rrf2	20
3. Materials and Methods	22
3.1 Materials	22
3.1.1 Biochemical reagents	22
3.1.2 Bacterial strains	23
3.1.3 Plasmids	23
3.1.3.1 Plasmid pRKPhoA	23
3.1.3.2 Plasmid pNMB	27
3.1.3.3 Plasmid pNMP	27
3.1.3.4 Plasmid pNSB	27

Section	Page

3.1.3.5 Plasmid pCSP 27
3.1.3.6 Plasmid pΔRRF 30
3.1.4 Growth media 30
3.1.5 Growth conditions 31
3.2 Methods 32
3.2.1 Standard protocols 32
3.2.1.1 DNA isolations 32
3.2.1.2 DNA enzymatic manipulations 32
3.2.1.3 DNA Electrophoresis 32
3.2.1.4 Gel isolation of DNA 32
3.2.1.5 Southern blotting 32
3.2.1.6 Colony filter hybridization 33
3.2.1.7 Transformation and conjugation 33
3.2.1.8 SDS PAGE 33
3.2.1.9 Western blotting 35
3.2.1.10 Computer programs 35
3.2.2 Bacteriophage T7 expression system 35
3.2.3 Polyclonal antiserum generation 36
3.2.4 Alkaline phosphatase fusions 36
3.2.4.1 Expression of *phoA* fusions in *E. coli* 37
3.2.4.2 Alkaline phosphatase activity measurements 37
3.2.5 Analysis of potential helix-turn-helix motifs 38
3.2.6 *D. vulgaris* mutagenesis 38
3.2.7 *D. vulgaris* growth rates 40
3.2.8 Operon expression analysis 41

4. Results 42
4.1 Overexpression of operon components in *E. coli* 42
4.1.1 Orf2 overexpression 42
4.1.2 Orf3 overexpression 42
4.1.3 Orf6 overexpression 44
4.2 Anti-Orf6 antisera generation 44
4.2.1 Western blot analysis of Orf6 44
4.3 Orf2-alkaline phosphatase fusions 46
4.3.1 Expression of *orf2-phoA* fusions in *E.coli* 46
4.3.2 Alkaline phosphatase activities of fusions 51
4.4 *hmc* operon expression 54
4.4.1 Western blot analysis of operon expression levels during growth on different electron donors 54
4.5 Analysis of a potential helix-turn-helix motif in Rrf2 57

Section	Page
4.6 Generation of an *rrf1,2*-deficient strain of *D. vulgaris* Hildenborough	58
4.6.1 Southern blot analysis of the gene deletion procedure	58
4.6.2 Growth rates of wild type and mutant *D. vulgaris* Hildenborough	63
4.6.3 Western blot analysis of operon expression levels after deletion of genes *rrf1,2*	70
5. Discussion	74
5.1 Overexpression of Orf2, Orf3 and Orf6 in *E.coli*	74
5.2 Cellular localization of Orf6	75
5.3 Membrane topology of Orf2	76
5.4 Differential expression of the *hmc* operon	78
5.5 Role of the *rrf1,2* genes in *D. vulgaris* Hildenborough	81
5.6 Role of the *hmc* operon in *D. vulgaris* Hildenborough	85
6. References	89

List of Tables

Table	Page
Table 3-1. Chemical reagents and suppliers.	24
Table 3-2. Bacterial strains, vectors and plasmids used.	25
Table 4-1. Sizes and relative expression levels of Orf2-PhoA fusion proteins.	51
Table 4-2. Alkaline phosphatase (AP) activities of cultures expressing *orf2-phoA* fusions.	53
Table 4-3. Relative *hmc* operon expression levels.	57
Table 4-4. Helix-turn-helix weight matrix scores of Rrf2.	58
Table 4-5. Normalized *hmc* operon expression levels comparing wild type and mutant strains.	73

List of Figures

Figure	Page
Figure 1-1. The *hmc* operon of *D. vulgaris* Hildenborough.	6
Figure 1-2. Cysteine group alignments of several iron-sulfur cluster proteins.	7
Figure 1-3. Orf2 hydropathy plot.	8
Figure 1-4. Comparison of Orf2 N-terminus and hydrogenase-type signal sequences.	9
Figure 1-5. Model of the interaction of *hmc* operon proteins.	12
Figure 3-1. Map of the inserts within plasmids pTORF2, pTORF3 and pTORF6.	28
Figure 3-2. Orf2-PhoA fusions.	29
Figure 3-3. Generation of the *D. vulgaris* Hildenborough mutant strain RK100.	39
Figure 4-1. SDS PAGE of *hmc* operon components overexpressed in *E. coli.*	43
Figure 4-2. Western blot analysis of mouse anti-Orf6 antibody titre.	45
Figure 4-3. Detection of native Orf6 in *D. vulgaris* Hildenborough.	47
Figure 4-4. Orf6 hydropathy plot.	48
Figure 4-5. Comparison of pJRMR+ and pJRMR- transconjugants.	49
Figure 4-6. Western blot of Orf2-PhoA fusion proteins.	50
Figure 4-7. Plate indicating which fusion plasmid transformants express active alkaline phosphatase.	52
Figure 4-8. Column graph of Orf2-PhoA fusion alkaline phosphatase activities after induction with IPTG.	53
Figure 4-9. Western blot analysis of *hmc* operon during growth with different electron donors.	56
Figure 4-10. Southern blot verifying integration of plasmid pΔRRF into the *D. vulgaris* Hildenborough chromosome.	60
Figure 4-11. Southern blot indicating the presence of two types of integrant.	61

Figure **Page**

Figure 4-12. Southern blot including RK1-RK100 mixture. 62
Figure 4-13. Southern blot showing purified RK100. 64
Figure 4-14. Southern blot indicating deletion of *rrf1,2*. 65
Figure 4-15. Growth curves of *D. vulgaris* Hildenborough strains in minimal media where lactate was used as electron donor. 67
Figure 4-16. Growth curves of *D. vulgaris* Hildenborough strains in Postgate medium C. 68
Figure 4-17. Growth curves of *D. vulgaris* Hildenborough strains in minimal media where hydrogen was used as electron donor. 69
Figure 4-18. Growth curves of *D. vulgaris* Hildenborough strains in minimal media where pyruvate was used as electron donor. 71
Figure 4-19. Western blot analysis of *hmc* operon of *D. vulgaris* Hildenborough wild type and mutant strains. 72
Figure 5-1. Model of *hmc* operon regulation by Rrf1 and Rrf2. 87
Figure 5-2. Model of the role of the *hmc* operon in electron transfer from hydrogen. 88

Abbreviations and Symbols

≈: approximately equal to
A: alanine
Å: angstrom = 10^{-10} m
ADP: adenosine diphosphate
Ala: alanine
AMP: adenosine monophosphate
Amp^r: ampicillin resistant
AP: alkaline phosphatase
APS: adenosine-5'-phosphosulfate
Arg: arginine
A_{600}: absorbance at 600 nm wavelength
Asp: aspartate
atm: atmospheres
ATP: adenosine triphosphate
BCIP: 5-bromo-4-chloro-3-indolyl-β-D-phosphopyranoside
bp: base pairs
BSA: bovine serum albumin (fraction V)
C: cysteine
C-terminal: carboxy-terminal
ca.: *circa* (approximately)
CheY: chemotaxis reponse regulatory factor of *E. coli*
Ci: Curies
Cm^r: chloramphenicol resistant
D: aspartate
Δ: indicates gene deletion
dCTP: deoxycytidine triphosphate
DmsA-C: dimethyl sulfoxide reductase subunits of *E. coli*
DNA: deoxyribonucleic acid
dNTPs: deoxynucleoside triphosphates
E: glutamate
e^-: electrons
e^-_{in}: cytoplasmic electrons

EDTA: ethylenediaminetetraacetic acid
F: phenylalanine
FdhA-D: formate dehydrogenase subunits of *W. succinogenes*
FDH_H: formate dehydrogenase-H
FDH_N: formate dehydrogenase-N
FdnG-I: nitrate-inducible formate dehydrogenase subunits of *E. coli*
FHL: formate hydrogen lyase
g: standard gravity
G: glycine
Gly: glycine
h: hours
H: histidine
H^+_{in}: cytoplasmic protons
H^+_{out}: periplasmic protons
HGT: high-gelling temperature
Hmc: high molecular weight cytochrome *c* of *D. vulgaris* Hildenborough
HyaA-F: hydrogenase-1-associated proteins of *E. coli*
I: isoleucine
IgG: immunoglobulin G
Ile: isoleucine
IPTG: isopropylthiogalactoside
K: lysine
kbp: kilobase pairs = 10^3 base pairs
kDa: kilodaltons = 10^3 Daltons = 10^3 grams/mole
Km^r: kanamycin resistant
L: leucine
LB: loading buffer
Leu: leucine
LGT: low-gelling temperature
M: methionine
MBq: megabecquerels = 10^6 Becquerels
mRNA: messenger RNA
N: asparagine
N-terminal: amino-terminal

NADH: nicotinamide adenine dinucleotide
NAD(P): nicotinamide adenine dinucleotide (phosphate)
Nal^r: nalidixic acid resistant
NarL, NarX: nitrate induction regulatory factors of *E. coli*
NBT: nitroblue tetrazolium
Orf1-Orf8: FHL complex proteins of *E. coli*
Orf2-Orf6: proteins encoded by open reading frames 2-6 of *hmc* operon of *D. vulgaris* Hildenborough
P: proline
PAGE: polyacrylamide gel electrophoresis
% (v/v): percent volume by volume = mL/100 mL total volume
% (w/v): percent weight by volume = g/100 mL total volume
P_{hmc}: promoter of *D. vulgaris* Hildenborough *hmc* operon
PhoA: alkaline phosphatase of *E. coli*
PhoB: phosphorus assimilation response regulatory factor of *E. coli*
P_i: inorganic phosphate
P_{lac}: promoter of *E. coli lac* operon
*p*NPP: paranitrophenyl phosphate
Q: glutamine
R: arginine
RNA: ribonucleic acid
Rrf1, Rrf2: response regulatory factors of *D. vulgaris* Hildenborough
S: serine
SD: standard deviation
SDS: sodium dodecylsulfate
Spo0F: sporulation stage 0 response regulatory factor of *B. subtilis*
spp.: species (plural)
Str^r: streptomycin resistant
t: time
T: threonine
TCA: trichloroacetic acid
Tris: Tris(hydroxymethyl) methylamine
U: units of enzyme activity
UV: ultraviolet

V: valine
W: tryptophan
x: times
X: unspecified amino acid residue
X-Gal: 5-bromo-4-chloro-3-indolyl-β-D-galactopyranoside
Y: tyrosine
YjeB: hypothetical peptide encoded downstream of the *E. coli purA* gene

1. Introduction

Sulfate-reducing bacteria are a unique group of anaerobic microorganisms found in a variety of environmental niches. Many of the redox enzymes and redox proteins discovered in sulfate-reducers have been well described and this has led to the development of metabolic models for these bacteria. Molecular biological studies of *Desulfovibrio* spp. have assigned more definitive roles to these various proteins by describing their cellular localization and potential structure and function based on sequence analysis. One very interesting and unique group of proteins has been discovered to be encoded by the *hmc* operon of *Desulfovibrio vulgaris* subspecies *vulgaris* Hildenborough (hereafter denoted *D. vulgaris* Hildenborough). This operon has been found to encode a transmembrane redox protein complex which may play an important metabolic role within these bacteria. The present study describes a molecular biological analysis of the *hmc* operon which was undertaken in an attempt to characterize the role of some of its components and to determine the function of the complex as a whole. Before discussing this work, it would be helpful to review what is known of *D. vulgaris* metabolism and to describe what has been elucidated from sequence analyses of the *hmc* operon as well as to compare this operon to similar systems found in other bacteria.

1.1 *Desulfovibrio vulgaris* metabolism

Sulfate-reducing eubacteria of the genus *Desulfovibrio* have been studied with regards to their metabolism for 100 years. Sulfate-reducers, in general, are defined by their usage of sulfate as the principal electron acceptor in respiration. As in many biological systems, energy production in the form of ATP synthesis is coupled to electron transport by a proton gradient across the bacterial inner membrane. This results in a reducing cytoplasmic environment and a high periplasmic proton concentration. The proton-motive force drives the synthesis of ATP by an ATPase complex. Such a complex has not been described in these bacteria but is assumed to exist. Sulfate reduction to sulfide occurs in the cytoplasm of *Desulfovibrio* spp. by a

series of reactions with adenosine-5'-phosphosulfate (APS) and bisulfite as intermediates. The four cytoplasmic enzymes: ATP sulfurylase, APS reductase, bisulfite reductase and pyrophosphatase (Peck, 1993) catalyze the reaction (Voordouw, 1995):

$$SO_4^{2-} + ATP + 8H^+_{in} + 8e^- \rightarrow HS^- + AMP + 2P_i$$

Water has been omitted from the equation. The investment of two high energy phosphate bonds is restored by proton-driven and/or substrate-level phosphorylation of ADP to ATP (Voordouw, 1995). H^+_{in} refers to cytoplasmic protons (as opposed to periplasmic protons: H^+_{out}). Electrons participating in sulfate reduction are transported to the reaction site via one of three cytoplasmic electron carriers: desulforedoxin, rubredoxin or flavodoxin. Of these carriers, flavodoxin is the one most likely to donate electrons to the sulfate reduction pathway due to its low reduction potential.

In *Desulfovibrio vulgaris*, the reduction of sulfate occurs by such electron donors as lactate, pyruvate, formate or hydrogen as well as other compounds such as metallic iron (Postgate, 1984; Odom, 1993). Lactate and pyruvate are incompletely oxidized to acetate and carbon dioxide. Lactate oxidation to pyruvate is catalyzed by a poorly characterized NAD(P)-independent, membrane-bound lactate dehydrogenase (Hansen, 1993; Voordouw, 1995):

$$lactate \rightarrow pyruvate + 2H^+_{in} + 2e^-$$

Pyruvate is oxidized to acetate and carbon dioxide via acetyl coenzyme A and acetylphosphate intermediates (Peck, 1993; Voordouw, 1995):

$$pyruvate + ADP + P_i \rightarrow acetate + CO_2 + ATP + 2H^+_{in} + 2e^-$$

Thus, the oxidation of 2 mol of lactate per mol of sulfate proceeds as follows (Voordouw, 1995):

$$2\ lactate + SO_4^{2-} \rightarrow 2\ acetate + 2\ CO_2 + HS^-$$

The oxidation of pyruvate is coupled to sulfate reduction in the reaction (Peck, 1993; Voordouw, 1995):

$$4 \text{ pyruvate} + 2ADP + 2P_i + SO_4^{2-} \rightarrow 4 \text{ acetate} + 4CO_2 + 2ATP + HS^-$$

It can be seen that, unlike growth on pyruvate, growth on lactate offers no net formation of ATP by substrate-level phosphorylation. Instead, it requires coupled, proton-driven ATP synthesis (Voordouw, 1995). To explain this form of ATP synthesis, Odom & Peck (1981) proposed the hydrogen cycling hypothesis. The hypothesis postulates that the electrons formed in the cytoplasm during lactate and pyruvate oxidation (see above) cannot participate in sulfate reduction directly but must combine with cytoplasmic protons in this reaction:

$$2H^+_{in} + 2e^-_{in} \rightarrow H_2$$

The hydrogen produced by this cytoplasmic hydrogenase diffuses to the periplasm where the reverse reaction, that of hydrogen oxidation, is catalyzed by periplasmic hydrogenases resulting in a proton buildup outside the membrane. The major problem with this hypothesis is the requirement for a cytoplasmic hydrogenase, something which has not been found universally among *Desulfovibrio* spp. The existence of another mechanism of active proton export such as one associated directly with the membrane-bound lactate dehydrogenase would be a possible solution to this problem but no such mechanism has been discovered (Voordouw, 1995).

D. vulgaris can grow, albeit sluggishly, on formate/SO_4^{2-} media utilizing formate as sole electron donor (Postgate, 1984; Peck, 1993). Periplasmic formate dehydrogenase has been found to use purified cytochrome c_{553} as electron acceptor in *D. vulgaris* Miyazaki (Hansen, 1993; Yagi, 1979). Cytochrome c_{553} is a periplasmic, monoheme, c-type cytochrome thought to function as the electron acceptor for oxidation of formate and/or lactate although its absence in some *Desulfovibrio* spp. demonstrates that it is not required for this function (Odom & Peck, 1984). The oxidation of formate

by formate dehydrogenase proceeds via a reaction in which two periplasmic protons are formed:

$$\text{formate} \rightarrow CO_2 + 2H^+_{out} + 2e^-$$

D. vulgaris can grow chemolithotrophically with molecular hydrogen as sole electron donor and acetate and carbon dioxide as the carbon source. This growth was first described by Badziong *et al.* (1978; 1979) and proceeds by the overall reaction (Voordouw, 1995):

$$4H_2 + SO_4^{2-} + ADP + P_i \rightarrow HS^- + ATP$$

As can be seen from this reaction, growth on hydrogen results in the net synthesis of 1 mol of ATP per mol of sulfate reduced (Badziong *et al.*, 1979). While the [NiFeSe] hydrogenase found in many *Desulfovibrio* spp. likely functions in hydrogen evolution (proton reduction), hydrogen oxidation occurs via the periplasmic [Fe] and/or [NiFe] hydrogenases giving rise to a scalar proton gradient (Voordouw *et al.*, 1990):

$$H_2 \rightarrow 2H^+_{out} + 2e^-_{out}$$

The [Fe] and [NiFe] hydrogenases can donate the 2 electrons to periplasmic cytochrome c_3, a tetrahemic *c*-type cytochrome of known structure which is found ubiquitously among *Desulfovibrio* spp. (Higuchi *et al.*, 1984; Postgate, 1984), and/or to the similar high-molecular-weight cytochrome *c* (Hmc) described in the next section (Pollock *et al.*, 1991). The next electron transport step requires the presence of a transmembrane redox link which can shuttle electrons from the periplasm to the cytoplasm where they participate in sulfate reduction. This role is potentially fulfilled by the proteins encoded by the *hmc* operon of *D. vulgaris* Hildenborough.

1.2 The *hmc* operon

The *hmc* operon of *D. vulgaris* Hildenborough is 7.7 kbp long and contains eight open reading frames denoted *hmc, orf2* through *orf6, rrf1* and *rrf2* (Figure 1-1). The encoded proteins Hmc and Orf2 to Orf6 are proposed to comprise the transmembrane redox protein complex and Rrf1 and Rrf2 are cytoplasmic proteins which likely serve some regulatory function. The promoter-proximal open reading frame is the *hmc* gene which codes for a 55.7 kDa high-molecular-weight cytochrome *c* (Hmc) described by Pollock *et al.* (1991). This cytochrome possesses 16 *c*-type hemes 12 of which are present in three tetraheme cytochrome c_3-like domains giving a 65.5 kDa holoprotein. Cloning of the gene for Hmc into the broad-host-range vector pJRD215 has led to the expression of the native protein complete with covalently-bound hemes in *D. desulfuricans* G200 (*ibid*). The protein has been shown to be periplasmically located possessing a 31 amino acid N-terminal signal sequence (*ibid*) but it is not known for sure whether this protein is attached to the membrane. Different fractionation protocols have given conflicting data regarding the membrane association of this protein (Rossi *et al.*, 1993).

The second gene of the operon is *orf2* which encodes a 40.0 kDa transmembrane redox protein. Orf2 is postulated to contain four [4Fe-4S] iron-sulfur clusters based on its high homology with DmsB, the electron transferring subunit of *E. coli* dimethyl sulfoxide reductase (Bilous *et al.*, 1988), and with FdnH, the iron-sulfur protein of *E. coli* nitrate-inducible formate dehydrogenase (Berg *et al.*, 1991). DmsB, FdnH and Orf2 share cysteine cluster alignments with several known bacterial iron-sulfur proteins (Figure 1-2). Unlike the other members of this redox protein family, Orf2 contains two potential transmembrane regions based on sequence hydrophobicity (Figure 1-3). One of these hydrophobic regions is located near the N-terminus in a sequence region homologous to that of atypical signal sequences present in hydrogenase small subunits. These signal sequences share a conserved sequence, the consensus box RRXFXK and are found at the N-terminus of the hydrogenase small subunit. The Orf2 sequence is not identical but quite similar to this sequence (Figure 1-4). The most notable feature of the signal sequence in hydrogenases is that it may act to export both

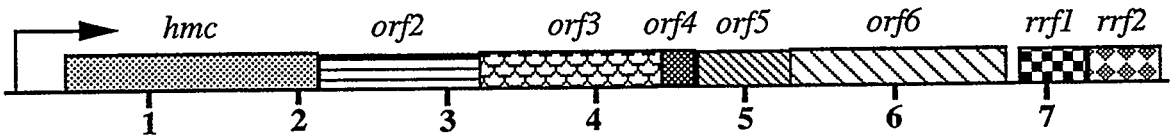

Fig. 1-1. The *hmc* operon of *D. vulgaris* Hildenborough. The scale is in kbp.

```
I.   Orf2 DvH   48-RCIGCRKCEQACNEV
     DmsB Ec    13-RCTGCKTCELACKDY
     FdnH Ec    38-TCIGCKACQVACSEW
     Orf2 Ec    11-LCIGCHTCEAACSET
     NarH Ec    15-KCIGCHTCSVTCKNV
     FdhB Ws    15-RCIDCHGCDVACKEA

II.  Orf2 DvH   109-QCNHCLEPACASACFVKAFTKNP-DGSVTYDGSLCVGCRYCMVACPFNV
     DmsB Ec     66-SCNHCEDPACTKVCPSGAMHKRE-DGFVVVDEDVCIGCRYCHMACPYGA
     FdnH Ec     99-GCIDCEDPGCLKACPSAGAIIQYANGIVDFQSENCIGCGYCIAGCPFNI
     Orf2 Ec     50-LCHHCEDAPCAVVCPVNAITRV--DGAVQLNESLCVSCKLCGIACPFGA
     NarH Ec    183-LCEHCLNPACVATCPSGAIYKREEDGIVLIDQDKCRGWRMCITGCPYKK
     FdhB Ws     58-ACMHCSDAPCAQVCPVDCFYVRA-DGIVLHDKEKCIGCGYCLYACPFGA

III. Orf2 DvH   169-IQKCTMCH----------------HPRLAEGKLPGCVEICPKEALTFGR
     DmsB Ec    123-MTKCDGCY----------------DRVAEGKKPICVESCPLRALDFGP
     FdnH Ec    157-VYKCTLCV----------------DRVSVGQEPACVKTCPTGAIHFGT
     Orf2 Ec    140-AVKCDLCS----------------FDEQGPACARMCPTKALHLVD
     NarH Ec    241-SEKCIFCY----------------PRIEAGQPTVCSETCVGRIRYLGV
     FdhB Ws    120-MDKCTFCAGGPEETHSEKEYKLYGQNRIAEGKVPVCAAMCSTKALLAGD
```

Fig. 1-2. Sequence group alignments of several iron-sulfur cluster proteins. Cysteine residues are in underlined, boldface type. Abbreviations are as described in Figure 1-4 (Bokrantz *et al.*, 1991; Böhm & Böck, 1990; Berg *et al.*, 1991).

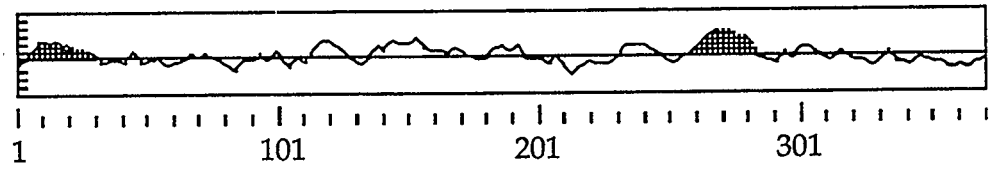

Fig. 1-3. Orf2 hydropathy plot according to Kyte & Doolittle (1982). Regions above the line are hydrophobic and below are hydrophilic. The scale runs from +4.5 (top) to -4.5 (bottom). Regions predicted to be capable of spanning the membrane have been shaded. The scale is in amino acid residue units.

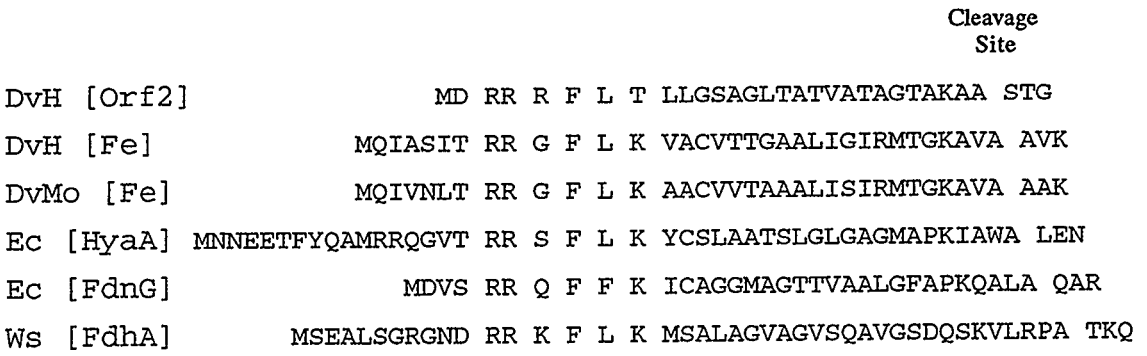

Fig. 1-4. Comparison of Orf2 N-terminus and hydrogenase-type signal sequences. The sequences have been aligned relative to the consensus box (RRXFXK). DvMo, *D. vulgaris* subsp. *oxamicus* Monticello; DvH, *D. vulgaris* Hildenborough; Ec, *E. coli* ; Ws,*W. succinogenes* (Voordouw, 1993; Menon *et al.*, 1990; Berg *et al.*, 1991; Bokrantz *et al.*, 1991).

subunits of the hydrogenase enzyme cooperatively. It is ineffective if only one of the two is expressed (Nivière *et al.*, 1992). Although the mechanism of protein export which utilizes this signal has yet to be elucidated, it is believed to be involved in the export of polypeptides which contain iron-sulfur clusters (Voordouw, 1993). The other hydrophobic segment of Orf2 is followed by a highly charged 85 residue C-terminal peptide in which 48% of the amino acids are charged (55% of these are acidic and 45% are basic). The function of this charged region has not been speculated upon.

The next three proteins encoded by the *hmc* operon are Orf3 (43.2 kDa), Orf4 (5.8 kDa) and Orf5 (25.3 kDa). These are predicted to be highly hydrophobic integral membrane proteins. All three share some sequence similarity with different chains of the NADH-ubiquinol oxidoreductase complex but this small degree of homology is mostly due to the high hydrophobicity which the proteins share. The primary structure of Orf5 does resemble that of cytochrome *b* suggesting that this polypeptide may carry a heme *b* prosthetic group (Rossi *et al.*, 1993). An intramembrane redox prosthetic group is required for efficient electron transfer through the 30 Å membrane of *D. vulgaris* Hildenborough (Pollock, 1992). The protein possesses six histidines, three of which reside within predicted membrane-spanning regions, a characteristic of cytochrome *b* proteins (Degli Esposti, 1989). Degli Esposti (1989) has described "specifically-enriched residues" commonly found surrounding intramembrane histidines in cytochromes *b*. The sequence of Orf5 possesses many of these residues further supporting the possibility that this protein might be a cytochrome *b*.

Orf6 is a redox protein which is potentially attached to the cell membrane from the cytoplasmic side. The 52.7 kDa polypeptide contains two putative [4Fe-4S] iron sulfur clusters as based on cysteine cluster alignments with the [Fe] hydrogenase large subunit of *D. vulgaris* Hildenborough (Voordouw & Brenner, 1985). Overall, Orf6 does not share significant homology with any other known proteins (Rossi *et al.*, 1993).

The last two genes of the *hmc* operon encode the cytoplasmic proteins Rrf1 (14.8 kDa) and Rrf2 (16.6 kDa). Rrf1 likely belongs to the family of bacterial response regulatory proteins due to its strong homology with members of this family such as Spo0F, involved in *B. subtilis* sporulation

stage 0 regulation (Trach *et al.*, 1988), and PhoB, involved in *E. coli* phosphorus assimilation (Makino *et al.*, 1986). These response regulators are part of a two-component signal transduction system and are phosphorylated at a conserved aspartyl residue by a histidine protein kinase. This occurs within a conserved N-terminal domain of *ca.* 100 residues. Once activated through phosphorylation, the response regulator can control a wide range of cellular activities such as motility and gene expression (Stock *et al.*, 1990). This response can be elicited through the C-terminal output domain portion of the protein (Parkinson & Kofoid, 1992) which sometimes functions as a DNA binding domain (*eg.* PhoB; Makino *et al.*, 1986). In the case of Spo0F, the protein consists solely of the N-terminal phosphorylation domain and functions by means of phosphotransfer (Burbulys *et al.*, 1991). Rrf1 resembles Spo0F in possessing primarily the phosphorylation domain. This domain is followed by only a short C-terminal tail which contains 25% prolines and 25% threonines.

Rrf2 shares homology with a hypothetical 15.6 kDa protein, denoted YjeB, encoded by the region downstream of the *purA* gene of *E. coli* (Wolfe & Smith, 1988). This homology, however, gives no information about the role of Rrf2 since a function has not been ascribed to YjeB. Rrf2 does contain an intriguing sequence of residues matching the consensus for helix-turn-helix DNA-binding domains described by Pabo & Sauer (1984). The sequence of this region of Rrf2 is shown below with consensus residues in underlined, bold-face type:

$$K_{28}\,D\;I\;\underline{\mathbf{A}}\;Q\;R\;Q\;\underline{\mathbf{G}}\;I\;S\;V\;K\;Y\;\underline{\mathbf{L}}\;E\;K\;\underline{\mathbf{L}}\;I\;R_{46}$$

The possibility that this protein contains a DNA-binding motif is very plausible considering that it follows a putative response regulatory protein. As mentioned above, these response regulators are often associated with some DNA-binding function.

Rrf1 and Rrf2 were named differently than the previous proteins encoded by the *hmc* operon due to the lack of proof that they are controlled by the *hmc* promoter. There is the potential for the formation of a stem-loop transcription termination structure between the genes *orf6* and *rrf1*.

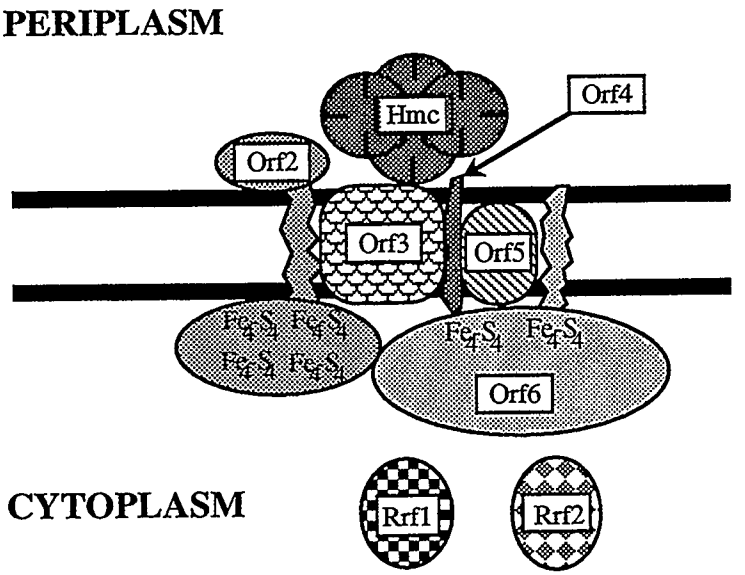

Fig. 1-5. Model of the interaction of *hmc* operon proteins.

However, there is also no discernable promoter region following this structure suggesting that *rrf1,2* would be transcribed from the *hmc* promoter. The stem-loop may serve in transcriptional regulation of these two genes by allowing only a fraction of mRNA transcripts to contain the *rrf1,2* sequence due to partial readthrough of the operon. This hypothesis has been supported by the low levels of expression of native Rrf1 observed within *D. vulgaris* Hildenborough (Rossi *et al.*, 1993).

A schematic representation of how the proteins encoded by the *hmc* operon might interact with one another is illustrated in Figure 1-5. *D. vulgaris* Hildenborough has three different periplasmic hydrogenases: the [Fe], [NiFe] and [NiFeSe] hydrogenases. An interesting hypothesis proposed by Pollock *et al.* (1991) is that each of the three cytochrome c_3 domains of Hmc interacts specifically with one of these three enzymes. Electrons from hydrogen oxidation would then be transferred from the hydrogenase to Hmc and shuttled through the membrane via the transmembrane complex formed by Orf2 to Orf6 where they wind up in the cytoplasm ready to participate in sulfate reduction (Rossi *et al.*, 1993). This model of electron transfer proposed for the *hmc* operon solves the problem of linking periplasmic hydrogen oxidation to cytoplasmic sulfate reduction.

1.3 Analogous operons

There are no other operons described which combine the gene of a cytochrome with those of a redox protein complex and regulatory proteins. It is for this reason that the operons described in this section bear only limited similarity to the *hmc* operon. The operons outlined here share a common overall structural design incorporating catalytic, electron transfer and membrane anchor proteins into a multi-subunit transmembrane electron transport complex. Some of these complexes possess hydrogenases and some contain components which are significantly homologous to proteins encoded by the *hmc* operon.

1.3.1 The *hyc* operon of *E. coli*

E. coli can ferment glucose to a number of organic compounds such as

formate. In the absence of external electron acceptors such as oxygen or nitrate, formate can be decomposed to hydrogen and carbon dioxide by the formate hydrogenlyase (FHL) complex (Birkmann *et al.*, 1987). This complex consists of redox carriers and the specific isozymes formate dehydrogenase-H (FDH_H) and hydrogenase-3 (Schlensog & Böck, 1990). During studies of this system in *E. coli*, sequencing revealed the *hyc* operon which is found to contain eight open reading frames on an 8 kbp fragment located in the 58/59 min region of the chromosome (Böhm *et al.*, 1990). The genes appear to encode a unique hydrogenase and redox carriers linking formate oxidation to proton reduction in the FHL system.

The fifth open reading frame encodes Orf5, a protein which is significantly similar to conserved regions of [NiFe] hydrogenase large subunits. Much like the *hmc* operon, Orf2 and Orf6 of the *hyc* operon are iron-sulfur proteins containing four and two such clusters, respectively. Orf2 of the *hyc* operon is comparable to Orf2 of the *hmc* operon as seen in Figure 1-2. Genes *orf3* and *orf4* of the *hyc* operon encode hydrophobic integral membrane proteins. The proteins Orf3 and Orf4 possess hydrophilic stretches that are homologous to regions within NADH-ubiquinol oxidoreductase found between its membrane-spanning helices. Orf7 encoded by this operon shares a high degree of similarity with protein G of the chloroplast NADH-ubiquinol oxidoreductase complex. Orf1 (17.6 kDa) and Orf8 (15.5 kDa) share no sequence homology with any known protein. Although a biochemical role has not been assigned to the group of *hyc* gene products as a whole, all of the components are required for FHL complex formation (Böhm *et al.*, 1990).

1.3.2 The *hya* operon of *E. coli*

In anaerobiosis, *E. coli* can produce hydrogen during fermentation and oxidize it for fumarate reduction during anaerobic respiration. A complex regulatory system responds to a wide variety of signals and substrates in the control of anaerobic hydrogen metabolism. Three hydrogenases have been described in *E. coli* which are synthesized in response to cellular requirements under different physiological conditions (Menon *et al.*, 1990). Hydrogenase-2 is a respiratory uptake enzyme coupled to fumarate reduction (Sawers *et al.*, 1985) and hydrogenase-3 has a role in the FHL pathway described above

(Böhm *et al.*, 1990). While the physiological role of hydrogenase-1 has not yet been defined, it has been found to be a unique nickel-containing protein associated with the cell membrane (Sawers & Boxer, 1986). The genes encoding the structural subunits of [NiFe] hydrogenase-1 have been cloned and sequenced. The genes encoding the small and large subunits are the first two in a 5.5 kbp operon with four additional open reading frames. The operon is designated *hya* (Menon *et al.*, 1990).

As mentioned above, the first two genes of the *hya* operon, *hyaA* and *hyaB*, encode the small and large subunits of hydrogenase-1, respectively. These proteins are highly homologous to [NiFe] hydrogenase subunits of other organisms complete with the inclusion of the characteristic unique long signal sequence found at the N-terminus of the small subunit (Figure 1-4; *ibid*).

The third gene encodes HyaC which is a very hydrophobic integral membrane protein with as many as six transmembrane helices. This protein is not unlike Orf3 of the *hmc* operon which possesses as many as ten such helices (Rossi *et al.*, 1993). It has been shown that deletions made within the *hyaC* gene result in the appearance of multiple forms of membrane-bound hydrogenase-1 suggesting that this protein may have a more complex role than simply anchoring the enzyme into the membrane as originally thought (Menon *et al.*, 1991).

The last three open reading frames of the *hya* operon encode proteins HyaD, E and F. None of these gene products has been found to be homologous to other proteins (Menon *et al.*, 1990) but data suggest that HyaD and HyaE may act as a complex involved in the processing of nascent hydrogenase-1 structural subunits. Evidence for this is their requirement to obtain the final correct conformation of the enzyme complete with prosthetic groups (Menon *et al.*, 1991). Although *hyaA-E* are sufficient to encode active hydrogenase-1, it has been shown that wild type activity is generated only with the inclusion of *hyaF* in this transcriptional unit. HyaF may be involved in the enhancement of nickel incorporation within the nascent hydrogenase polypeptide due to the absence of any HyaF-dependent activity change in nickel-supplemented growth (Menon *et al.*, 1991).

1.3.3 The *dms* operon of *E. coli*

Dimethyl sulfoxide reductase is a terminal electron transfer enzyme located in the membrane which enables the respiratory growth of *E. coli* on the electron acceptor dimethyl sulfoxide, provided that a suitable electron donor and carbon source such as glycerol are also present (Weiner *et al.*, 1993). This heterotrimeric enzyme is encoded by the *dmsA, B, C* genes. DmsA contains the molybdenum cofactor molybdopterin and is involved in the catalytic functioning of the enzyme. DmsB is an electron transferring subunit containing four [4Fe-4S] iron-sulfur clusters. As mentioned above, this protein bears a strong resemblance to Orf2 of the *hmc* operon throughout its iron-sulfur cluster domains sharing 38.1% identity in a 168 residue overlap (Figure 1-2). Together, DmsA and DmsB form the catalytic domain of dimethyl sulfoxide reductase. DmsC is an integral membrane protein which anchors the catalytic domain to the cytoplasmic surface of the cell membrane. This highly hydrophobic polypeptide has eight membrane-spanning helices and is required in its entirety to bind DmsAB to the membrane and provide optimal stability for the catalytic dimer (Weiner *et al.*, 1993). Proteins such as HyaC of the *hya* operon and Orf3,4 of the *hmc* operon likely serve roles similar to DmsC functioning as membrane anchors for the complex and stabilizing it against thermal denaturation. There is even speculation that some of these DmsC-like proteins are capable of proton translocation (Bilous *et al.*, 1988). DmsC has also been found to be required for menaquinol oxidase activity of dimethyl sulfoxide reductase due to its possession of an important histidyl residue (Weiner *et al.*, 1992).

1.3.4 The *fdh* operon of *Wolinella succinogenes*

Wolinella succinogenes is an anaerobic bacterium which generates energy for growth exclusively by phosphorylation coupled to electron transport (Kröger & Winkler, 1981). It contains a membrane-bound formate dehydrogenase which catalyzes the oxidation of formate by menaquinone. The membrane-associated fumarate reductase then reoxidizes the resulting menaquinol forming a redox partnership between fumarate and formate. Components of the formate dehydrogenase are encoded by the four genes of the *fdh* operon (Bokranz *et al.*, 1991).

FdhA is the first encoded protein of the *fdh* operon. It contains the molybdenum cofactor molybdopterin guanine dinucleotide (Jankielewicz *et al.*, 1994) and formate binding site. The subunit also carries the irregular N-terminal signal sequence associated with hydrogenase small subunits (Figure 1-4) suggesting its periplasmic localization. This N-terminal region of FdhA is followed by what appears to be an iron-sulfur cluster of atypical spacing. The second protein encoded, FdhB, contains 16 cysteine residues arranged in clusters typical of those observed in DmsB of *E. coli* and Orf2 of *D. vulgaris* (Figure 1-2). FdhC is a hydrophobic protein which is identical to the 25 kDa subunit of formate dehydrogenase. It is predicted to have four membrane-spanning helices and represents the cytochrome *b* which carries the menaquinone reactive site of the enzyme. The formate dehydrogenase complex of *W. succinogenes* appears to be composed of two moles of FdhA for every mole of FdhBC. The function of the last protein, FdhD, has not been determined (Bokranz *et al.*, 1991).

1.3.5 The *fdn* operon of *E. coli*

The *fdn* operon encodes the three subunits of nitrate-inducible formate dehydrogenase-N (FDH_N) in *E. coli*. The enzyme exchanges electrons with quinone and nitrate reductase thereby coupling formate oxidation to nitrate respiration in anaerobiosis. The enzyme active site is located in the 110 kDa α subunit encoded by *fdnG*. This subunit contains the molybdenum cofactor and selenocysteine and also possesses an atypical hydrogenase-type signal peptide (Figure 1-4) and iron-sulfur cluster very similar to FdhA described above (Berg *et al.*, 1991). FdnH is the β subunit of FDH_N. It contains four iron-sulfur clusters homologous to those described above (Figure 1-2) followed by a transmembrane region and then a highly charged C-terminus. Although this pattern of primary structure is very similar to that seen in Orf2 of the *hmc* operon, there is no N-terminal signal sequence. The role of cytochrome *b* is fulfilled by FdnI which has three transmembrane regions, two of which contain histidyl residues (*ibid*). Nitrate induction of the *fdn* operon is mediated by the response regulatory protein, NarL, which responds to phosphorylation by the histidine protein kinase NarX (Stock *et al.*, 1990).

There are other operons which share the overall structural design of those mentioned in this section. Examples such as the *frd* and *nar* operons of *E. coli* which encode fumarate and nitrate reductase, respectively, also represent gene clusters resembling the *hmc* operon (Lemire *et al.*, 1982; Blasco *et al.*, 1989).

2. Objectives

The cloning and sequencing of the *hmc* gene of *D. vulgaris* Hildenborough revealed the presence of seven additional open reading frames comprising the *hmc* operon. Sequence analysis suggested that this operon encodes a transmembrane redox protein complex (Rossi *et al.*, 1993). The experiments described in this work have the common goal of establishing, in greater detail, the nature and function of the *hmc* operon in this bacterium. Specifically, experiments have been designed which will: (1) confirm the open reading frames suggested by the sequence of the *hmc* operon, (2) overexpress operon components for the development of antibodies, (3) determine the membrane topology of Orf2, (4) analyze *hmc* operon expression level fluctuations in an attempt to characterize operon function and (5) define the potentially regulatory role of the proteins Rrf1 and Rrf2.

2.1 Overexpression of selected *hmc* operon genes in *E. coli*

The first objective of this research project is to overexpress some of the open reading frames comprising the *hmc* operon within *E. coli*. The reasons for this goal are twofold: (1) high-level expression of expected sized proteins would confirm the open reading frames suggested by the DNA sequence of the *hmc* operon, and (2) a large overproduction of a given protein could be used in the generation of antibodies against that protein. Polyclonal antisera generated against individual components of the Hmc protein complex would be a very valuable tool for use in later studies.

2.2 Determination of the membrane topology of Orf2

As discussed in the introduction, Orf2 is an iron-sulfur protein homologous to several other proteins which have been discovered in different bacterial systems (Figure 1-2). A feature common to all of the members of this redox protein family is the cytoplasmic localization of their iron-sulfur clusters. The localization of Orf2 has previously been presumed

to have the same membrane topology as the other members of the family. The N-terminal hydrophobic region was hypothesized by Pollock (1992) to be an amphipathic membrane anchor lying along the inner side of the cell membrane giving rise to cytoplasmic localization of the iron-sulfur clusters as seen in Figure 1-5. The similarity observed in this study between the Orf2 N-terminus and hydrogenase signal peptides indicates the possibility that Orf2 is largely periplasmic. If this hypothesis is proven, Orf2 is endowed with a membrane topology which is unique among its class of proteins. Experiments with PhoA fusions may establish the membrane topology of Orf2.

2.3 Expression analysis of the *hmc* operon

As mentioned above, the primary goal of this study is to aid in understanding the function of the proteins encoded by the *hmc* operon of *D. vulgaris* Hildenborough. Sequence analysis has suggested that a transmembrane redox protein complex is formed by Hmc and Orf2 to Orf6. The similarity between Hmc and the hydrogenase electron acceptor cytochrome c_3 has further suggested that the membrane complex might play some role in hydrogen oxidation. A way to determine the involvement of the operon components in electron transfer is to grow these bacteria on different electron donating substrates and record possible changes in the level of expression of *hmc* operon components. Use of polyclonal sera in Western blotting will allow monitoring of operon protein expression levels.

2.4 Functional analysis of proteins Rrf1 and Rrf2

The sequence of the *rrf1* gene has implied that Rrf1 serves as a response regulator (Rossi *et al.*, 1993). The potential for a DNA-binding domain within Rrf2 raises the possibility that these two proteins work cooperatively and that their function is one of transcriptional modulation. The fact that *rrf1* and *rrf2* are encoded immediately downstream of the *hmc* operon, and may be part of this operon, points to the likelihood that the proteins Rrf1 and Rrf2 regulate the transcription of this operon in particular. The function of these proteins

and their effect upon *hmc* operon expression will be investigated by construction of a deletion mutant which does not express Rrf1 and Rrf2.

3. Materials and Methods

3.1 Materials

3.1.1 Biochemical reagents

DNA manipulation enzymes were purchased from Pharmacia, Boehringer Mannheim Biochemicals, Promega and New England Biolabs. The radiochemical [α-^{32}P]-dCTP (370 MBq/mL) used in random hexamer labeling and the radiochemical Tran^{35}S-Label™ (70% L-[^{35}S]-methionine, 15% L-[^{35}S]-cysteine; 437 MBq/mL) used in protein labeling were from ICN Biomedicals, Inc. Random hexanucleotide primers, *Bam*HI linkers and *Hin*dIII linkers were obtained from the Regional DNA Synthesis Laboratory (University of Calgary, Calgary, Canada). Deoxynucleoside triphosphates (dNTPs) used in labeling and endrepair were purchased from Pharmacia. Salmon sperm DNA (sodium salt) was from Amersham Life Sciences. Three enzymes were used in plasmid DNA isolation. Lysozyme and proteinase K were from Boehringer Mannheim Biochemicals or Merck while ribonuclease was from Sigma Chemical Co. The *lac* operon inducer isopropylthiogalactoside (IPTG) was from United States Biochemical Corporation and the β-galactosidase chromogenic substrate 5-bromo-4-chloro-3-indolyl-β-D-galactopyranoside (X-Gal) was purchased from Gold Biotechnology, Inc. Bactotryptone and yeast extract were from Difco Laboratories. The antibiotics ampicillin (sodium salt), chloramphenicol and nalidixic acid (sodium salt) were obtained from Sigma Chemical Co. and kanamycin sulfate and rifampicin were from Boehringer Mannheim Biochemicals as was bovine serum albumin (fraction V). Low- (LGT) and High- (HGT) gelling temperature agarose were purchased from Gibco BRL and Boehringer Mannheim Biochemicals, respectively. The ethidium bromide used to stain DNA during electrophoresis was from Sigma Chemical Co. Acrylamide and N,N'-methylenebisacrylamide were from Boehringer Mannheim Biochemicals and BDH Ltd. SDS PAGE electrophoresis low molecular weight markers were from Bio-Rad Laboratories (for the prestained markers) and Pharmacia. The Western blot anti-mouse and anti-rabbit immunoglobulin G alkaline phosphatase conjugates as well as the

chromogenic substrates nitroblue tetrazolium (NBT) and 5-bromo-4-chloro-3-indolyl-β-D-phosphopyranoside (BCIP) were purchased from Promega. The alkaline phosphatase substrate disodium *p*-nitrophenyl phosphate was obtained from Sigma Chemical Co. The nitrogen and mixed gases (5% H_2, 10% CO_2, 85% N_2) used for anaerobic growth of *Desulfovibrio* were purchased from Praxair Canada, Inc. All remaining chemical reagents which were used are listed in Table 3-1.

3.1.2 Bacterial strains

All bacterial strains used are described in Table 3-2. *E. coli* DBH4 was originally obtained from J. Beckwith but all other strains were available in the laboratory.

3.1.3 Plasmids

All plasmids used are described in Table 3-2. The genes of these were expressed in *E. coli, D. desulfuricans* G200 or *D. vulgaris* Hildenborough. Plasmid pT7-7 and M13 phage mGP1-2 were originally obtained from S. Tabor (Tabor & Richardson, 1987). W. B. R. Pollock generated plasmid pP6A (Pollock *et al.*, 1991). Plasmid pJH5304 was constructed by J. van Helvoort, pJK64 by J. K. Voordouw and plasmids pJRMR- and pJRMR+ by M. Rossi (Rossi *et al.*, 1993). Plasmids pPho3 and pΦDP2 were constructed by H. Deckers (Deckers & Voordouw, 1993). Plasmids pMOB2, pMOB3 and pNOT19 were obtained from H. P. Schweizer (Schweizer, 1992). The steps involved in the construction of plasmids pTORF2, pTORF3 and pTORF6 have been described elsewhere (Rossi *et al.*, 1993). The inserts cloned to create these three plasmids can be seen in Figure 3-1.

3.1.3.1 Plasmid pRKPhoA. Plasmid pP6A (Pollock *et al.*, 1991) was digested with *Hin*dIII and the 2.7 kbp fragment, which encompasses the 3'-end of *hmc*, all of *orf2* and the 5'-end of *orf3*, was isolated by LGT agarose gel electrophoresis. Plasmid pRKPhoA was constructed by ligating this 2.7 kbp fragment with *Hin*dIII-digested, alkaline phosphatase-treated pPho3 (Deckers & Voordouw, 1993) placing it 28 bp upstream of the *phoA* coding region (Fig. 3-2, Table 3-2).

Table 3-1. Chemical reagents and suppliers.

Reagent	Supplier
Boric acid, chloroform, ethylenediaminetetraacetic acid (EDTA), ferrous sulfate heptahydrate, glacial acetic acid, glycerol, hydrochloric acid, methanol, Nonidet P-40, potassium dihydrogen orthophosphate, potassium nitrate, sodium carbonate, sodium chloride, sodium citrate, sodium dodecylsulfate (SDS), sodium formate, sodium hydroxide, 70% sodium lactate solution, sodium molybdate dihydrate, sodium pyruvate, sodium sulfate, sucrose, Triton X-100	BDH Ltd.
Ammonium chloride, ammonium sulfate, L-ascorbic acid, bromophenol blue, butanol, calcium chloride dihydrate, calcium sulfate, cobaltous chloride hexahydrate, ferrous chloride tetrahydrate, magnesium chloride hexahydrate, magnesium sulfate heptahydrate, potassium chloride, sodium phosphate dibasic, sodium perchlorate, trichloroacetic acid (TCA), zinc chloride	Fisher Scientific Co.
Bromophenol blue, Coomassie brilliant blue, dithiothreitol, Ficoll 400, gelatin, nitrilotriacetic acid, Nonidet P-40, polyethyleneglycol (PEG) 8000, polyvinylpyrrolidone, Triton X-100, xylene cyanole	Sigma Chemical Co.
Glycine, N-2-hydroxyethylpiperazine-N'-2-ethanesulfonic acid (HEPES), phenol	Boehringer Mannheim Biochemical
Isoamyl alcohol, thioglycollic acid	Aldrich Chemical Corporation, Inc.
Tris(hydroxymethyl) methylamine	ICN Biomedicals, Inc.
Sodium acetate	MCB Reagents
Ficoll 400	Pharmacia
Acetone	Caledon Laboratories
95% Ethanol	Stanchem
Manganous chloride tetrahydrate	Allied Chemical
2-mercaptoethanol	Mallinckrodt, Inc.

Table 3-2. Bacterial strains, vectors and plasmids used.

Strain, vector or plasmid	Genotype, comment(s) and/or reference
D. vulgaris Hildenborough	NCIMB 8303; isolated from clay soil near Hildenborough, Kent, United Kingdom (Postgate, 1984); source of the *hmc* operon (Pollock *et al.*, 1991; Rossi *et al.*, 1993)
D. vulgaris Hildenborough strain RK1	Integration strain which carries plasmid pΔRRF integrated into the chromosome at the downstream region of *orf6* (this study)
D. vulgaris Hildenborough strain RK100	Δ*rrf1,2*; Cm^r (this study)
D. desulfuricans G200	Spontaneous Nal^r derivative of *D. desulfuricans* G100A (Weimer *et al.*, 1988)
E. coli TG2[a]	Δ(*lac-pro*) *supE thi hsdM hsdR recA* F' [*traD36 proAB*$^+$ *lacZ*Δ*M15I*^{q}]
E. coli S17-1	*thi pro hsdR hsdM+ recA* RP4-2 (Tc::Mu, Km::Tn7) (Simon *et al.*, 1983)
E. coli DBH4[b]	Δ(*ara leu*) 7697 *araD*139 Δ(*lac*)x74 *galE galK* Str^r *malF-D3* *phoR*$^-$ *phoA*$^-$ ΔPvuII (F' *lacI*^{q} Z^+Y^+)
M13 phage mGP1-2[c]	Bacteriophage T7 Gene 1 (T7 RNA polymerase) inserted between *Bam*HI and *Sal*I sites of the *E. coli* cloning vector M13mp8 (Tabor & Richardson, 1987)
pUC8	*E. coli* cloning vector; Amp^r (Vieira & Messing, 1982)
pUC18, pUC19	*E. coli* cloning vectors; Amp^r (Yanisch-Perron *et al.*, 1985)
pT7-7[c]	*E. coli* expression vector containing a strong ribosome binding site downstream of the multiple cloning site; T7 RNA polymerase promoter ϕ10; Amp^r (Tabor, 1990)
pJRD215	IncQ group, broad-host-range cloning vector; Km^r, Sm^r (Davison *et al.*, 1987)
pP6A	Contains the *hmc* and *orf2* genes of *D. vulgaris* Hildenborough on a 3.7 kbp *Xho*I insert in pUC8 (Pollock *et al.*, 1991)
pJK64	Contains the *orf2, orf3, orf4* and *orf5* genes of *D. vulgaris* Hildenborough on a 4.7 kbp *Kpn*I insert in pUC18 (Rossi *et al.*, 1993)
pJH5304	Contains the last 1.2 kbp of the *orf6* gene and all of *rrf1* and *rrf2* of *D. vulgaris* Hildenborough on a 3.3 kbp *Xho*I-*Sph*I insert in pUC8 (Rossi *et al.*, 1993)
pTORF2	Contains the last 1.1 kbp of *orf2* of *D. vulgaris* Hildenborough on a 1.5 kbp *Bal*I-*Xho*I insert in pT7-7 (Rossi *et al.*, 1993; this study)
pTORF3	Contains the last 0.7 kbp of *orf3* of *D. vulgaris* Hildenborough on a 1.8 kbp *Xho*I insert in pT7-7 (Rossi *et al.*, 1993; this study)
pTORF6	Contains the last 1.2 kbp of *orf6* of *D. vulgaris* Hildenborough on a 3.3 kbp *Bam*HI insert in pT7-7 (Rossi *et al.*, 1993; this study)

pJRMR-	Contains the entire *hmc* operon of *D. vulgaris* Hildenborough without its promoter on an 8.3 kbp *Eco*RI-*Bam*HI insert in pJRD215 (Rossi *et al.*, 1993)
pJRMR+	Contains the entire *hmc* operon of *D. vulgaris* Hildenborough with its promoter on an 8.7 kbp *Eco*RI-*Bam*HI insert in pJRD215 (Rossi *et al.*, 1993)
pPho3	Contains the *E. coli phoA* gene without its signal sequence on a 4.0 kbp *Hin*dIII-*Sal*I insert in pUC19 (Deckers & Voordouw, 1993)
pRKPhoA	Contains the *orf2* gene of *D. vulgaris* Hildenborough on a 2.7 kbp *Hin*dIII fragment inserted upstream of the *phoA* gene in pPho3 (this study)
pNMB	Contains an in-frame fusion of the *D. vulgaris* Hildenborough *orf2* gene and *E. coli phoA* by deletion of the 1.4 kbp *Mlu*I-*Bam*HI fragment of pRKPhoA (this study)
pNMP	Contains an in-frame fusion of the *D. vulgaris* Hildenborough *orf2* gene and *E. coli phoA* by deletion of the 1.4 kbp *Mlu*I-*Pst*I fragment of pRKPhoA (this study)
pNSB	Contains an in-frame fusion of the *D. vulgaris* Hildenborough *orf2* gene and *E. coli phoA* by deletion of the 1.5 kbp*Sma*I-*Bam*HI fragment of pRKPhoA (this study)
pCSP	Contains an in-frame fusion of the *D. vulgaris* Hildenborough *orf2* gene and *E. coli phoA* by deletion of the 0.5 kbp*Sma*I-*Pst*I fragment of pRKPhoA (this study)
pΦDP2	Contains the upstream 0.7 kbp of the *D. vulgaris* Hildenborough *dcrA* gene under the control of that bacteria's *cyc* promoter and ribosome binding site fused in frame to the *phoA* gene in pPho3 (Deckers & Voordouw, 1993)
pNOT19[d]	*E. coli* cloning vector pUC19 with a *Not*I site replacing the *Nde*I site (Schweizer, 1992)
pMOB2[d]	Mobilization cassette containing *oriT* of the self-transmissable plasmid RP4 and *B. subtilis sacBR* genes; Km^r (Schweizer, 1992)
pMOB3[d]	Mobilization cassette containing *oriT* of the self-transmissable plasmid RP4 and *B. subtilis sacBR* genes; Km^r, Cm^r (Schweizer, 1992)
pRRFH	Contains 3.3 kbp *Bam*HI insert of pJH5304 encompassing the *rrf1,2* genes of *D. vulgaris* Hildenborough with a 0.6 kbp *Stu*I-*Bsm*I deletion replaced by a *Hin*dIII site cloned in pUC8 (this study)
pRRFCm	Contains 3.3 kbp *Bam*HI insert of pJH5304 encompassing the *rrf1,2* genes of *D. vulgaris* Hildenborough with a 0.6 kbp *Stu*I-*Bsm*I deletion replaced by Cm^r gene on a 0.8 kbp *Hin*dIII insert all cloned in pUC8 (this study)
pRRFNOT	Contains 3.3 kbp *Bam*HI insert of pJH5304 encompassing the *rrf1,2* genes of *D. vulgaris* Hildenborough with a 0.6 kbp *Stu*I-*Bsm*I deletion replaced by a Cm^r gene all cloned in pNOT19 (this study)

pΔRRF	Contains 3.3 kbp *Bam*HI insert of pJH5304 encompassing the *rrf1,2* genes of *D. vulgaris* Hildenborough with a 0.6 kbp *StuI-BsmI* deletion replaced by a Cm^r gene; also has *oriT* of RP4 and *B. subtilis sacBR* genes on a 4.7 kbp *Not*I insert cloned in pNOT19 (this study)

[a] Constructed from *E. coli* JM101 by T. J. Gibson and M. D. Biggin at the Laboratory of Molecular Biology, MRC Centre, Cambridge, United Kingdom

[b] Obtained from J. Beckwith, Department of Microbiology and Molecular Genetics, Harvard Medical School, Boston, Mass., USA

[c] Obtained from S. Tabor, Department of Biological Chemistry, Harvard Medical School, Boston, Mass., USA

[d] Obtained from H. P. Schweizer, Department of Microbiology and Infectious Diseases, University of Calgary Health Sciences Centre, Calgary, Alberta, Canada

3.1.3.2 Plasmid pNMB. This plasmid was constructed following the restriction of pRKPhoA with *Mlu*I and *Bam*HI, end-repair with DNA polymerase I Klenow fragment and re-ligation. This resulted in the in-frame fusion of the first 81 amino acids of Orf2 to the 8th amino acid of PhoA (Figure 3-2, Table 3-2; Li *et al.*, 1988).

3.1.3.3 Plasmid pNMP. This plasmid was constructed by digesting pRKPhoA with *Mlu*I and *Pst*I, end-repair with Klenow polymerase, alkaline phosphatase treatment and ligation with *Bam*HI linkers. The result was an in-frame fusion of the first 81 amino acids of Orf2 to the 13th amino acid of PhoA and the generation of a new Arg-Ile-Arg sequence at the point of fusion (Figure 3-2, Table 3-2).

3.1.3.4 Plasmid pNSB. This plasmid was constructed by digesting pRKPhoA with *Sma*I and *Bam*HI, end-repair with Klenow polymerase and re-ligation. The result was an in-frame fusion of the first 34 amino acids of Orf2 to the 8th residue of PhoA (Figure 3-2, Table 3-2).

3.1.3.5 Plasmid pCSP. This plasmid was constructed by digesting pRKPhoA with *Pst*I and partially digesting with *Sma*I before isolating a 6.3 kbp fragment by LGT agarose gel electrophoresis. This fragment was end-repaired with Klenow polymerase and self-ligated to yield an in-frame

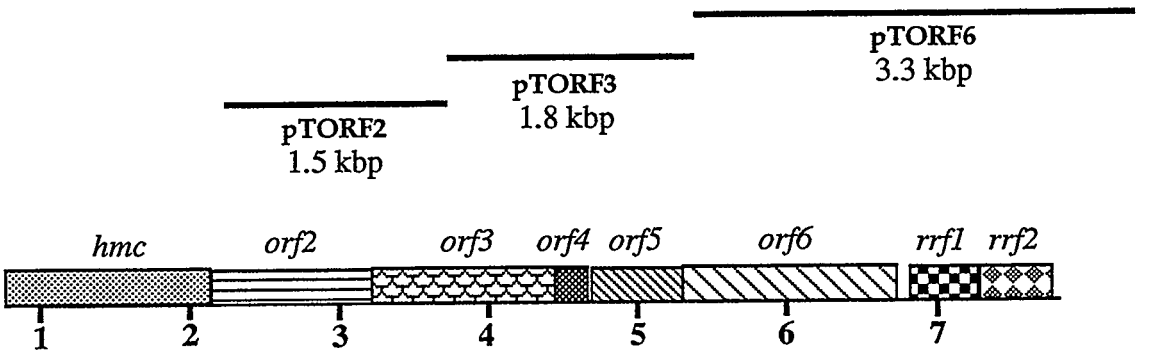

Figure 3-1. Map of the inserts within plasmids pTORF2, pTORF3 and pTORF6. The inserts are shown above the *hmc* operon to indicate which portions of the operon are included in each construction. All fragments were inserted into the multiple cloning site of pT7-7 to give the final plasmid (Rossi *et al.*, 1993). The scale is in kbp.

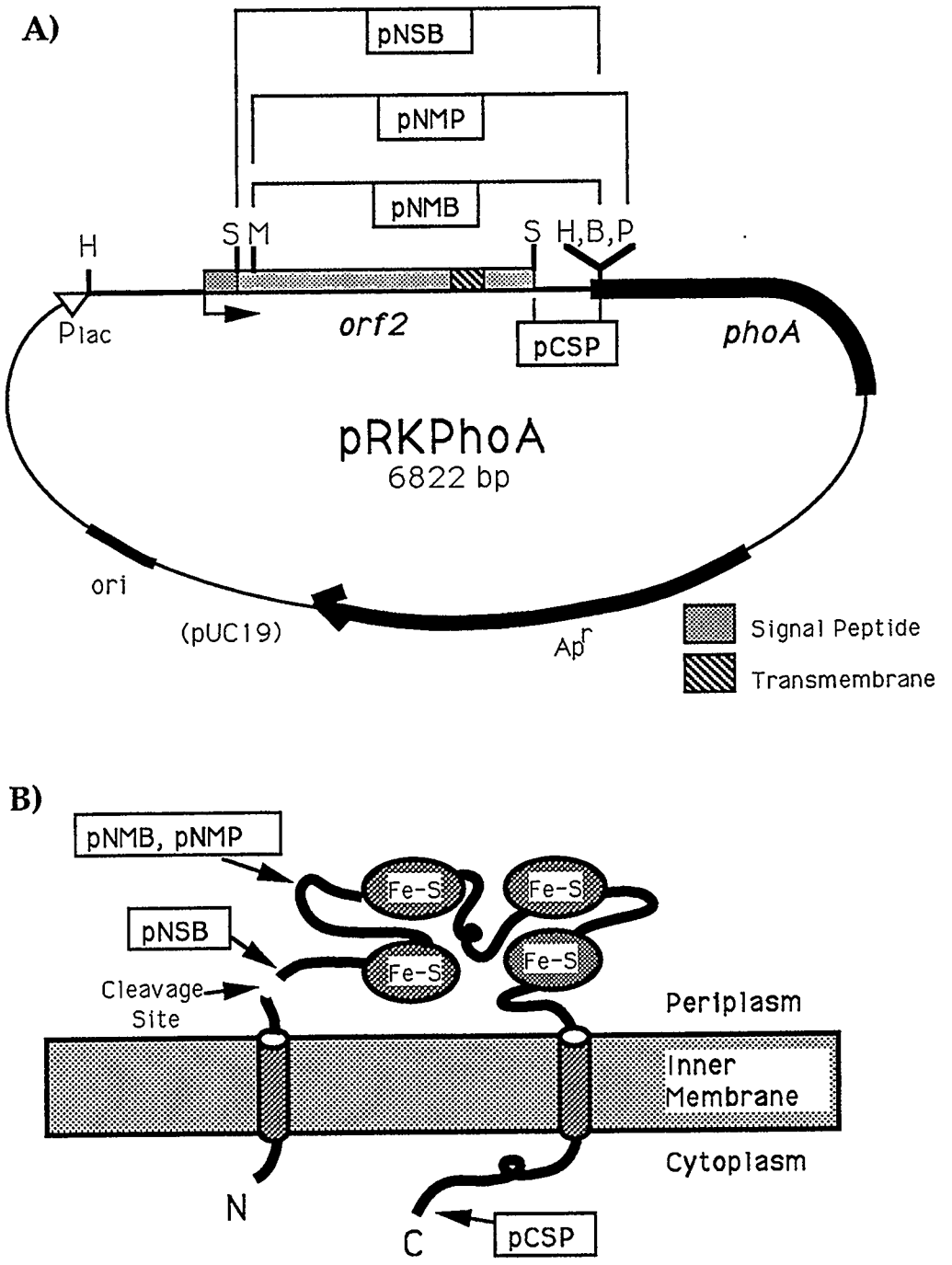

Fig. 3-2. Orf2-PhoA fusions. **A)** Fusion plasmids shown in boxes were constructed by deleting the indicated regions of plasmid pRKPhoA. **B)** Fusion plasmids express PhoA fused to truncations of Orf2 at the indicated points. B, *Bam*HI; H, *Hin*dIII; M, *Mlu*I; P, *Pst*I; S, *Sma*I.

fusion of the first 365 amino acids of Orf2 to the 13th residue of PhoA (Fig. 3-2, Table 3-2).

3.1.3.6 Plasmid pΔRRF. Plasmid pJH5304 (Rossi *et al.*, 1993) was restriction-digested with *Stu*I and *Bsm*I, end-repaired with Klenow polymerase and ligated with *Hin*dIII linkers resulting in the generation of plasmid pRRFH which possessed a deletion of 0.6 kbp spanning the genes *rrf1* and *rrf2* and a *Hin*dIII site in place of this deletion. Plasmid pMOB3 (Schweizer, 1992) was digested with *Hin*dIII and its 0.8 kbp fragment encoding chloramphenicol acetyltransferase or Cm^r was isolated by LGT agarose gel electrophoresis and ligated with *Hin*dIII-digested pRRFH to yield pRRFCm. *E. coli* TG2 (pRRFCm) transformants were positively selected on Cm plates. The pUC8 region of pRRFCm was replaced with plasmid pNOT19 (Schweizer, 1992) by digesting pNOT19 and pRRFCm with *Bam*HI and ligating the 3.6 kbp insert of pRRFCm with the linearized pNOT19 providing a single *Not*I site in the resulting plasmid pRRFNOT. Plasmid pMOB2 (Schweizer, 1992) was digested with *Not*I and the 4.7 kbp region encoding *sacBR* and *oriT* was ligated with pRRFNOT which had been digested with the same enzyme and treated with alkaline phosphatase. This last ligation resulted in the construction of the self-transmissable plasmid pΔRRF (Figure 3-3, Table 3-2). *E. coli* TG2 (pΔRRF) transformants were positively selected on Cm plates and negatively selected on plates containing 5% (w/v) sucrose.

3.1.4 Growth media

All *E. coli* cultures were grown in TY (tryptone-yeast extract) broth or on TY plates which are described in Sambrook *et al.* (1989). For labeling of *E. coli* with Tran^{35}S-Label™, cells were resuspended in M9 minimal medium which is also described by Sambrook *et al.* (1989).

D. vulgaris Hildenborough (wild type and mutants) and *D. desulfuricans* G200 were cultured in Postgate medium C (0.5 g/L KH_2PO_4, 1 g/L NH_4Cl, 4.5 g/L Na_2SO_4, 0.06 g/L $CaCl_2 \cdot 6H_2O$, 0.06 g/L $MgSO_4 \cdot 7H_2O$, 6 g/L sodium lactate, 1 g/L yeast extract, 0.004 g/L $FeSO_4 \cdot 7H_2O$, 0.3 g/L sodium citrate$\cdot 2H_2O$ in distilled H_2O, pH 7.5), plated on Postgate medium E (0.5 g/L KH_2PO_4, 1 g/L NH_4Cl, 1 g/L Na_2SO_4, 1 g/L $CaCl_2 \cdot 6H_2O$, 2 g/L $MgSO_4 \cdot 7H_2O$, 3.5 g/L sodium lactate, 1 g/L yeast extract, 0.1 g/L ascorbic acid, 0.1 g/L

thioglycollic acid, 0.5 g/L $FeSO_4 \cdot 7H_2O$, 15 g/L agar in tap H_2O, pH 7.6) and stored in Postgate medium B (0.5 g/L KH_2PO_4, 1 g/L NH_4Cl, 1 g/L Ca_2SO_4, 2 g/L $MgSO_4 \cdot 7H_2O$, 3.5 g/L sodium lactate, 1 g/L yeast extract, 0.1 g/L ascorbic acid, 0.1 g/L thioglycollic acid, 0.5 g/L $FeSO_4 \cdot 7H_2O$ in tap H_2O, pH 7.2; Postgate, 1984). Expression studies and growth profiles of *D. vulgaris* Hildenborough strains were performed while growing the bacteria on minimal hydrogen/SO_4^{2-} medium (2.5 g/L sodium acetate, 6.6 g/L $(NH_4)_2SO_4$, 1.8 g/L NaCl, 0.9 g/L KH_2PO_4, 0.36 g/L $MgCl_2 \cdot 6H_2O$, 0.26 g/L $CaCl_2 \cdot 2H_2O$, in distilled water, pH 6.8 with Na_2CO_3) with 1.25% (v/v) trace elements solution (12.8 g/L NTA, pH 6.5 with NaOH, 1 g/L $FeCl_2 \cdot 4H_2O$, 0.5 g/L $MnCl_2 \cdot 4H_2O$, 0.3 g/L $CoCl_2 \cdot 6H_2O$, 0.2 g/L $ZnCl_2$, 50 mg/L $Na_2MoO_4 \cdot 2H_2O$, 20 mg/L H_3BO_3; Brandis & Thauer, 1981). The lactate, pyruvate and formate variations of this medium differ only in the replacement of 30 mM sodium acetate with one of 30 mM sodium lactate (4.8 g/L 70% solution), 30 mM sodium pyruvate (3.3 g/L) or 30 mM sodium formate (2.0 g/L).

3.1.5 Growth conditions

E. coli liquid cultures were typically incubated in 5.0 mL medium plus the appropriate antibiotic (100 µg/mL ampicillin, 10 µg/mL chloramphenicol or 100 µg/mL kanamycin) at 37°C and shaking at 250 rpm. Plated cultures were incubated at 37°C on 25 mL of medium plus antibiotic, isopropylthiogalactoside (IPTG, 0.4 mg/mL) and chromogenic substrate if appropriate. Plates were stored at 4°C after growth.

Desulfovibrio were stored for long periods in 20 mL Postgate medium B at 4°C in capped, nitrogen-flushed tubes. Growth of cultures took place in liquid medium or on 30 mL plates plus antibiotic (10 µg/mL chloramphenicol, 100 µg/mL kanamycin or 200 µg/mL nalidixic acid) incubated at 35°C in a Forma Scientific Anaerobic Chamber filled with an atmosphere of 5% (v/v) H_2, 10% (v/v) CO_2 and 85% (v/v) N_2. For use in growth profiles and expression studies, some cultures were grown in 100 mL capped bottles flushed with nitrogen and incubated at 35°C.

3.2 Methods

3.2.1 Standard protocols

3.2.1.1 DNA isolations. Plasmid DNA was isolated from *E. coli* using the Triton X-100 lysis procedure described by Voordouw *et al.* (1985). Total DNA was isolated from *Desulfovibrio* using the method described by Marmur (1961).

3.2.1.2 DNA enzymatic manipulations. Restriction endonuclease digestions, ligation reactions using T_4 DNA ligase, 5'-end dephosphorylation with calf intestine alkaline phosphatase, end-repair reactions using the DNA polymerase I Klenow fragment and radiolabel incorporation of [α-^{32}P]-dCTP using random hexamer priming and Klenow polymerase were performed as described by Sambrook *et al.* (1989).

3.2.1.3 DNA Electrophoresis. Electrophoresis was carried out using HGT (high-gelling temperature) agarose for size fractionation and LGT (low-gelling temperature) agarose for routine use and DNA fragment isolation. Agarose concentrations used were either 0.7% or 1.0% (w/v) in TAE (40 mM Tris-acetate, 2.0 mM EDTA, pH 8.0) and electrophoresis was run in *ca.* 800 mL of TAE in a BRL Model H5 gel apparatus as described by Voordouw *et al.* (1985).

3.2.1.4 Gel isolation of DNA. Size fractionated DNA fragments were isolated from 1.0% (w/v) LGT agarose gels and purified by phenol extraction as described elsewhere (Sambrook *et al.*, 1989) with a couple of changes. The DNA-agarose bands were melted at 68°C for 15 min and diluted 2.5x with TE (10 mM Tris-HCl, 0.1 mM EDTA, pH 8.0) before two phenol extraction procedures. Following phenol extraction the sample was extracted with dry butanol until the sample volume was concentrated to *ca.* 50 µL before ethanol precipitation of the DNA.

3.2.1.5 Southern blotting. DNA was electrophoresed in either digested or undigested form through 0.7% (w/v) HGT agarose gels as described above. Following electrophoresis, the DNA was denatured, neutralized and transferred to Hybond-N membrane (from Amersham) overnight as described by Sambrook *et al.* (1989). The Hybond-N blots were washed for 5 min in 6x SSC (1x SSC is 15 mM sodium citrate, pH 7.2, 150 mM NaCl), dried

and UV-irradiated for 5 min on a Fisher Biotech 321 nm transilluminator (8000 mW/cm^2) to cross-link the DNA to the membrane. Prehybridization of the blot involved incubation in a solution of 6x SSC, 0.5% (w/v) SDS, 5x Denhardt solution (1x Denhardt is 1% (w/v) Ficoll 400, 1% (w/v) polyvinylpyrrolidone, 1% (w/v) BSA) and 3 mg salmon sperm DNA at 68°C for 3 h. Radiolabeled probes were generated by random hexamer priming and incorporation of deoxynucleotide triphosphates (dNTPs) and [α-^{32}P]-dCTP as described above. The labeled probe was added to the prehybridization solution after the 3 h incubation period and the Southern blots were hybridized at 68°C for 16 h. Following hybridization, the blots were washed 4x 2 min at room temperature in 6x SSC and once for 1 h at 68°C in 6x SSC, 0.5% (w/v) SDS. Blots were then dried at room temperature, wrapped in Saran wrap and autoradiographed at -70°C for 1 to 16 h.

3.2.1.6 Colony filter hybridization. *E. coli* transformants were screened for desired plasmid DNA by probing the colonies with a radiolabeled probe. The bacterial colonies were grown on nitrocellulose filters (from Schleicher & Schuell), lysed, neutralized and dried as outlined previously (Voordouw *et al.*, 1985). Filters were then baked at 75°C under vacuum for 50 min before prehybridizing, hybridizing and autoradiographing as for a Southern blot.

3.2.1.7 Transformation and conjugation. Plasmid DNA was transformed into *E. coli* using the $CaCl_2$ method (Sambrook *et al.*, 1989). Plasmid DNA was conjugated into *D. vulgaris* Hildenborough and *D. desulfuricans* G200 using *E. coli* S17-1 transformant donors as described previously (Rossi *et al.* 1993). The mating mixtures were spread on Postgate medium E plates containing 100 µg/mL kanamycin (Km) and 200 µg/mL nalidixic acid (Nal) for pJRD215-based plasmids conjugated into *D. desulfuricans* G200 and 10 µg/mL chloramphenicol (Cm) for pΔRRF conjugations.

3.2.1.8 SDS PAGE. The size fractionation of proteins by sodium dodecylsulfate polyacrylamide gel electrophoresis was performed as described previously (Laemmli, 1970). Running gels were typically 12.5% (w/v) acrylamide/ 0.33% (w/v) bisacrylamide in 0.3 M Tris-acetate, pH 8.8 and 0.1% (w/v) SDS. Stacking gels were 5% (w/v) acrylamide/ 0.13% (w/v) bisacrylamide in 0.125 mM Tris-acetate, pH 6.8 plus 0.1% (w/v) SDS.

Electrophoresis was performed in a running buffer of 25 mM Tris-HCl, 192 mM glycine, pH 8.3 and 0.1% SDS.

Whole cell samples for SDS PAGE were prepared by harvesting ice-chilled cells in a Sorvall RC-5B centrifuge at 12 000 xg for 10 min at 4°C. The pellet was resuspended in 1 mL cold 50 mM Tris-HCl, pH 7.4 which was spun for 1 min at 16 000 xg in a Beckman Microfuge E at 4°C. The pellet of cells was resuspended in water (half the desired final volume) and then an equal volume of 2x sample loading buffer (LB) (1x LB is 50 mM Tris-HCl, pH 6.8, 100 mM dithiothreitol, 2% (w/v) SDS, 0.1% (w/v) bromophenol blue and 10% (v/v) glycerol) before the sample tube was immersed in a boiling water bath for 5 to 8 min and stored at -70°C. The final volume of the denatured sample in LB was related to the initial bacterial culture harvested as follows:

$$\text{Final volume (mL)} = \frac{[\text{cell density (Klett units)}] \times [\text{culture volume (mL)}]}{3333.}$$

This relationship was found empirically to yield crude cell extract concentrations that were sufficient for analysis when loading 20 µL of sample in each gel lane. Cell densities were determined with a Klett-Summerson Photoelectric Colorimeter using a #66 red filter and blanked with water.

Membrane fractions were prepared by harvesting bacterial cultures as above but then resuspending in 4 mL cold 50 mM Tris-HCl, pH 7.4 and breaking the cells with two passes through a French Pressure cell. The samples were spun 10 min at 12 000 xg and 4°C to remove unbroken cells and then the supernatant was spun for 1 h at 100 000 xg in a Beckman Model L5-50 Ultracentrifuge using a Ti-50 rotor. The pelleted membrane fraction was denatured in LB, boiled and stored as described above.

Soluble cell fractions were prepared from the supernatant resulting after ultracentrifugation of broken cells (above). This fraction was precipitated with 5% (v/v) trichloroacetate (TCA) at 0°C for 20 min before being spun at 12 000 xg and 4°C for 10 min. The pellet was washed once with 1 mL of 65% acetone and spun in a similar fashion for 2 min. The soluble fraction was resuspended in LB, boiled and stored as above.

SDS polyacrylamide gels which needed to be autoradiographed were dried prior to autoradiography. Gels were soaked in a 50% (v/v) methanol, 5% (v/v) glycerol solution for 30 min before drying onto Whatman 3mm chromatography paper with an LKB 2003 Slab Gel Dryer for 2 h.

3.1.2.9 Western blotting. Size-fractionated proteins were transferred electrophoretically from polyacrylamide gel to nitrocellulose membrane as described by Towbin *et al.* (1979). Transfer occurred at 40 mA for 16 h in a Bio-Rad transfer tank filled with transfer buffer composed of 39 mM glycine, 48 mM Tris-HCl, pH 8.3, 0.037% (w/v) SDS and 20% (v/v) methanol (Sambrook *et al.*, 1989). Following transfer, the nitrocellulose filter was blocked for 3 h in 7% (w/v) gelatin, 0.1 M NaCl and 0.1 M Tris-HCl, pH 7.4. Primary antibody incubation was performed for 16 h in Buffer A (0.16 M NaCl, 10 mM Tris-HCl, pH 7.4, 0.1% (w/v) Nonidet P-40) plus 4 µL antiserum. The blot was washed 4x 10 min in Buffer A and incubated for 1 h in Buffer A plus 4 µL anti-mouse or anti-rabbit IgG alkaline phosphatase conjugate. The blot was washed further in Buffer A for 2x 10 min and then 2x 10 min in AP (alkaline phosphatase) buffer (0.1 M NaCl, 0.1 M Tris-HCl, pH 9.5, 0.1% (w/v) $MgCl_2$) before developing in AP buffer plus 0.1% (v/v) 50 mg/mL BCIP (5-bromo-4-chloro-3-indolyl-β-D-phosphopyranoside) and 0.2% (v/v) 50 mg/mL NBT (nitroblue tetrazolium) in the dark for 5 to 30 min.

3.2.1.10 Computer programs. DNA of known sequence was analyzed with respect to restriction endonuclease cut sites and translated peptide sequence and proteins of known sequence were analyzed regarding weight and hydropathy using the Staden programs (Staden, 1984; Staden & McLachlan, 1982). Protein primary structure comparisons were performed with the FASTA program of the GCG package (Devereux *et al.*, 1984).

3.2.2 Bacteriophage T7 expression system

Fusion proteins of Orf2, Orf3 and Orf6 were overexpressed in *E. coli* using the bacteriophage T7 expression system developed by Tabor & Richardson (1985). *E. coli* TG2 cells were transformed with the pT7-7 derivatives pTORF2, pTORF3 or pTORF6 and grown to an $A_{600}\approx0.6$ before overexpression of the protein of interest was induced by infection of the bacteria with M13 phage mGP1-2 (which carries the T7 RNA polymerase gene

under the control of the *lac* promoter), using a multiplicity of infection of 10, and addition of IPTG (0.24 mg/mL of cells) as described previously (Tabor & Richardson, 1987; 1985). The cells were incubated at 37°C for 2 h, chilled on ice, harvested and suspended in water and then SDS PAGE LB and run on SDS PAGE as described above. Alternatively, the induced cultures were harvested and resuspended in M9 minimal medium and 80 µg rifampicin was added (Dougan & Sherratt, 1977). The cells were incubated at 42°C for 15 min and labeled for 15 min with 10 µCi of Tran^{35}S-Label™ before preparing in sample buffer as described above and analyzing following SDS PAGE and autoradiography.

3.2.3 Polyclonal antiserum generation

E. coli TG2 (pTORF6) transformants overexpressing a 47 kDa truncated Orf6 protein via the bacteriophage T7 expression system were lysed and the proteins were size-fractionated by SDS PAGE. The overexpressed protein was excised from the polyacrylamide gel and used to generate mouse polyclonal anti-Orf6 serum as described by Winston *et al.* (1990). The protein bands of the unstained gel were visualized with cold 0.1 M KCl and the excised gel slice was homogenized in a minimal volume of PBS (phosphate-buffered saline: 137 mM NaCl, 2.7 mM KCl, 4.3 mM $Na_2HPO_4 \cdot 7H_2O$, 1.4 mM KH_2PO_4) by forcing the suspension through successively smaller gauge needles. Approximately 400 µl of polyacrylamide-PBS mixture containing 40 µg of antigen was administered to each of two mice via an intraperitoneal injection. The mice were boosted with the same amount of antigen after 21 days and bled out 7 days later. The blood samples were incubated at 37°C for 1.5 h to allow a clot to form before being spun 5 min at 16 000 xg to remove the clot. The supernatant was stored in 100 µL aliquots at -70°C before use in Western blotting.

3.2.4 Alkaline phosphatase fusions

In order to determine the membrane topology of Orf2, *phoA* gene fusions were prepared and investigated with regards to alkaline phosphatase activity as described previously (Deckers & Voordouw, 1993; San Millan *et al.*, 1989; Michaelis *et al.*, 1983). In-frame genetic fusions were constructed which

resulted in truncations of Orf2 joined to the entire alkaline phosphatase polypeptide which is enzymatically inactive if it is retained in the cytoplasm of the bacteria (Manoil & Beckwith, 1986).

3.2.4.1 Expression of *phoA* fusions in *E. coli*. The *orf2-phoA* fusion plasmids were transformed into *E. coli* DBH4 which were grown at 37°C for 16 h with 50 µg IPTG added per mL culture. The cultures were harvested and prepared for SDS PAGE as above. The polyacrylamide gels were Western blotted using polyclonal antibodies generated in mice against *E. coli* alkaline phosphatase (Deckers & Voordouw, 1993) and the size and expression level of the immunoreactive bands was analyzed. The latter was quantitatively determined in the same manner as for *hmc* operon expression levels described below in section 3.2.8.

3.2.4.2 Alkaline phosphatase activity measurements. Alkaline phosphatase activity was visualized through growth of *E. coli* DBH4 transformants on plates inoculated with IPTG (16 µg/mL medium) and the chromogenic substrate BCIP (40 µg/mL medium) which yielded blue colonies in the presence of active alkaline phosphatase (Deckers & Voordouw, 1993).

The enzyme activity was measured as the rate of hydrolysis of the substrate *p*-nitrophenyl phosphate (*p*NPP) as described by Brickman & Beckwith (1975). *E. coli* DBH4 transformants were grown at 37°C for 16 h in the presence or absence of IPTG (0.1 mg/mL cells) before permeabilizing the cells with 0.4% (v/v) chloroform and SDS (8 µg/mL culture) for 30 min at room temperature. Following permeabilization, the cells were harvested by cenrifugation in an IEC Centra-7R Refrigerated Centrifuge for 10 min at 1750 xg and 4°C and resuspended in 5 mL of 1 M Tris-HCl, pH 8.0 and the absorbance at 600 nm was recorded for a 1.0 mL 10-fold dilution (diluted in 1 M Tris-HCl, pH 8.0) to give a measure of cell density. Upon addition of 0.2 mg *p*NPP to the cuvette, the absorbance at 550 nm (to provide a correction factor for absorbtion of the cells) and 420 nm (to determine *p*NPP hydrolysis) was monitored over time for the 10-fold dilutions (Brickman & Beckwith, 1975). The following formula was used to determine the units of alkaline phosphatase activity present in the cultures:

$$\text{Units}/A_{600} = \frac{1000 \times [\,(A_{420}-1.75\times A_{550})_{tB} - (A_{420}-1.75\times A_{550})_{tA}\,]}{(tB-tA)\,A_{600}}$$

where t = time (minutes).

3.2.5 Analysis of potential helix-turn-helix motifs

The amino acid sequence of Rrf2 was investigated for the presence of a potential DNA-binding domain in the form of a helix-turn-helix motif using a method of motif detection and evaluation developed by Dodd & Egan (1990). The primary structure of Rrf2 was analyzed and found to contain the sequence Ala-X_3-Gly-X_5-Leu-X_2-Leu which is a consensus commonly found among helix-turn-helix-containing proteins (Pabo & Sauer, 1984). Each of 22 amino acids surrounding this consensus was evaluated by comparison with the sequences of all proteins known to contain this motif.

3.2.6 *D. vulgaris* mutagenesis

The genes *rrf1* and *rrf2* of *D. vulgaris* Hildenborough were deleted using a method of double homologous recombination developed by R. Fu (unpublished). A schematic representation of the mutagenesis method is presented in Figure 3-3. The method utilizes Cm resistance to select positively for the first recombination event resulting in integration of a foreign self-transmissable plasmid into the host chromosome. The lethality of the *B. subtilis sacB* gene in Gram negative bacteria grown on sucrose is used to select for the second recombination event which results in plasmid excision and mutagenesis (Schweizer, 1992; Hynes *et al.*, 1989). *E. coli* S17-1 was transformed with the integration plasmid pΔRRF and the transformants were used to donate the plasmid to *D. vulgaris* Hildenborough through conjugation as described above. Single colonies of integrants were selected on plates with 10 μg/mL Cm and 25 μg/mL Km (used to select against *E. coli* since *D. vulgaris* is Km^r) incubated anaerobically at 35°C for 4 days. The integration frequency was determined by counting the number of Cm^r colonies obtained and dividing this by the number of total viable cells as determined from a control plate with only Km. After culturing in Postgate medium C plus 10 μg/mL Cm, total DNA was prepared from purified

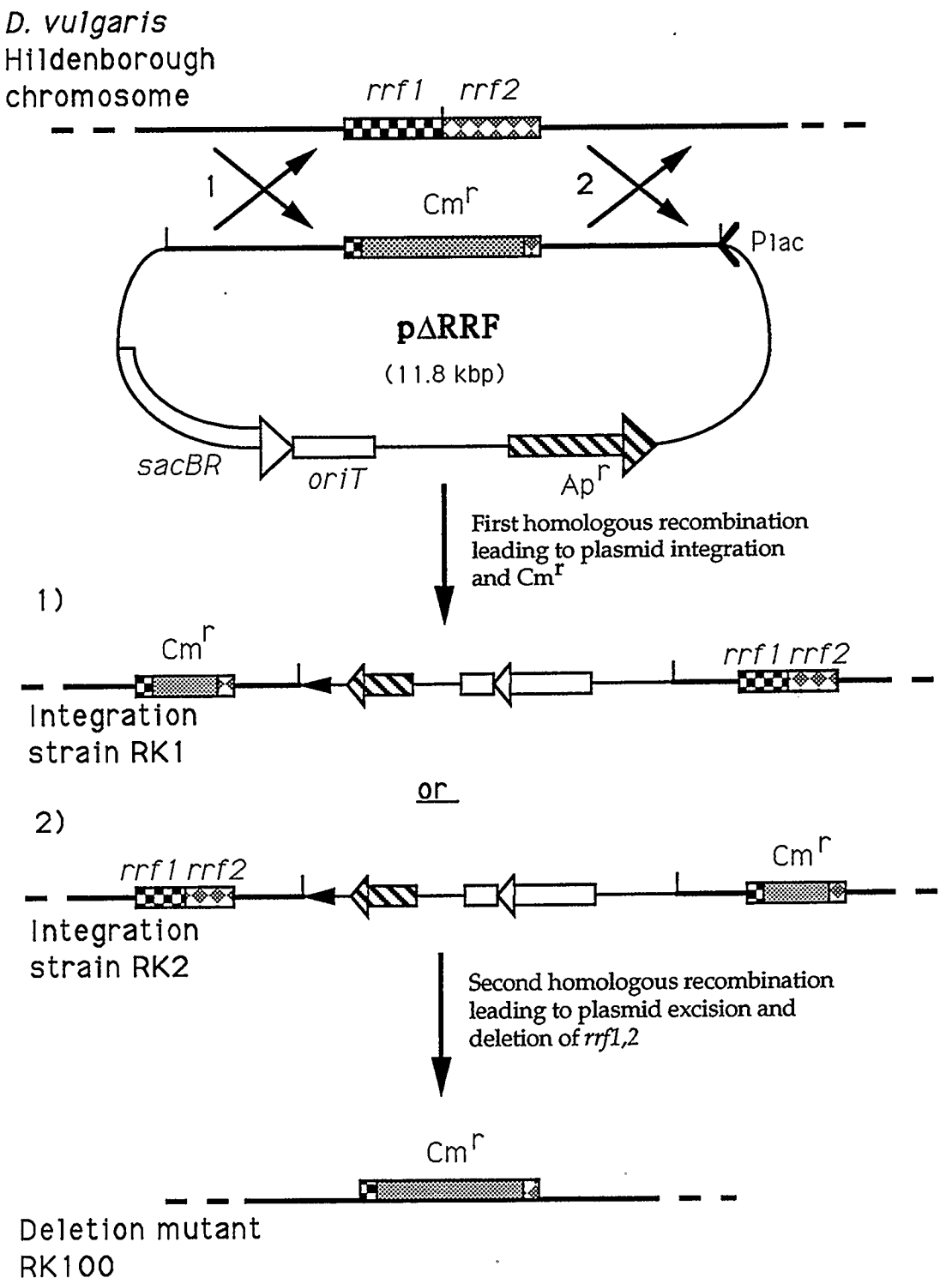

Fig. 3-3. Generation of the *D. vulgaris* Hildenborough mutant strain RK100.

colonies and Southern blotted to verify the integration of pΔRRF into the *D. vulgaris* chromosome and determine the nature of the event. Representatives of the integrant strain RK1 were grown in Postgate medium C with 10 μg/mL Cm and 7% (w/v) sucrose at 35°C and/or plated on Postgate medium E with 10 μg/mL Cm and 5% (w/v) sucrose to select for the second recombination event which would lead to excision of the counter-selectable marker, *sacB*. Total DNA was prepared from individual colonies which were cultured as above with Cm and 7% (w/v) sucrose and Southern blotted to check for the second recombination. Samples found eventually to contain the mutant strain (RK100) were plated on 10 μg/mL Cm, 5% (w/v) sucrose plates to colony-purify the strain and cultured as above before preparing total DNA and Southern blotting to verify the presence of purified colonies of the *D. vulgaris* Hildenborough *rrf1,2*-deficient mutant RK100.

3.2.7 *D. vulgaris* growth rates

The growth rates of *D. vulgaris* Hildenborough wild type and mutant strain RK100 on different media were compared to elucidate phenotypic differences between the two strains. Both strains were cultured in Postgate medium C before inoculating 0.5 mL of each into 5 mL minimal lactate/SO_4^{2-} with 1.25% (v/v) trace elements and growing for 24 h at 35°C. The bacteria were sub-cultured in lactate/SO_4^{2-} plus trace elements in this manner twice more to lower yeast extract levels to a negligible level before 100 mL cultures of the same were inoculated. Once these cultures had grown for 40 h, the cell densities were measured using a Klett-Summerson Photoelectric Colorimeter. Aliquots which contained the same amount of cells were removed from both the wild type and mutant cultures and harvested by centrifugation for 1.5 min at 16 000 xg and 4°C before resuspending in the new media on which growth would be monitored (*i.e.* one of hydrogen/SO_4^{2-}, pyruvate/SO_4^{2-} or lactate/SO_4^{2-}) and using these resuspended aliquots to inoculate the test cultures. The test cultures were grown in triplicate in 3 mL volumes open to the 5% H_2, 10% CO_2, 85% N_2 atmosphere of the anaerobic chamber at 35°C or in 50 mL volumes within sealed 100 mL bottles under *ca.* 1 atm nitrogen at 35°C and the cell densities were monitored over time using the colorimeter.

3.2.8 Operon expression analysis

The expression level of the *hmc* operon was analyzed during growth on various media differing in electron donating substrate through the determination of the relative levels of Hmc and Orf6 proteins present on Western blots. Cultures of *D. vulgaris* Hildenborough wild type or mutant strain RK100 were grown in the medium of interest at 35°C until mid-log phase (as determined by growth rates) before being chilled on ice, harvested, resuspended in water and denatured in SDS PAGE LB as described above. The cell extracts were electrophoresed using SDS PAGE and Western blotted with either anti-Orf6 serum or affinity column-purified anti-Hmc serum generated in rabbits (Rossi *et al.*, 1993). These blots carried multiple lanes of cell extract each of which represented a different medium for the bacteria. They displayed either Orf6 or Hmc at a given intensity in each lane depending on which antibodies were used. The Western blots were imaged using a Hewlett-Packard ScanJet IIc and the relative intensities of immunoreactive bands present in each lane on the same blot were compared using the Image 1.31f Gelscan software. The band intensity for a particular immunoreactive protein in one lane was plotted and the area under the resulting peak was determined. The same was done for all lanes on a particular blot. The area values representing band intensities were normalized by giving the lane with the highest area a new value of 100% and scaling all other lanes accordingly. Stained polyacrylamide gels were examined through visual analysis to verify that the same concentration of cell extract had been loaded in each well. A difference as low as 1.2x was readily apparent.

4. Results

4.1 Overexpression of operon components in *E. coli* [1]

The bacteriophage T7 expression system was used to overexpress truncated versions of proteins Orf2, Orf3 and Orf6 which were fused at their N-terminus to the short leader peptide found encoded on the pT7-7 vector. The fusion proteins were expressed in *E. coli* TG2 and analyzed by SDS PAGE.

4.1.1 Overexpression of Orf2

The expected size of the fusion protein expressed by *E. coli* TG2 (pTORF2) transformants induced with IPTG is 39 kDa. A band corresponding to this molecular weight could not be visualized by staining the polyacrylamide gels after SDS PAGE of whole cell samples. Upon labeling of the cells with Tran^{35}S-Label™ and autoradiography, a radiolabeled band corresponding to the predicted 39 kDa could be seen on the autoradiogram (Figure 4-1, lane 2).

4.1.2 Overexpression of Orf3

The expected size of the fusion protein expressed by *E. coli* TG2 (pTORF3) transformants upon induction is 28 kDa. A band of this size was not visualized after staining of whole cell samples on SDS polyacrylamide gels, but very weak bands running at 30 kDa and 25 kDa could be seen following translabeling of the cells (Figure 4-1, lane 3). These bands may correspond to Orf3 as well as the full length protein Orf5 which is encoded in its entirety within pTORF3 and has a predicted size of 25 kDa. In addition to these two bands, radioactive aggregated material was observed at the top of the gel suggesting that the extreme hydrophobic nature of Orf3 may have prevented proper denaturation and resolution of this protein by SDS PAGE (Figure 4-1, lane 3).

---

[1] This work has been published (Rossi *et al.*, 1993). No further reference to this publication will be made.

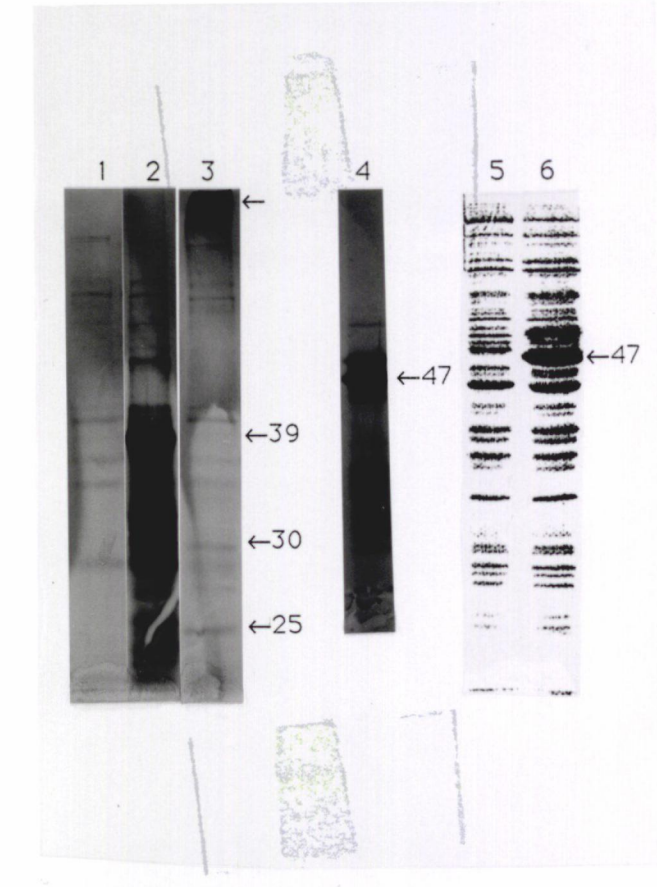

Fig. 4-1. SDS PAGE of *hmc* operon components overexpressed in *E. coli*. The labeled proteins were expressed from plasmids pT7-7 (lane 1), pTORF2 (lane 2), pTORF3 (lane 3) and pTORF6 (lane 4). The stained proteins were expressed from plasmids pT7-7 (lane 5) and pTORF6 (lane 6). Note that lanes 1,2,3, lane 4 and lane 5 originate from three different polyacrylamide gels which accounts for the scale differences. Molecular weights of proteins are indicated in kDa.

4.1.3 Overexpression of Orf6

The expected size of the fusion protein expressed by *E. coli* TG2 (pTORF6) transformants upon induction is 47 kDa. A band running at 47 kDa could be seen to be highly overexpressed in the whole cell samples run on SDS PAGE. The protein could be visualized by staining of the SDS polyacrylamide gel as well as by autoradiography of translabeled cells (Figure 4-1, lanes 4 & 6). The origin of the slightly higher molecular weight band above the expected fusion protein was unknown.

4.2 Anti-Orf6 antiserum generation

As described above, the bacteriophage T7 expression system yielded a high level of overexpression of Orf6 fusion protein. This expression level was suitable for the development of anti-Orf6 antiserum. Using the method of Winston et al. (1990), *E. coli* TG2 (pTORF6) transformants were used to generate mouse polyclonal antiserum.

4.2.1 Western blot analysis of Orf6

The development of an anti-Orf6 antibody titre in the injected mice was monitored through Western blot analysis. There was an increase in anti-Orf6 antibody titre generated in one of the two mice injected with the Orf6 suspension prepared from SDS polyacrylamide gel. The preimmune serum obtained from the mouse before immunization showed no immunoreactivity towards *E. coli* TG2 (pTORF6) whole cell samples (Figure 4-2, Blot 1, lane 2). Using the same whole cell sample, a distinct band corresponding to the 47 kDa Orf6 fusion protein became apparent upon incubation of the blot with mouse serum extracted 19 days after the first immunization (Figure 4-2, Blot 2, lane 2). A booster inoculation and 7 days wait caused the anti-Orf6 titre to reach a high level (Figure 4-2, Blot 3, lane 2). At this time the mouse was bled out to harvest the serum. *E. coli* TG2 (pT7-7) crude cell extracts were not found to be immunoreactive at any time (Figure 4-2, lane 1).

The ability of the anti-Orf6 serum to detect native Orf6 was tested. The antiserum was incubated with Western blots of *D. vulgaris* Hildenborough

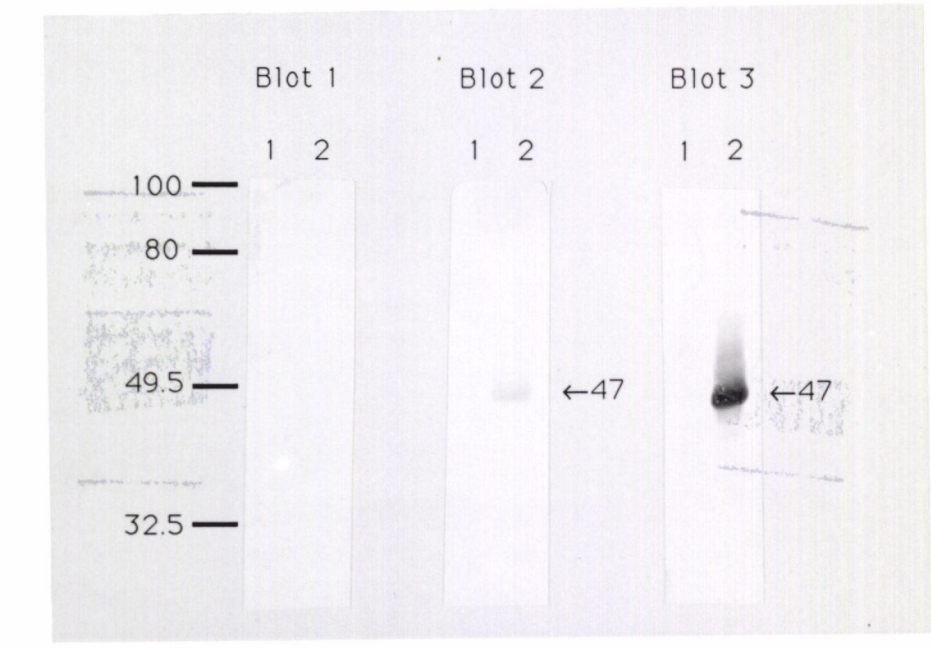

Fig. 4-2. Western blot analysis of mouse anti-Orf6 antibody titre. The plasmids expressed in each blot are pT7-7 (lane 1) and pTORF6 (lane 2). Blots were incubated with preimmune serum (Blot 1), first immunization serum (Blot 2) and boosted immunization serum (Blot 3). Molecular weights are in kDa.

whole cells and membrane and soluble fractions. The native Orf6 was immunoreactive and ran at 53 kDa as expected (Figure 4-3) in both the whole cell and membrane fraction. The soluble fraction showed very little immunoreactivity suggesting that Orf6 is membrane-bound as hypothesized previously (Rossi *et al.*, 1993). A hydropathy plot of Orf6 fails, however, to reveal precisely where a membrane associated region could be found within the protein sequence since there are a few regions with moderate, but none with extreme, hydrophobicity (Figure 4-4).

The anti-Orf6 serum was tested with respect to its detection of Orf6 expressed in the transconjugant *D. desulfuricans* G200 (pJRMR+) (which should express the entire *hmc* operon of *D. vulgaris* Hildenborough) and in *D. desulfuricans* G200 (pJRMR-) which lacks the putative *hmc* promoter so should not express any of the operon (Rossi *et al.*, 1993). Whole cell, membrane and soluble fractions were blotted and the results are shown in Figure 4-5. Once again, Orf6 was found to be membrane-associated yielding bands for the whole cell and membrane fractions of the pJRMR+ transconjugant only. The transconjugant containing pJRMR-, which lacks the 0.4 kbp upstream of *hmc*, gave only a very faint band in the whole cell sample suggesting that this upstream region is important for *hmc* operon expression.

4.3 Orf2 -alkaline phosphatase fusions

4.3.1 Expression of *orf2-phoA* fusions in *E. coli*

The fusion plasmids pNMB, pNMP, pNSB and pCSP were transformed into *E. coli* DBH4 and whole cell samples were analyzed for Orf2-PhoA fusion proteins by Western blotting (Figure 4-6). *E. coli* DBH4 transformed with plasmid pRKPhoA served as a negative control for expression and pΦDP2 transformants served as a positive control since they had been shown to express a 65 kDa protein as expected (Deckers & Voordouw, 1993). The observed sizes of the Orf2-PhoA fusion proteins corresponding to each fusion plasmid are listed in Table 4-1. The Western blot of the various induced transformants showed that all of the expected size fusions were present in the cells and, despite the presence of a high background, each fusion represented

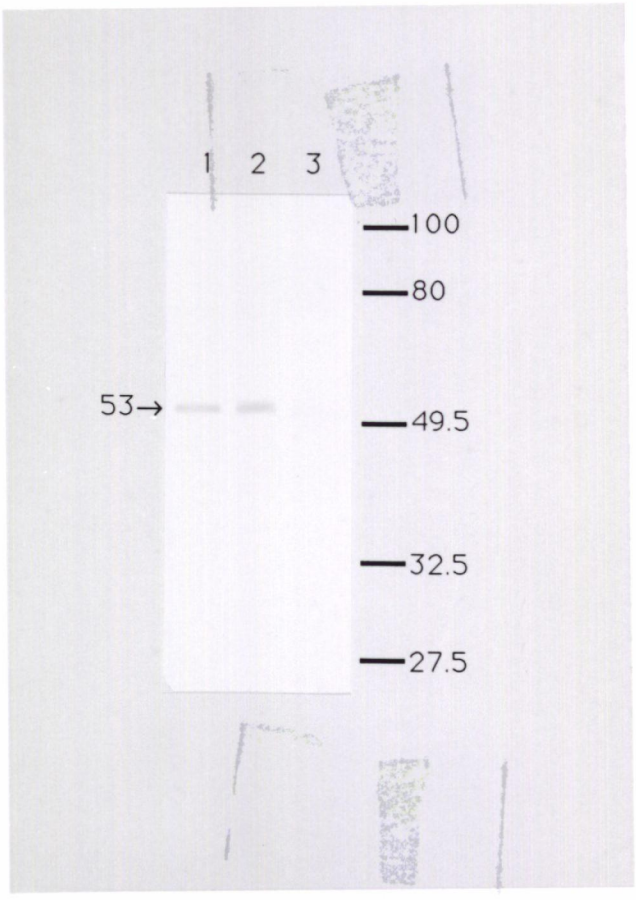

Fig. 4-3. Detection of native Orf6 in *D. vulgaris* Hildenborough. Lane 1) whole cell extracts; lane 2) membrane fraction; lane 3) cell soluble fraction. Molecular weights are in kDa.

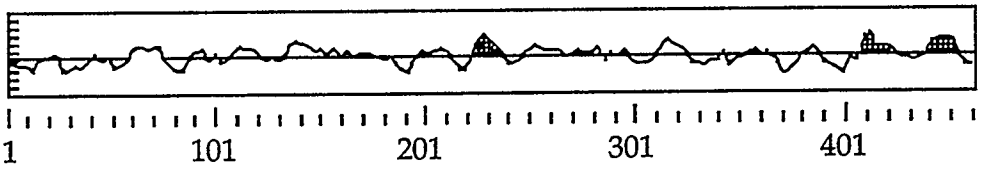

Fig. 4-4. Orf6 hydropathy plot. Regions which might span the membrane have been shaded. The axes of the plot are described in Figure 1-3. The scale is in amino acid residue units.

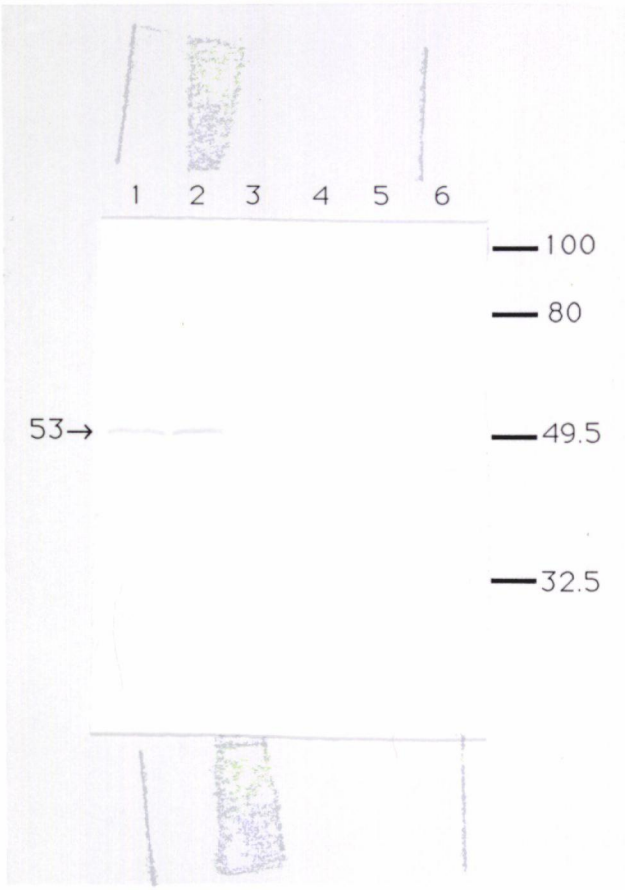

Fig. 4-5. Comparison of pJRMR+ and pJRMR- transconjugants. The lanes represent G200 (pJRMR+) whole cell (lane 1), membrane (lane 2), soluble fraction (lane 3), and G200 (pJRMR-) whole cell (lane 4), membrane (lane 5), soluble fraction (lane 6). Molecular weights are in kDa.

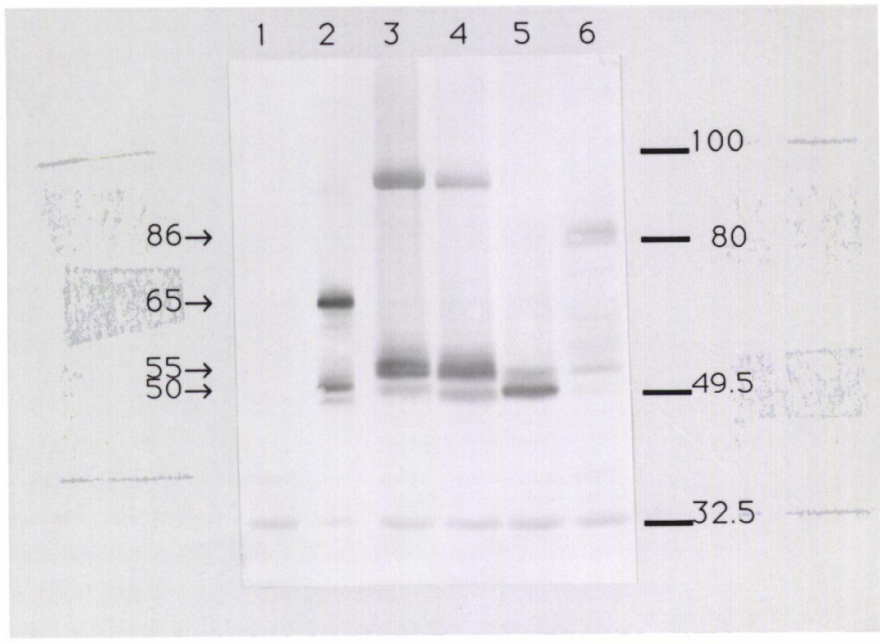

Fig. 4-6. Western blot of Orf2-PhoA fusion proteins. The blot was incubated with anti-PhoA antibodies. The fusion plasmids shown expressed by *E. coli* DBH4 are pRKPhoA (lane 1), pΦDP2 (lane 2), pNMB (lane 3), pNMP (lane 4), pNSB (lane 5) and pCSP (lane 6). Molecular weights are in kDa.

Table 4-1. Sizes and relative expression levels of Orf2-PhoA fusion proteins.

Fusion Plasmid Expressed	Expected Size (kDa)	Observed Size (kDa)	Relative Expression
pRKPhoA	None	None	N/A
pΦDP2	60.0	63	N/A
pNMB	55.1	52	100%
pNMP	55.0	52	96%
pNSB	49.7	47	52%
pCSP	85.5	84	21%

the principal immunoreactive species within the sample (Figure 4-6). The differences in expression of the various fusions was accounted for by normalizing their levels to that produced by pNMB which was given a value of 100% (Table 4-1). The pCSP transformants expressed significantly less fusion protein than those expressing N-terminal fusions suggesting that its C-terminal fusion was degraded rapidly within the cell. The high molecular weight bands in Figure 4-6, lanes 3 and 4 were not included in expression level determinations since their origin was unknown. Plasmid pRKPhoA expressed no immunoreactive protein as expected due to the absence of a ribosome-binding site immediately upstream of the *phoA* gene.

4.3.2 Alkaline phosphatase activities of fusions

Active alkaline phosphatase could be tested for in *orf2-phoA* fusion plasmid transformants plated with IPTG and BCIP (Figure 4-7). The only colonies not producing a blue pigment contained pCSP or the negative control plasmid pRKPhoA. This suggested that these transformants fail to express active alkaline phosphatase.

The alkaline phosphatase activities which resulted from each *orf2-phoA* fusion plasmid, both in the presence and absence of IPTG, in *E. coli* DBH4 are shown in Table 4-2 and Figure 4-8. Activities were first determined

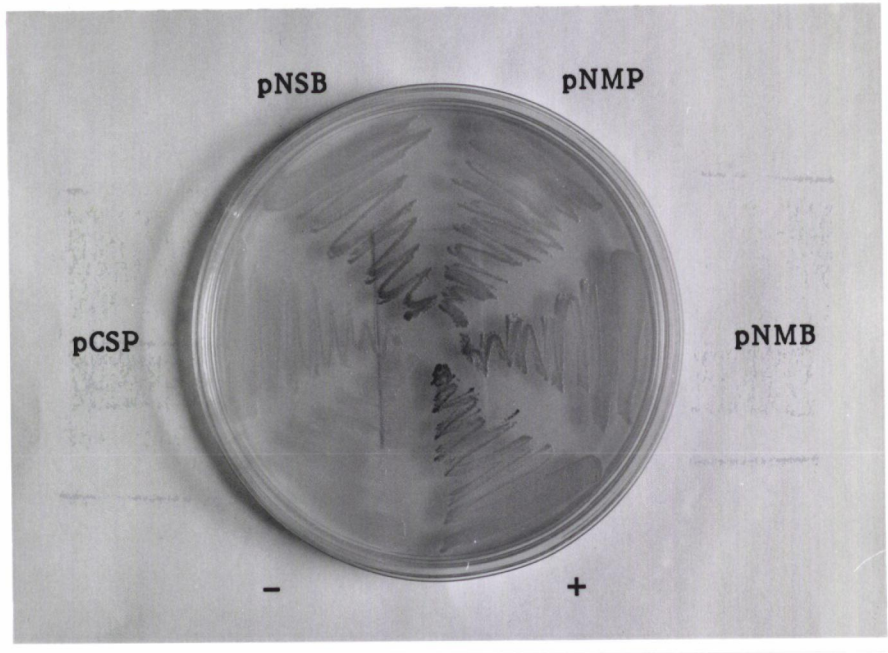

Fig. 4-7. Plate indicating which fusion plasmid transformants express active alkaline phosphatase. Colonies are *E. coli* DBH4 transformants plated on a TY-plate containing IPTG and BCIP. The "-" refers to plasmid pRKPhoA and "+" refers to plasmid pΦDP2.

Table 4-2. Alkaline phosphatase (AP) activities of cultures expressing *orf2-phoA* fusions.

Plasmid expressed	AP activity (Units/A_{600}) Uninduced	Induced with IPTG
pRKPhoA	0.60	1.1 ± 0.17
pNMB	10	900 ± 132
pNMP	6.6	620 ± 103
pNSB	15	930 ± 150
pCSP	0.78	49 ± 8.1

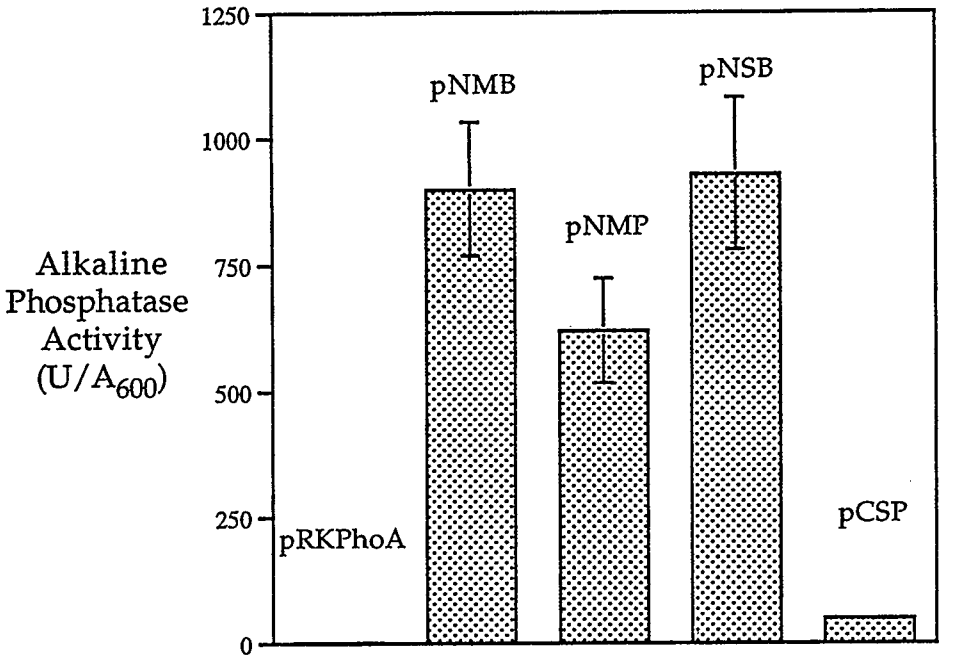

Fig. 4-8. Column graph of Orf2-PhoA fusion alkaline phosphatase activities after induction with IPTG. Error bars indicate the maximum discrepancy encountered over a minimum of five readings.

for transformed cultures in the absence of the Plac inducer, IPTG, and were found to possess universally low expression never exceeding 15 Units/A_{600} (Table 4-2). This indicated that expression of active enzyme was controlled by the *lac* promoter. The induced activities resulting from expression of the N-terminal fusion plasmids which link *phoA* to *orf2* upstream of its transmembrane region were substantially higher than the C-terminal fusion which joined *phoA* to *orf2* downstream of this region (Figure 3-2B). This suggested that these N-terminal fusions export PhoA to the periplasmic space where it is enzymatically active. Consequently, the N-terminus and bulk of Orf2 must be located in the periplasmic space while the C-terminus is cytoplasmic. Plasmid pNSB, which only fuses the signal peptide region of Orf2 to alkaline phosphatase, resulted in the highest enzyme activity (although only slightly higher than pNMB), suggesting further that this region does in fact function as a signal sequence. The activity observed for pNMP transformants was *ca.* 35% lower than that of the other two N-terminal fusion cultures due perhaps to the introduction of an Arg-Ile-Arg sequence at the junction of Orf2 and PhoA encoded by this plasmid. These two extra positive charges may have hindered protein export slightly by adherence to the 'positive inside' rule (von Heijne, 1992).

The activity level for the C-terminal fusion was higher than that of the negative control culture, but both possessed values which were very low in comparison to the N-terminal fusions. For reasons described by Derman & Beckwith (1995), these activity values were not zero and could be seen to rise very slowly over the course of several hours due to slow folding of alkaline phosphatase into its native conformation during cell stasis.

4.4 *hmc* operon expression

4.4.1 Western blot analysis of operon expression levels during growth on different electron donors

D. vulgaris Hildenborough was grown on media differing in electron-donating substrate and the expression levels of the *hmc* operon were monitored through Western blot analysis of Hmc and Orf6 using specific polyclonal sera. The bacteria were cultured using lactate, pyruvate or formate

as electron donor and carbon source both in the presence and absence of 5% (v/v) hydrogen. They were also cultured in a chemolithotrophic growth medium using 5% hydrogen as electron donor and acetate as carbon source. Western blots comparing protein expression resulting from growth with these different substrates are shown in Figure 4-9. As determined by the immunoreactive band intensities, the Hmc expression levels relative to chemolithotrophic growth did not differ from those obtained for Orf6 by more than 16%. This suggests that both proteins are influenced equally by substrate changes. For each of the three blots shown in Figure 4-9, the band intensity for each lane was compared to its neighboring lane(s) on a particular blot as described in section 3.2.8. Bands could not be compared between separate blots directly since varying development times yielded differences in band intensity from blot to blot. However, if a given sample was present on more than one blot, then the expression level for that sample could act as a numerical bridge allowing comparison of two blots to give expression levels relative to chemolithotrophic growth on hydrogen as sole electron donor for which expression was the highest (100%). The resulting relative expression levels are listed in Table 4-3.

Growth on lactate/hydrogen and pyruvate/hydrogen gave similar *hmc* operon expression levels which were 58% of that observed during chemolithotrophic growth. The absence of hydrogen lowered expression levels even further in lactate and pyruvate media where values became 37% and 27% of that of growth on hydrogen, respectively. These results demonstrate that *hmc* operon components are present in detectable quantities within the cell during growth on hydrogen, lactate or pyruvate. The level of operon expression is positively dependent on the presence of hydrogen with chemolithotrophic growth yielding the highest level.

The bacteria were unable to grow in the minimal media which used formate as electron donor and carbon source in the absence of hydrogen. Also, the bacteria were unable to grow in a negative control medium of acetate/nitrogen supporting the observation that *D. vulgaris* is an incomplete oxidizer, meaning that it cannot use acetate as an electron donor for sulfate reduction (Postgate, 1984).

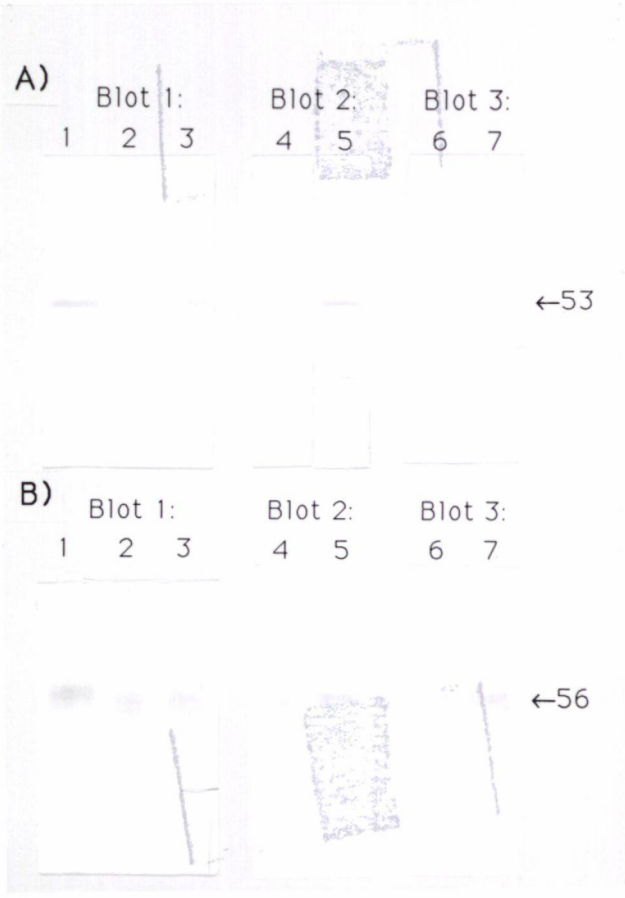

Fig. 4-9. Western blot analysis of *hmc* operon during growth with different electron donors. **A)** Incubated with anti-Orf6 serum; **B)** incubated with anti-Hmc serum. Each lane represents *D. vulgaris* Hildenborough grown in minimal media with different electron donors. Lane 1) hydrogen; lanes 2 & 5) lactate/hydrogen; lanes 3 & 7) pyruvate/hydrogen; lane 4) lactate; lane 6) pyruvate. Molecular weights are in kDa.

Table 4-3. Relative *hmc* operon expression levels.

Electron Donor	Expression Level Relative to Hydrogen: Hmc	Orf6	Avg.
hydrogen	100%	100%	100%
lactate/hydrogen	50%	66%	58%
pyruvate/hydrogen	50%	66%	58%
lactate	33%	40%	37%
pyruvate	25%	29%	27%

4.5 Analysis of a potential helix-turn-helix motif in Rrf2

A 22 amino acid region of Rrf2 was subjected to the weight matrix developed by Dodd & Egan (1990) and the results of this are shown in Table 4-4. The total score awarded for this section of Rrf2 was 1446. This total score was substituted into the following formula to obtain a standard deviation (SD) score (Dodd & Egan, 1990):

$$\text{SD score} = \frac{(\text{total score} - 238.71)}{293.61}$$

The resulting SD score of 4.1 was obtained for Rrf2. A list of SD scores obtained for a set of known proteins was found in Dodd & Egan (1990) and these values corresponded to the percentage likelihood of helix-turn-helix formation. The score of 4.1 corresponded to a greater than 90% probability that this region of Rrf2 forms a helix-turn-helix DNA-binding motif (*ibid*).

Table 4-4. Helix-turn-helix weight matrix scores of Rrf2.

Motif position	-2	-1	1	2	3	4	5	6	7	8	9	10	11	12	13	14
Sequence	V	S	I	K	D	I	A	Q	R	Q	G	I	S	V	K	Y
Score	17	96	101	70	109	116	238	90	76	-131	202	128	174	-16	-100	-40

Motif position	15	16	17	18	19	20	
Sequence	L	E	K	L	I	R	Total score = 1446
Score	97	-101	38	37	122	123	

4.6 Generation of an *rrf1,2*-deficient strain of *D. vulgaris* Hildenborough

4.6.1 Southern blot analysis of the gene deletion procedure

The steps towards the generation of the mutant *D. vulgaris* Hildenborough strain RK100 were monitored closely with Southern blot analysis of total chromosomal DNA to find out at which point the selection procedures (growth on Cm and/or growth on sucrose) pressured some fraction of the bacterial population to undergo recombination and mutate.

The initial conjugation of the plasmid pΔRRF and purification of Cm^r colonies led to integrants whose DNA was Southern blotted to verify that the plasmid had integrated into their chromosome by probing undigested total DNA with radiolabeled *cat* (Cm^r) gene (Figure 4-10). The frequency of integration was determined to be 1 integrant/ 1.4 x 10^6 cells. All of the seven purified cultures selected on Cm plates were found to be integrants. Hybridization with the *cat* probe and the difference between the size of this hybridization and that of the undigested plasmid pΔRRF (Figure 4-10, lane 9) indicated plasmid integration as opposed to mere propagation of the plasmid

within the cell. Propagation should not occur due to the lack of a *D. vulgaris*-useable plasmid origin of replication.

The next step was to investigate the nature of these integrants (*ie.* whether the integration occurred upstream or downstream of the *rrf* genes; Figure 3-3) by probing digested DNA with radiolabeled fragments. The chromosomal DNA was digested with *Eco*RI and probed with either a 4.4 kbp *Eco*RI fragment generated from pΔRRF downstream of *rrf2* (Figure 4-11A) or a 1.7 kbp *Eco*RI fragment from pΔRRF upstream of *rrf1* (Figure 4-11B). The probes contained both chromosomal DNA as well as vector DNA sequence. The resulting Southern blots revealed the presence of two types of integrant. One of these, called Type-I and occurring with about 43% frequency, corresponded well with RK1 as it is described in Figure 3-3 by displaying the retention of the 4.4 kbp downstream *Eco*RI region but having the 1.7 kbp upstream fragment increase to 7.2 kbp due to an integration event within that region (Figure 4-11, lane 1). The other integrant, Type-II, comprised the rest of the integration population but could not be described from its hybridization patterns. Both the upstream and downstream probes hybridized to Type-II DNA but not in the pattern expected of RK2 integrants (Figure 3-3). The DNA of this strain was probed with numerous probes (of which only two are shown) but all hybridizations were to the same 11.0 kbp fragment and so the nature of Type-II was never determined (Figure 4-11, lane 2). The expected wild type chromosomal regions hybridized to the probes in all lanes shown in this figure. Sucrose-selection went ahead using the RK1 strain.

Several rounds of culturing and colony purification in the presence of 5-7% sucrose were required before a noticeable fraction of integrant cells underwent a second recombination event to become the mutant strain RK100. Colony-purified RK1 was initially plated on Postgate medium E plates with Cm (10 μg/mL) and 5% sucrose (w/v). Single colonies were picked and cultured in Postgate medium C/Cm before preparing total DNA. The DNA was digested with *Hin*dIII and probed with a radiolabeled 1.3 kbp *Hin*dIII fragment generated from the region downstream of *rrf2* in pΔRRF. This probe would give different hybridization patterns for *D. vulgaris* Hildenborough wild type, strain RK1 and strain RK100 DNA. All samples examined in this round of sucrose selection were found to be RK1, however,

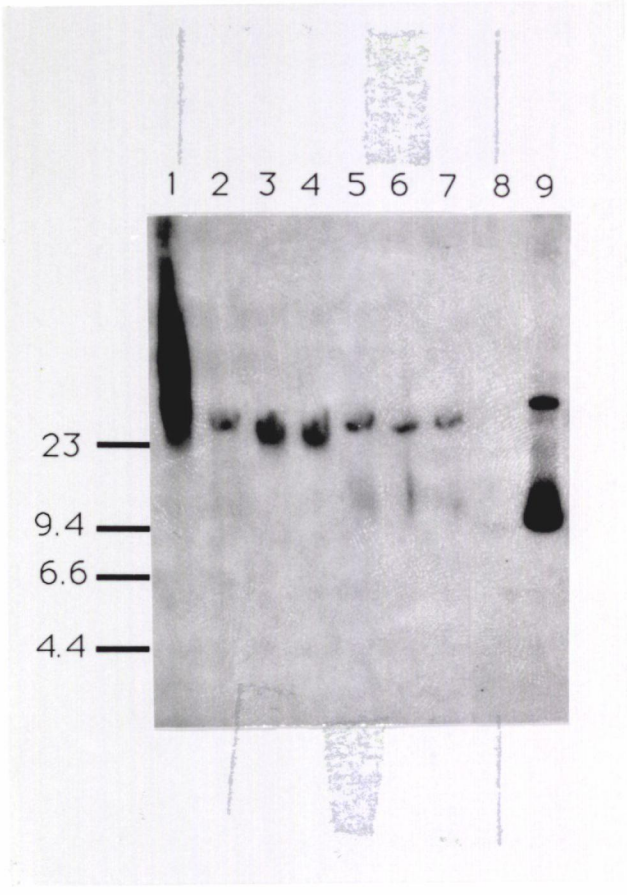

Fig. 4-10. Southern blot verifying integration of plasmid pΔRRF into the *D. vulgaris* Hildenborough chromosome. The blot was probed with the gene for Cm^r. Lanes 1-7) Integrants; lane 8) Wild type bacteria; lane 9) Undigested plasmid pΔRRF. Markers are in kbp.

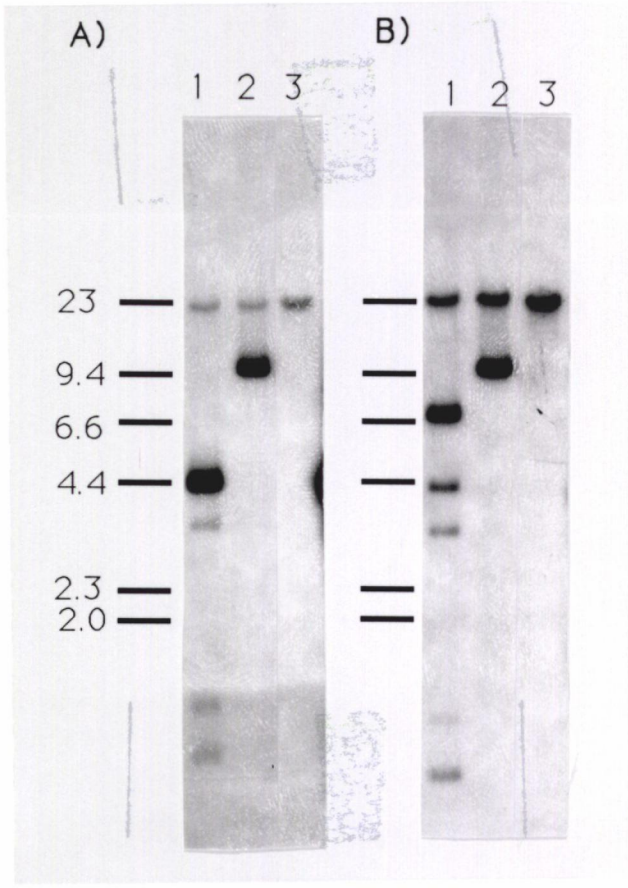

Fig. 4-11. Southern blot indicating the presence of two types of integrant. **A**) Probed with 4.4 kbp downstream fragment. **B**) Probed with 1.7 kbp upstream fragment. The *Eco*RI-digested DNA belong to integrant Type I (lane 1), integrant Type II (lane 2) and wild type *D. vulgaris* Hildenborough (lane 3). Note that the presence of extra bands in lane 1 is due to impurities present in the probe. Markers are in kbp.

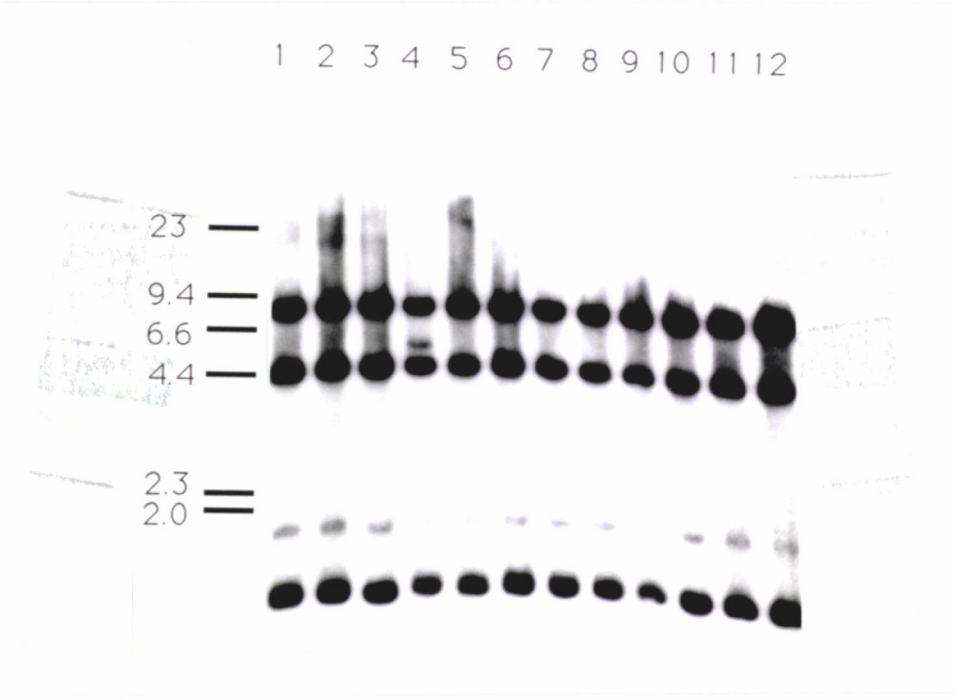

Fig. 4-12. Southern blot including RK1-RK100 mixture. Lane 1) RK1 control DNA; lanes 2-12) DNA tested for the presence of a second recombination. Lane 4) RK1-RK100 mixture can be detected by the presence of a 5.5 kbp band. All DNA was digested with *Hin*dIII. Markers are in kbp.

one of the samples contained a stronger hybridization pattern for digestion fragments corresponding to the *sacB* and *cat* genes of the vector insert (data not shown). The reason for this slight difference in hybridization pattern was unknown but the culture from which this DNA had been prepared was treated separately from RK1 and denoted RK13. Cultures of both RK1 and RK13 were used to inoculate Postgate C/Cm/7% sucrose cultures which were grown at 35°C for nine days then at room temperature for 2 days before plating on Postgate E/Cm/5% sucrose to get single colonies. Twenty colonies from each plate were cultured separately in Postgate C/Cm/7% sucrose and their DNA was prepared and blotted. One of the RK13 cultures gave a 5.5 kbp band which represented RK100 seen in a mixture with RK1 (Figure 4-12, lane 4). This culture was plated and single colonies were purified. The Southern blot of DNA prepared from these pure cultures is shown in Figure 4-13. Lanes 2 and 4 in this figure indicate purified deletion mutant RK100 cultures. In total, 35% of blotted DNA samples were found to originate from purified RK100.

Once the purified mutant strain was generated, its DNA was probed with a radiolabeled 0.4 kbp *Pvu*II fragment obtained from plasmid pJH5304 and lying within the region deleted from genes *rrf1,2* (Figure 4-14). The absence of a band in lane 3 of this figure indicates the deletion of the region containing this fragment.

4.6.2 Growth rates of wild type and mutant *D. vulgaris* Hildenborough

Both mutant and wild type strains of *D. vulgaris* Hildenborough were grown on minimal media with either lactate/hydrogen, lactate, pyruvate/hydrogen, pyruvate or hydrogen serving as electron donors. The substrate/hydrogen mixtures were grown in the anaerobic chamber in free exchange with the 5% hydrogen atmosphere using sponge plugs. Cultures lacking hydrogen were grown in nitrogen-flushed bottles. Three test cultures were grown in each medium for each strain and the cell densities were monitored over time. The growth profiles plotted in Figures 4-15, 4-16, 4-17 and 4-18 display the resulting averaged patterns. Due to the buildup of H_2S, growth in nitrogen bottles resulted in the formation of FeS precipitate which interfered with cell density measurements. In the case of the lactate and

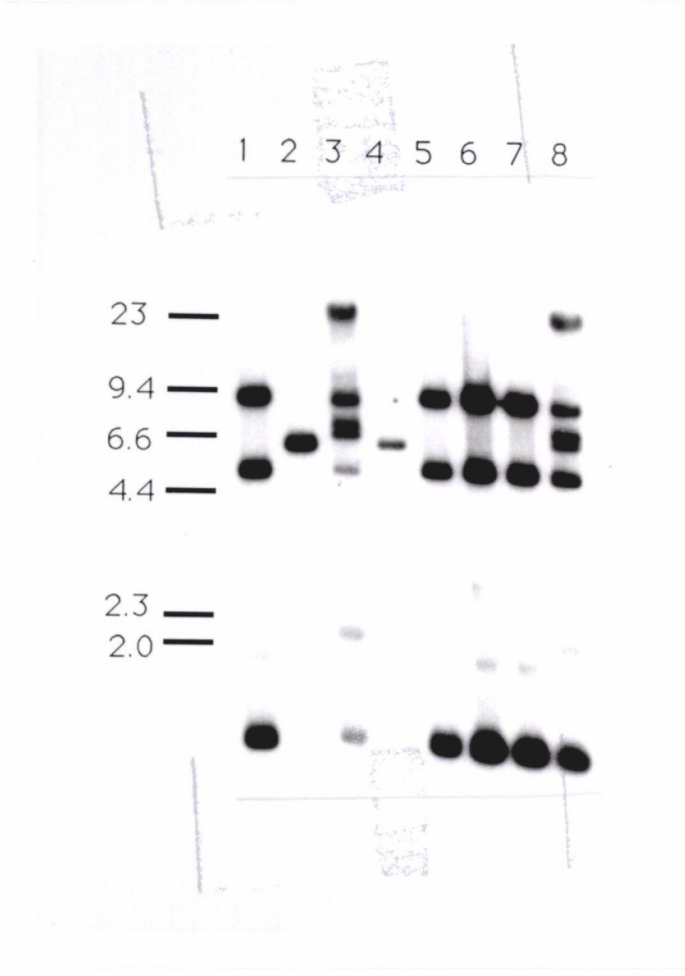

Fig. 4-13. Southern blot showing purified RK100. Lane 1) RK1 DNA control; lanes 2 & 4) RK100 mutants; lanes 3, 5-8) Test cultures containing only RK1. Note that lanes 3 & 8 contain incomplete digestions. All DNA was digested with *Hin*dIII. Markers are in kbp.

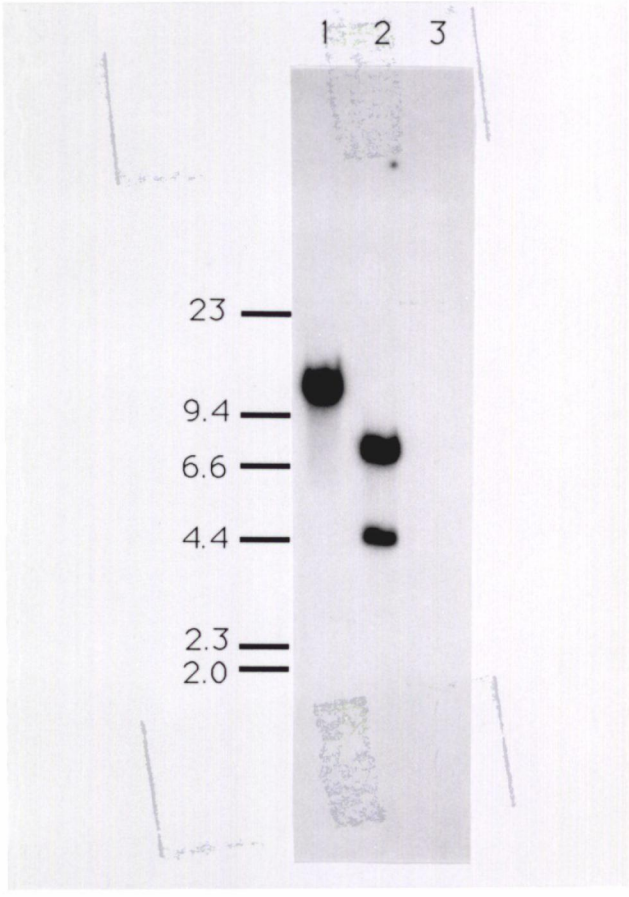

Fig. 4-14. Southern blot indicating deletion of *rrf1,2*. Lane 1) wild type; lane 2) RK1; lane 3) RK100. All DNA was digested with *Hin*dIII. Markers are in kbp.

pyruvate cultures, the growth curves were plotted only up to the point where a visible precipitate formed. This was usually after mid-log phase so that information obtained was still useful.

Growth of *D. vulgaris* Hildenborough on lactate resulted in a noticeable difference in the patterns observed for the wild type and mutant strains (Figure 4-15). Whether grown in the presence or absence of hydrogen, the wild type strain grew significantly faster on lactate than the mutant RK100 suggesting that the deletion of *rrf1,2* interferes with lactate metabolism in some way. The presence of 5% hydrogen also appears to hinder lactate utilization since it resulted in slower growth of both strains when compared to nitrogen cultures. Hydrogen led to a dramatic decrease in the RK100 rate of growth on lactate. For wild type bacteria, the time taken to get to the same point in mid-log phase increased from 28 h to 37 h and for the mutant the same change was from 46 h to 85 h. While rates were affected, cell saturation densities were quite similar for both strains of bacteria.

As described in the methods section 3.2.7, all cultures were started in Postgate medium C before sub-culturing in minimal lactate medium twice and then beginning the test cultures. Postgate medium C is a rich medium which uses lactate as electron donor substrate and contains yeast extract. The growth rates of *D. vulgaris* wild type and mutant RK100 were observed to be similar during growth on Postgate medium C plus 5% hydrogen possessing mid-log phase times of 18 and 24 h, respectively (Figure 4-16). It is interesting to note that with each successive dilution of yeast extract during sub-culturing, the growth rate of RK100 dropped relative to the wild type despite the fact that the same amount of cells was used for each inoculation (data not shown). These results suggest that RK100 is handicapped with respect to its growth on lactate but that this can be overcome if yeast extract is present.

Growth of the two strains on minimal medium with hydrogen as electron donor also resulted in marked differences in growth rates (Figure 4-17). Growth of the bacteria was quite sluggish when using hydrogen as sole electron donor most likely due to its low partial pressure within the anaerobic chamber. RK100 grew much faster on hydrogen than the wild type strain reaching mid-log phase in 145 h compared to the 241 h taken for the wild type. Thus, the mutant strain appears to be improved with regards to its

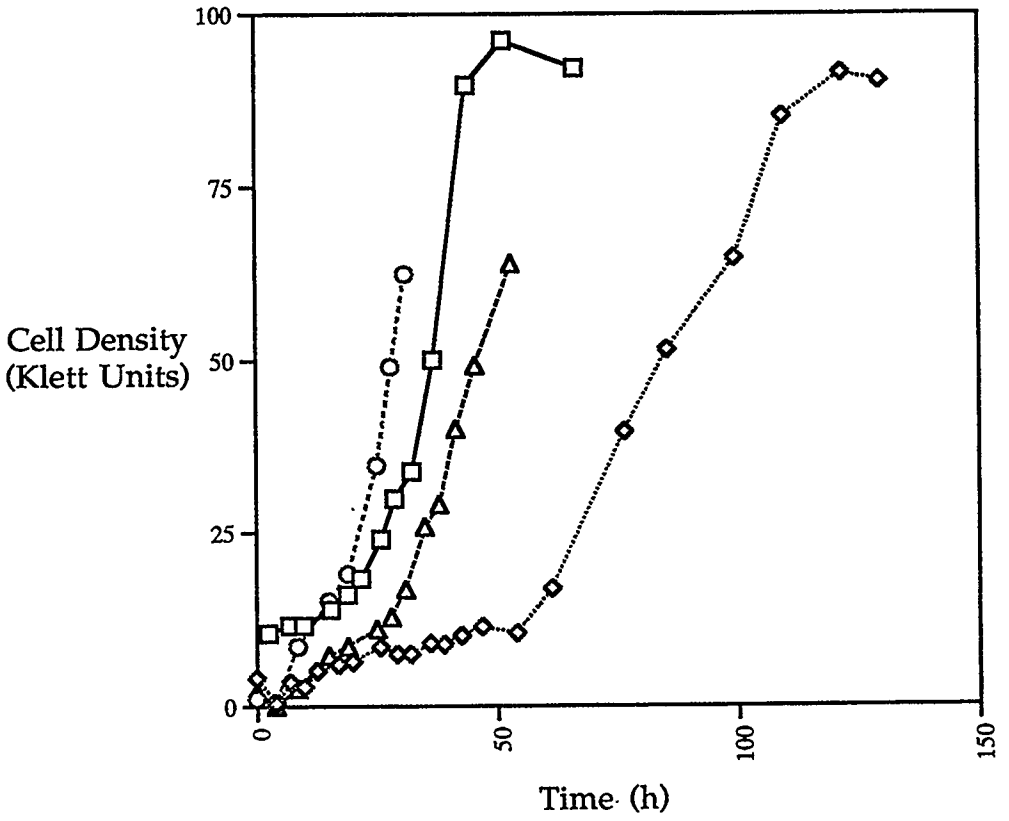

Fig. 4-15. Growth curves of *D. vulgaris* Hildenborough strains in minimal media where either lactate (----○---- wild type; ----△---- RK100) or lactate/hydrogen (—□— wild type; ·····◇····· RK100) was used as electron donor. Values represent averages of five data sets with ±8% error maximally.

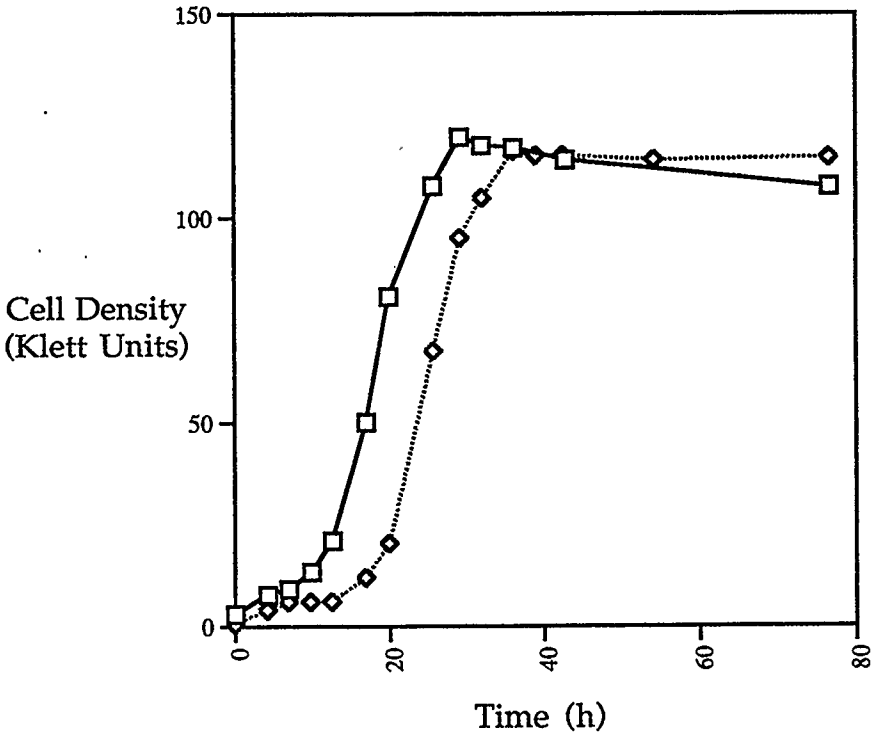

Fig. 4-16. Growth curves of *D. vulgaris* Hildenborough strains in Postgate medium C. —□— wild type; ·····◇····· RK100. Values represent averages from five data sets with ±7% error maximally.

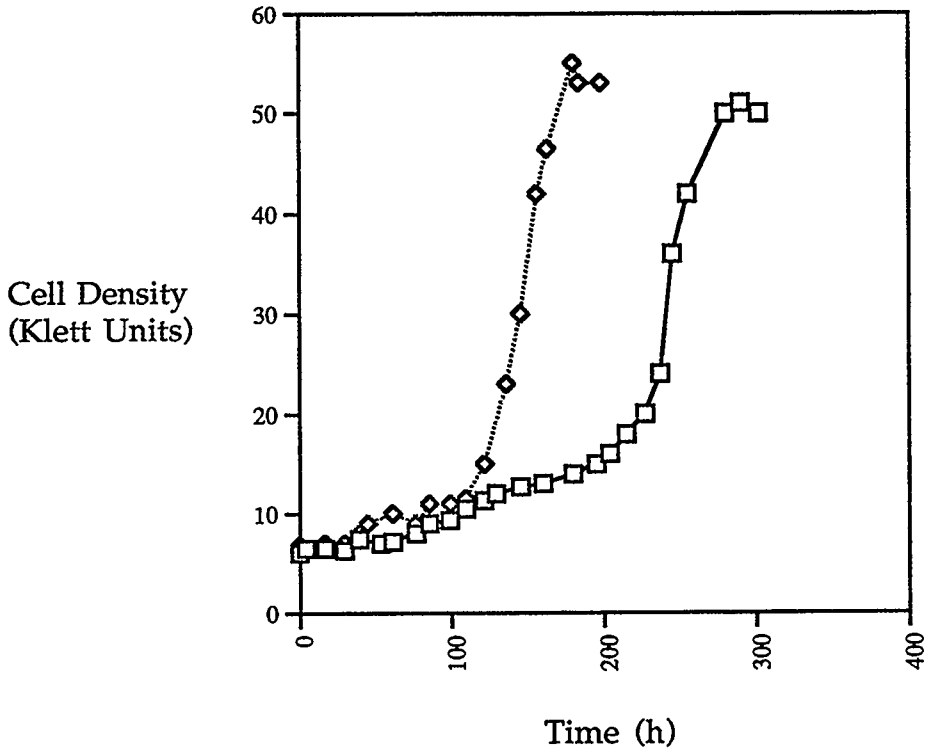

Fig. 4-17. Growth curves of *D. vulgaris* Hildenborough strains in minimal media where hydrogen was used as electron donor. —□— wild type; ·····◇····· RK100. Values represent averages from five data sets with ±8% error maximally.

adaptation to the usage of this substrate as an electron source. Again, final cell densities were similar for both strains.

Compared to growth of the different strains of *D. vulgaris* on lactate and hydrogen, growth on pyruvate as principal (or sole) electron donor differed much less (Figure 4-18). The growth rates of wild type and RK100 cells using pyruvate in nitrogen-flushed bottles were almost identical throughout the portion of the curve that was reliable (when the cultures were free of FeS precipitate). The wild type strain reached mid-log phase in 22 h compared to RK100 which reached the same point in 20 h. These rates were slightly faster than those seen for both strains in pyruvate plus 5% hydrogen. In this medium, *D. vulgaris* wild type cells reached mid-log phase in 28 h while it took RK100 37 h. As was seen with growth on lactate, the presence of hydrogen in the atmosphere had a negative influence on the growth rates of both strains on pyruvate, more notably RK100. Once again, cell saturation densities were similar for both strains having values about halfway between those observed for growth on lactate and growth on hydrogen.

4.6.3 Western blot analysis of operon expression levels after deletion of genes *rrf1,2*

Western blots using Hmc- and Orf6-specific antibodies were employed as described above in the comparison of *hmc* operon expression levels present in *D. vulgaris* Hildenborough wild type and RK100 strains. The blots are shown in Figure 4-19 and the normalized levels of relative expression in Table 4-5. The Hmc blot gave relative results which were similar to those of Orf6 differing maximally by only 12% between the two data sets. Growth of the two strains on hydrogen, lactate/hydrogen and pyruvate/hydrogen as electron donors were compared.

The general trend exhibited by the expression level comparison was that the RK100 mutant possessed higher *hmc* operon expression levels than the wild type. As seen in Table 4-5, growth of the bacteria on lactate/hydrogen resulted in RK100 expressing an average 2.0x more Hmc/Orf6 than the wild type. Growth on pyruvate/hydrogen gave 1.9x higher levels in RK100 than wild type and chemolithotrophic growth gave 2.5x higher levels in RK100. Thus, an average 2.1-fold increase in *hmc* operon expression levels are seen

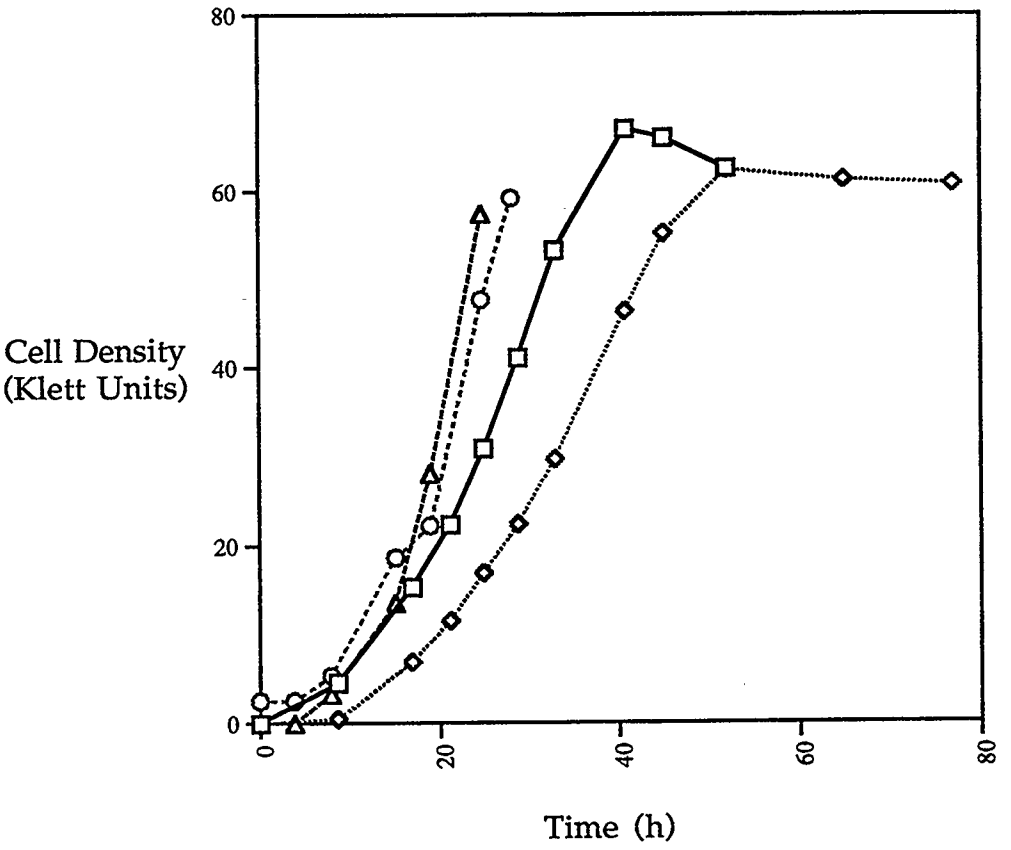

Fig. 4-18. Growth curves of *D. vulgaris* Hildenborough strains in minimal media where either pyruvate (----o---- wild type; ----Δ---- RK100) or pyruvate/hydrogen (—□— wild type; ·····◇····· RK100) was used as electron donor. Values represent averages from five data sets with ±8% error maximally.

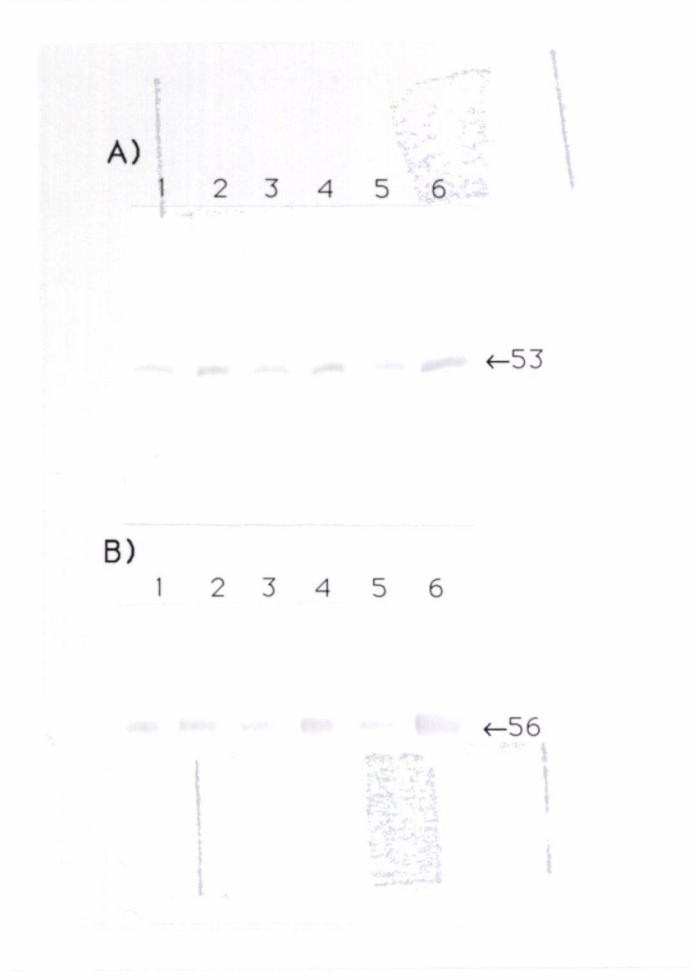

Fig. 4-19. Western blot analyses of *hmc* operon in *D. vulgaris* Hildenborough wild type and mutant strains. **A)** Incubated with anti-Orf6 serum; **B)** incubated with anti-Hmc serum. Lanes represent wild type grown on: lane 1) lactate/hydrogen; lane 3) pyruvate/hydrogen; lane 5) hydrogen as electron donors, and RK100 grown on: lane 2) lactate/hydrogen; lane 4) pyruvate/hydrogen; lane 6) hydrogen as electron donors. Molecular weights are in kDa.

Table 4-5. Normalized *hmc* operon levels comparing wild type and mutant strains.

Lane	Strain	Electron Donor	Expression Level Relative to RK100 on Hydrogen:		
			Hmc	Orf6	Avg.
1	wild type	lactate/hydrogen	31%	32%	32%
2	RK100	lactate/hydrogen	59%	71%	65%
3	wild type	pyruvate/hydrogen	31%	32%	32%
4	RK100	pyruvate/hydrogen	56%	65%	61%
5	wild type	hydrogen	41%	39%	40%
6	RK100	hydrogen	100%	100%	100%

in the mutant strain RK100 suggesting that the products of the genes *rrf1,2* play some role in repressing *hmc* operon expression.

It was also observed in these blots that the expression level of the wild type on hydrogen was lower relative to growth on lactate/hydrogen and pyruvate/hydrogen than what was seen previously (1.3x instead of the previous 1.7x; Figure 4-9, Table 4-3). This may have been due to a difference in the allowed growth time of the bacteria on hydrogen. For this blot, the wild type was harvested slightly prior to mid-log phase growth and this may have had an effect on the level of *hmc* operon expression. Perhaps the level rises to some maximal point during growth on hydrogen as the bacteria adapt to this substrate.

5. Discussion

5.1 Overexpression of Orf2, Orf3 and Orf6 in *E. coli*

The sequence of the chromosomal region downstream of the *D. vulgaris* Hildenborough *hmc* gene implied the presence of a total of eight open reading frames closely linked into a single, or maximally two, operon(s). Several of the putative peptides encoded by the *hmc* operon were found to have significant homologies with other known proteins. This condition by itself was good evidence that the deduced open reading frames comprising the *hmc* operon encoded authentic proteins. Actual verification of the existence of the various operon components would come with their visualization upon expression.

The overexpression of Orf2, Orf3 and Orf6 in *E. coli* led to the recognition of fusion peptides corresponding to sizes very similar to those expected by sequence analysis. An overexpressed protein corresponding probably to Orf5 was also visualized (Figure 4-1, lane 3). M. Rossi (1993) has used the bacteriophage T7 system to overexpress the 15 kDa Rrf1 protein and was able to see a 15.5 kDa band after SDS PAGE of cells expressing pTRRF1NP. The *hmc* gene has been overexpressed in *D. desulfuricans* G200 giving rise to a peptide of expected size upon conjugation of these bacteria with the plasmid pBPHmc-1 (Bruschi *et al.*, 1992). In all, as many as six of the eight open reading frames of the *hmc* operon have been overexpressed in *E. coli* or *D. desulfuricans* G200 and have given rise to polypeptides very near to or identical to their expected sizes. Collectively, these results validate the assignment of open reading frames in the *hmc* operon, as suggested by the sequence.

The expression levels of the Orf2 and Orf3 fusion proteins were lower than what was expected for this system of overexpression. Orf2 may have been degraded within the cell due to the nature of its fusion. The fusion point of Orf2 to the pT7-7 vector peptide lay within the putative signal peptide of Orf2 and, as will be discussed below, this disruption would eliminate the potential for protein export and might have resulted in accelerated intracellular degradation of Orf2. As discussed above, the

expression of Orf3 may have been diminished by the extreme hydrophobicity of this protein. The aggregation of material at the top of the SDS polyacrylamide gel (Figure 4-1, lane 3) suggested the inadequate denaturation of the expressed Orf3 fusion.

The bacteriophage T7 system was successfully used to produce a high amount of Orf6 fusion protein. The expression level of Orf6 which resulted from transformation of *E. coli* TG2 with plasmid pTORF6 constituted around 10% of total cellular protein (Figure 4-1, lane 6). This high level of overexpression was ample for usage in mouse anti-Orf6 antibody development which was useful in later studies.

5.2 Cellular localization of Orf6

Sequence analysis of Orf6 has revealed that this protein carries no fewer than three regions within its primary structure which are moderately hydrophobic and approximately 20 amino acids in length, indicating their potential to form transmembrane helices (Figure 4-4). A Robson secondary structure prediction performed by computer analysis of the Orf6 sequence also indicated that the three regions outlined in Figure 4-4 had high α-helical propensities. None of these regions is associated with a signal sequence consensus of any sort but, based on the presence of these hydrophobic regions as well as the hypothesis for the functioning of the *hmc* operon, Orf6 has been modeled in the past to be membrane associated (Rossi *et al.*, 1993; Figure 1-5).

After the development of anti-Orf6 antibodies which recognized the *E. coli* (pTORF6) 47 kDa fusion protein, the obvious next step was to test if the antiserum immunoreacted with the 53 kDa native Orf6 in *D. vulgaris* Hildenborough cells. It was this Western blot analysis of whole cell, membrane and soluble fractions of *D. vulgaris* which verified the membrane association of Orf6 (Figure 4-3). The absence of any Orf6 in the cell soluble fraction suggests that this redox protein sits against the cytoplasmic side of the cell membrane (due to the lack of a signal sequence) where it could logically play a more integral role in electron transfer through the membrane than if it were free in the cytoplasm. As mentioned, Orf6 lacks a high degree of hydrophobicity in any one region of sequence so it may be that the protein is

aided in its membrane association. The integral membrane proteins, Orf3 and/or Orf4 and/or Orf5, could anchor one of these regions into the membrane so that it does not need to be highly hydrophobic. In this position, the two iron-sulfur clusters of Orf6 could accept electrons from one of the membrane proteins, possibly Orf5 with its putative heme *b* , and donate these to a cytoplasmic electron carrier protein such as flavodoxin so they could be transported to the site of sulfate reduction.

5.3 Membrane topology of Orf2

The possession of four cysteine clusters found in a strictly conserved array has given Orf2 membership into a family of homologous bacterial redox proteins (Figure 1-2). These clusters are in sequence groups very similar to those shown to ligate iron-sulfur clusters in the bacterial ferredoxins (Graves *et al.*, 1985; Bruschi & Guerlesquin, 1988). The EPR properties of DmsB, the protein with which Orf2 shares the highest degree of sequence homology, indicate that this protein contains four [4Fe-4S] clusters (Cammack & Weiner, 1990). The members of this family which have been well characterized show that these clusters are observed to reside in the cytoplasmic space of their respective bacteria where they function as electron transfer subunits usually working in conjunction with a catalytic subunit (Berg *et al.*, 1991; Böhm *et al.*, 1990; Bokranz *et al.*, 1991; Weiner *et al.*, 1992).

The existence of two hydrophobic amino acid sequences within Orf2 has contrasted it with these other proteins (Figure 1-3). One of these (residues 261 to 284) is a good candidate for forming a membrane-spanning helix. This feature, by itself, is not novel among these redox proteins since FdnH (described in section 1.3.5) also contains a putative transmembrane helix. The other hydrophobic sequence (residues 9 to 25) of Orf2, while not extremely hydrophobic, is unique among this family of redox proteins. As described in the objectives (section 2.2), Orf2 was ascribed the same membrane topology as its homologs having cytoplasmic iron-sulfur clusters and with the N-terminal hydrophobic sequence forming an amphipathic helix lying against the inside of the membrane (Rossi *et al.*, 1993; Pollock, 1992; Figure 1-5). It was the close examination of a positively charged region just ahead of the N-

terminal sequence which brought this topology into question. This region bears similarity to the unusual signal sequences of hydrogenase small subunits. The Orf2 sequence differs from the consensus: RRXFXK, possessing instead: RRRFXT, but it may be that the presence of the extra arginine residue compensates for the missing lysine. The rest of the putative signal sequence was observed to be quite homologous to others of this type (Figure 1-4). In order to more definitively determine the membrane topology of Orf2, *orf2-phoA* genetic fusions were generated.

Alkaline phosphatase gene fusions are useful molecular tools which have been quite successful in determining the membrane topology of proteins (Deckers & Voordouw, 1993; Boyd *et al.*, 1993; Weiner *et al.*, 1993; Calamia & Manoil, 1990; San Millan *et al.*, 1989; Manoil & Beckwith, 1986). *E. coli* alkaline phosphatase, PhoA, can be readily translocated when attached to an appropriate signal sequence (Roof *et al.*, 1991; Manoil & Beckwith, 1985) and is found to be almost entirely dependent upon its export out of the cytoplasmic space for active functioning (Derman & Beckwith, 1991; Michaelis *et al.*, 1983). The only exception to this has been recently discovered in cells whose growth has been suspended. Cytoplasmic PhoA activity has been observed to increase gradually in these cells due to slow folding of the cytoplasmic enzyme into its native conformation (Derman & Beckwith, 1995). PhoA fusions are also useful with regards to their high sensitivity and ease of detection using substrates such as BCIP or *p*NPP (Brickman & Beckwith, 1975).

The activities resulting from the *orf2-phoA* gene fusions expressed in *E. coli* DBH4 have demonstrated that the N-terminus of Orf2 can act as a functional signal peptide. This indicates that the bulk of the protein, including its iron-sulfur clusters, is on the periplasmic side of the membrane while the highly charged C-terminus is cytoplasmic. Thus, Orf2 possesses a unique topology among its class of redox proteins, being the only member with periplasmic clusters. As hypothesized earlier, these clusters appear to be supported by the more reducing periplasm of *D. vulgaris* Hildenborough cells, which is unlike the periplasms of most other bacteria in which Orf2-like electron transfer proteins occur. This orientation of Orf2, while different from what was proposed previously (Rossi *et al.*, 1993; Pollock, 1992), helps to define the path of electron transfer through the Hmc-transmembrane

complex. Previously, it was difficult to say whether electrons passing through the membrane components would be accepted by the iron-sulfur clusters of Orf6 or Orf2 or both proteins since each seemed to be equally available (Rossi *et al.*, 1993; Figure 1-5). With this new knowledge of the topology of Orf2, a model emerges in which electrons could be transferred from Hmc to the iron-sulfur clusters of Orf2 before passage through the membrane to the clusters of Orf6 and on to sulfate reduction. This model also suggests that Hmc itself does not need to be membrane bound to pass electrons through the membrane. Instead, it can float freely through the periplasm and dock at Orf2 to donate its electrons.

5.4 Differential expression of the *hmc* operon

The sequence of the genes of the *hmc* operon has suggested that the first six proteins encoded could form a transmembrane redox protein complex. In part, the function of this complex was postulated from the homology between Hmc and cytochrome c_3, the electron acceptor for the [NiFe] and [Fe] hydrogenases. Hmc might accept electrons from hydrogenases just like cytochrome c_3 during hydrogen oxidation. Observation of the chemolithotrophic growth of *D. vulgaris* Hildenborough (Badziong & Thauer, 1978) implied the existence of a transmembrane redox link between periplasmic hydrogen oxidation and cytoplasmic sulfate reduction. Such a link had never been characterized but, upon its discovery, the protein complex encoded by the *hmc* operon became the most likely candidate.

In this research an attempt has been made to characterize the function of the *hmc* operon by expression analysis. Variations in operon expression levels observed under different controlled conditions must have been influenced by the changing environment. It can be assumed that the proteins encoded by an operon play some important role during a particular growth condition if the operon is activated. Decreasing operon expression under certain conditions indicates that the encoded proteins are no longer required. These assumptions were the basis for analyzing *hmc* operon expression.

Monitoring expression levels of the *hmc* operon during growth of *D. vulgaris* Hildenborough in the presence of various electron donors could

support or refute the hypothesis that the operon proteins serve as a redox link between hydrogen oxidation and sulfate reduction. Cultures were therefore grown in the presence of hydrogen, lactate, pyruvate and formate as electron donors. Many of the cultures were grown under mixed conditions with 5% hydrogen being present along with the test substrate because hydrogen was a component of the anaerobic chamber atmosphere.

Western blots were used to examine *hmc* operon expression levels. A more intense band on a Western blot indicates the presence of more protein. This may mean that (1) the gene encoding the protein in these cells was expressed at a higher level or that (2) these cells experienced less degradation of the observed protein than the others or that (3) some factor has increased the stability of the mRNA being translated. Measures were taken to reduce protein degradation within cell cultures prior to harvesting, or at least to keep degradation levels constant between cultures to avoid discrepancies. All cultures were harvested in exactly the same manner at equivalent points in the growth curve wherever possible. If protein degradation rates were influenced by differences in media substrates then some degree of inaccuracy would have been unavoidable. It was assumed that degradation rates were constant so that the Western blot expression analysis procedure with computer intensity comparisons allowed estimation of the effect of substrates on *D. vulgaris* Hildenborough *hmc* operon expression.

This assumption appears to have been reasonable because the same variations were observed for both Hmc and Orf6 expression levels with little discrepancy between them (section 4.4.1). This would be expected for two proteins under the influence of the same promoter. All expression analyses indicated the highest levels of operon expression in cells which had been grown in the presence of 5% hydrogen. Hydrogen had a definite activation effect upon *hmc* operon expression with the highest levels being discovered during chemolithotrophic growth (Figure 4-9, Table 4-3). Levels similar to chemolithotrophic growth were observed after growth on formate/hydrogen medium but, as discussed above (section 4.4.1), this was likely due to the bacteria's inability to use formate as an electron donor, only as a carbon source, in this minimal medium which lacked all but the bare necessities for growth. As mentioned in the introduction (section 1.1), formate can be used

as sole electron source for growth of *D. vulgaris* but the resulting growth rate is poor. Since no growth of the bacteria was observed in minimal formate medium within nitrogen-flushed bottles, it seems that the bacteria were unable to use this substrate as an electron source in the absence of more nutritional supplements such as vitamins, etc. Thus, the reason for high *hmc* operon expression in formate/hydrogen medium was the use of hydrogen as an electron donor.

Once well established, chemolithotrophic growth of the bacteria elicited *hmc* operon levels which were on average between 1.7-fold and 3.7-fold higher than those observed when another electron donor such as lactate or pyruvate was used (Table 4-3). Growth on these other substrates did result in detectable operon expression suggesting the requirement of the encoded complex even in the absence of hydrogen. The function of the *hmc* operon complex in the absence of hydrogen can be speculated upon. Perhaps, as hypothesized by Rossi *et al.* (1993), the transmembrane complex serves a second function in reverse electron flow. It may be that there is shuttling of cytoplasmic electrons evolved from lactate or pyruvate oxidation to the periplasm where they are used to reduce protons. The levels of *hmc* operon expression were observed to be 1.4-fold higher during growth on lactate than they were during growth on pyruvate (Table 4-3). Microcalorimetric studies performed by Traore *et al.* (1981) have shown that growth of these bacteria on lactate results in the liberation of 25% of evolved electrons into production of molecular hydrogen. The reason for this may be to lower sulfide concentrations within the growth culture and prevent hydrogen sulfide poisoning and/or to participate in interspecies hydrogen transfer with other bacteria such as methanogens as part of a mutually beneficial exchange. This trend is observed during pyruvate oxidation to a much lower extent where only 1 mol hydrogen per 10 mol pyruvate is produced (*ibid*). If the *hmc* operon transmembrane complex is required for electrons exiting to the periplasm in addition to their entry into the cytoplasm, then it can be seen why expression levels might be higher during growth on lactate than growth on pyruvate. All of the hypotheses presented in this section maintain that the function of the *hmc* operon is to produce a transmembrane redox protein

complex which passes electrons involved in hydrogen metabolism through the cell membrane of *D. vulgaris* Hildenborough.

5.5 Role of the *rrf1,2* genes in *D. vulgaris* Hildenborough

The sequence of genes *rrf1* and *rrf2* of *D. vulgaris* Hildenborough was very enlightening with regards to elucidating a possible function for their gene products. The strong sequence homology observed between Rrf1 and the CheY family of response regulatory proteins (Stock *et al.*, 1990) was the first indication that these two proteins might have an important regulatory function. In this study, sequence investigation of Rrf2 has shown that this protein contains a putative helix-turn-helix DNA-binding domain (section 4.5). As mentioned in the introduction (section 1.2), the association of a response regulator with a DNA-binding domain is not unusual. The combination of these two functions into a single-protein body plan is what is found in the response regulators OmpR, PhoB, NtrC, NifA and DctD (Stock *et al.*, 1990; Makino *et al.*, 1986; Ronson *et al.*, 1987). The genes *rrf1* and *rrf2* are separated on the *D. vulgaris* chromosome by only six base pairs. This indicates that a single point mutation could have occurred at some time in the past splitting one single gene which coded for a response regulatory protein with a DNA-binding output domain into two separate genes. It has been observed that many transmitter and receiver proteins possess a flexible AP-rich linker region which separates different domains (Radford *et al.*, 1989). This is not unlike the C-terminus of Rrf1 which is described in the introductory section 1.2. It is possible that this region was once the linker between the regulatory and output domains of one protein. Due to its flexibility, this linker region would play an important role in allowing the phosphorylated regulatory domain to interact with the output domain and effect a response (Parkinson & Kofoid, 1992). These two domains have also been described as being potentially autonomous (Ronson *et al.*, 1987) revealing how Rrf1 and Rrf2 could form a single cooperative unit despite their separation.

One of the best ways to determine the function of a gene or its encoded product is to delete the gene. With a measure of serendipity, a great deal about the gene function can be determined through phenotypic differences exhibited by the mutant. Deletion of a 567 bp fragment of the chromosome which spanned the *rrf1,2* genes of *D. vulgaris* Hildenborough removed the possibility of the production of functional proteins from these genes and resulted in noticeable phenotypic differences in this mutant, denoted RK100, relative to the wild type.

Western blot analysis has shown that the disruption of *rrf1,2* leads on average to a 1.9 to 2.5-fold increase in *hmc* operon expression levels (Figure 4-19, Table 4-5). This suggests that either the absence of intact *rrf1,2* genes stabilizes the *hmc* operon mRNA or that the proteins Rrf1 and Rrf2 repress transcription of the operon. The latter case shall be addressed here. The precise mode of repression cannot be determined from this data. It may be that the Rrf2 protein represses transcription by binding to the *hmc* promoter region after the protein's activation by the phosphorylated Rrf1. In this model, Rrf1 would be phosphorylated in response to the presence of pyruvate and/or lactate. One difficulty with this model is that the probable transcription of *rrf1,2* as part of the *hmc* operon presents a negative feedback scenario. The expression of Rrf1 and Rrf2 along with the other operon genes would lead to their own repression once Rrf1 is phosphorylated. An alternative is that Rrf2 might, by itself, have a natural tendency to bind the *hmc* promoter region and keep expression low (Figure 5-1). Activation would occur in the presence of hydrogen with a chain of events which causes Rrf1 to become phosphorylated. Phosphorylated Rrf1 could bind to Rrf2 and effect its removal from the promoter region. Thus, activation of the operon would create more Rrf1 and Rrf2 but the presence of hydrogen and phosphorylated Rrf1 would keep Rrf2 from binding to the promoter until hydrogen, and thus active Rrf1, levels decreased. Both of these models are supported by the increase in *hmc* operon levels seen in the absence of Rrf1 and Rrf2 in RK100 but it is also very possible that neither model is accurate. The regulation of expression of the *hmc* operon by these factors might be a very complicated process involving other gene products and promoter regions.

The results of the Western blots also displayed that there was not a common high level of expression noted for each mutant culture as would be expected for constitutive expression due to de-repression of the operon (Figure 4-19, Table 4-5). The RK100 levels were higher than observed in the wild type but still fluctuated depending on the electron donor. The highest overall expression appeared during chemolithotrophic growth just as for the wild type. This signifies that the expression of the *hmc* operon is regulated, at least in part, by the gene products of *rrf1,2* but also seems to be influenced by other unknown factors.

The most informative phenotypic observations were made during comparative growth of the two strains of bacteria on media which differed in the electron donating substrate present (section 4.6.2). Under chemolithotrophic conditions, the disruption of *rrf1,2* led to a significant increase in the growth rate of *D. vulgaris* Hildenborough (Figure 4-17). These results are consistent with what was described in the last section (section 5.4) with respect to *hmc* operon expression levels observed in wild type *D. vulgaris* Hildenborough. If the operon is important for hydrogen-associated electron transfer then it makes sense that removal of repressor proteins, such as in RK100, would lead to enhanced growth when using hydrogen as sole electron source.

The lactate growth rate was inhibited in the mutant strain leading to a significantly lower growth rate than observed in the wild type. Somehow, the generation of more Hmc-transmembrane complex had an adverse effect on growth on lactate, perhaps by disturbing electron transfer normally associated with the lactate dehydrogenase. Upon comparison with cultures grown under a nitrogen atmosphere, it was seen that the growth rate on lactate dropped in the presence of 5% hydrogen. An explanation for this may be that when hydrogen is present it is used in addition to lactate as an electron source. The use of both substrates simultaneously is supported by the increase in *hmc* operon expression observed in wild type *D. vulgaris* Hildenborough whenever 5% hydrogen is present in addition to lactate or pyruvate (sections 4.4 and 5.4). If the *hmc* operon is important for hydrogen usage then its expression would rise when hydrogen is present and being used as an electron source. Lactate oxidation might be inhibited in cultures

which are simultaneously oxidizing hydrogen due to the competition for reduceable periplasmic electron carriers, such as cytochrome c_3, which are common to both processes. Inhibition could also occur if electrons are shuttled out of the cytoplasm to the periplasm during lactate oxidation (as discussed above in section 5.4) via the Hmc-transmembrane complex. The reverse flow of electrons resulting from hydrogen oxidation in the periplasm could lead to decreased efficiency of lactate-associated electron transfer. Another reason for slower growth on lactate in the presence of hydrogen could be product inhibition since, as observed, these cells produce molecular hydrogen as a byproduct of lactate utilization (Traore *et al.*, 1981; section 5.4). These models all assume that it is the presence of hydrogen which inhibits growth on lactate and not the presence of lactate which enhances growth using hydrogen as electron donor. This is because lactate is likely the preferred oxidation substrate as evidenced by the faster growth associated with lactate cultures. This may not be the case in RK100 where the higher *hmc* operon levels improve the cell's ability to use hydrogen as the electron donor. This would explain why growth of RK100 on lactate/hydrogen was so much slower than that of the wild type (Figure 4-15). Not only was lactate usage somehow inhibited by the presence of more Hmc-transmembrane complex, but chemolithotrophic growth was enhanced. It could be that lactate is playing only a minor role in electron donation under these conditions.

A slight decrease in growth rate showed that growth on pyruvate was the least affected by the deletion of the *rrf1,2* genes. Thus, the higher operon expression is not as influential during growth on pyruvate (Figure 4-18). This is supported by the low levels of *hmc* operon observed in wild type *D. vulgaris* Hildenborough grown on this substrate (Figure 4-9, Table 4-3). If the *hmc* operon is unimportant for growth on pyruvate as an electron donor then its expression level may not make as big an impact on the observed growth rate on pyruvate as if the components were more consequential. The presence of 5% hydrogen led to slightly decreased growth rates for both strains on pyruvate. This decrease, which was more noticeable in RK100, may have been due to usage of some hydrogen as electron donor (more in RK100) in addition to pyruvate. This might compromise the pyruvate oxidation process by creating competition for cytoplasmic electron carriers.

5.6 Role of the *hmc* operon in *D. vulgaris* Hildenborough

All of the investigations performed during this research project have had the common goal of describing the role of the *hmc* operon in *D. vulgaris* Hildenborough. The results obtained have been enlightening and have led to the development of several models illustrating how different components encoded by the operon might function within this unique bacterial complex. The data presented help to define the membrane association of Orf6, the membrane topology of Orf2, the role of Rrf1 and Rrf2 and the function of the Hmc-transmembrane complex. These models can be combined into an overall conception of the mode of action of the *hmc* operon.

A speculative version of the pathway of hydrogen electron transfer during chemolithotrophic growth proceeds as follows. The extracellular hydrogen concentration rises and hydrogen diffuses into the cytoplasm of *D. vulgaris* Hildenborough. An unknown histidine-protein-kinase sensor is autophosphorylated (Stock *et al.*, 1990) in response to the presence of hydrogen within the cell. This sensor phosphorylates Rrf1 at Asp-53 causing a gross conformational change (Parkinson & Kofoid, 1992; Rossi *et al.*, 1993; Stock *et al.*, 1990) within that protein. The activated Rrf1 complexes Rrf2 which is bound to the bacterial chromosome at the *hmc* promoter region. It binds Rrf2 causing it to be removed from the DNA. Transcription of the *hmc* operon rises leading to more Hmc, Orf2 to Orf6 and, at a much lower level, more Rrf1 and Rrf2 (Figure 5-1).

The transmembrane complex assembles. Hmc is exported to the periplasm. The bulk of Orf2 is also exported with the aid of helper proteins then its signal peptide is cleaved. Orf3, Orf4 and Orf5 insert into the membrane, binding to the transmembrane helix of Orf2 and holding it in place. Orf6 inserts a hydrophobic tail into the membrane where it is also bound by this integral membrane complex.

In the periplasm, hydrogen is oxidized to protons and electrons primarily by the [Fe] hydrogenase (which has lower affinity but higher activity than the [NiFe] hydrogenase; Voordouw, 1993). The electrons evolved are passed to the *c*-type hemes of Hmc. Hmc docks at Orf2 where it channels the electrons to the iron-sulfur clusters of Orf2 which in turn pass them down to

the heme *b* of Orf5. Orf5 transfers the electrons to the iron-sulfur clusters of Orf6 which pass them to flavodoxin. Flavodoxin carries the electrons through the cytoplasm to where they can participate in sulfate reduction (Figure 5-2).

The flow of electrons utilized in hydrogen production during lactate oxidation would follow the reverse pathway. Electrons would be carried to Orf6 where they migrate back through the membrane to Orf5 then to Orf2 and Hmc before being used in proton reduction by the [NiFeSe] hydrogenase (Voordouw, 1993).

From these models, it can be seen that all of the molecular biological data accumulated regarding the *hmc* operon has led to a greater understanding of the how the hydrogen metabolism of these bacteria may proceed. There are numerous future studies which would further enhance our understanding of this operon. These could include (1) the investigation of the *hmc* operon mRNA levels in the mutant strain RK100 as well as mRNA stabilty, (2) a *phoA*-fusion based investigation of the membrane topology of Orf6 as well as the use of fractionation experiments to determine if Orf3,4,5 are required for Orf6 membrane association, (3) the deletion of the entire *hmc* operon and investigation of the effects of this on chemolithotrophic growth or growth on other reductants, (4) radioactive phosphate labeling of Rrf1, (5) investigation of potential DNA sites for Rrf2 binding and (6) spectroscopic characterization of Orf2 investigating its iron-sulfur clusters and Orf5 in search of a heme *b* prosthetic group.

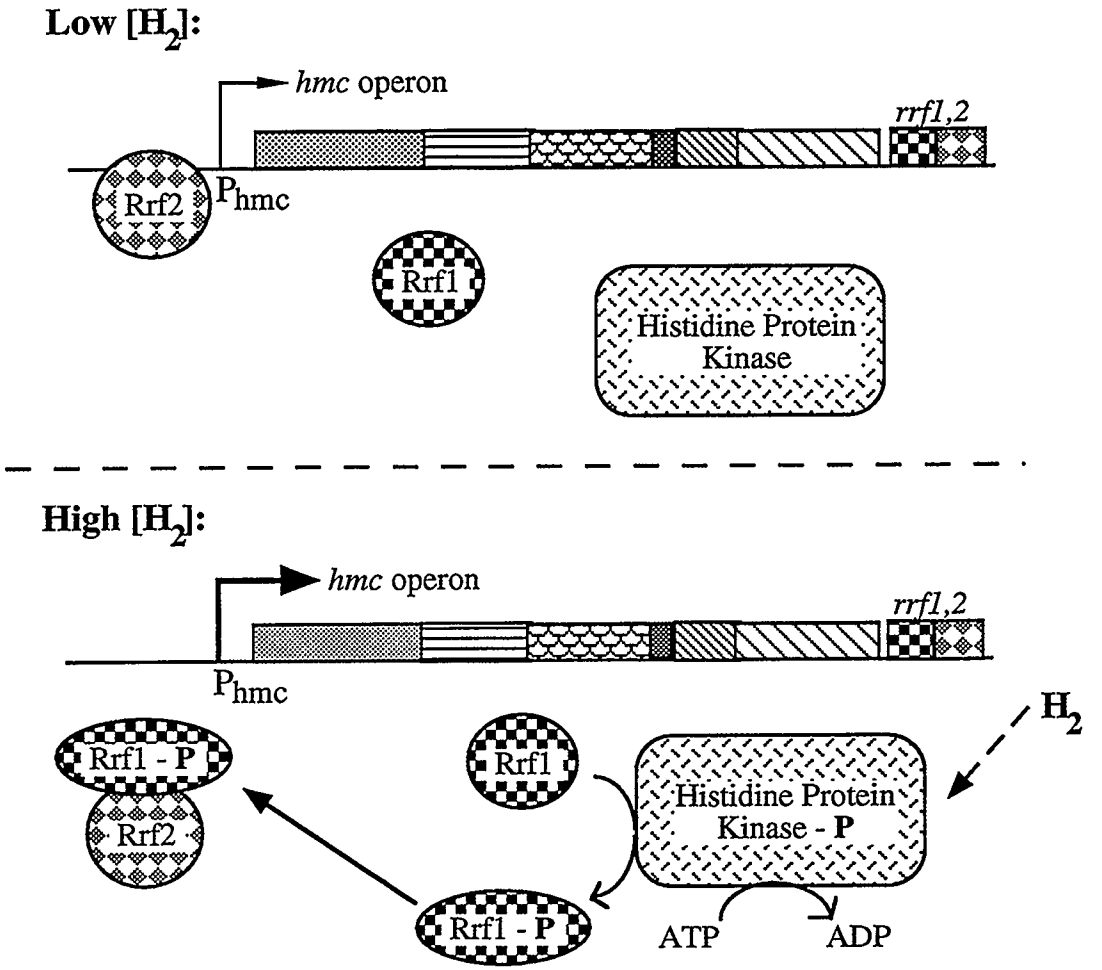

Fig. 5-1. Model of *hmc* operon expression regulation by Rrf1 and Rrf2. This model is purely speculative but illustrates a possible mode of action for these proteins based on the data presented.

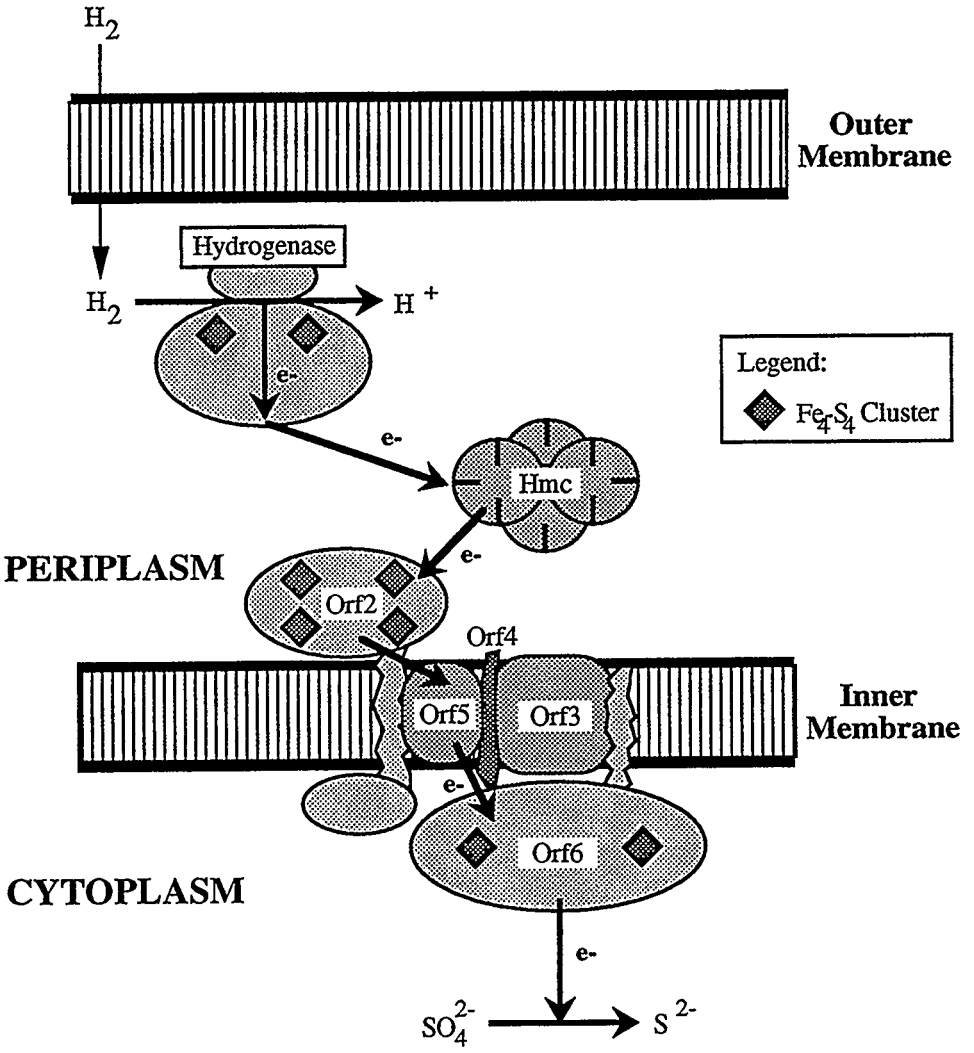

Fig. 5-2. Model of the role of the *hmc* operon in electron transfer from hydrogen. The boldface arrows represent electron transfer during chemolithotrophic growth.

6. References

Badziong, W. & R.K. Thauer (1978). *Arch. Microbiol.* **117**: 209-214.

Badziong, W., B. Ditter & R.K. Thauer (1979). *Arch. Microbiol.* **123**: 301-305.

Berg,. B.L., J. Li, J. Heider & V. Stewart (1991). *J. Biol. Chem.* **266**: 22380-22385.

Bilous, P.T., S.T. Cole, W.F. Anderson & J.H. Weiner (1988). *Mol. Microbiol.* **2**: 785-795.

Birkmann, A., F. Zinoni, G. Sawers & A. Böck (1987). *Arch. Microbiol.* **148**: 44-51.

Blasco, F., C. Iobbi, G. Giordano, M. Chippaux & V. Bonnefoy (1989). *Mol. Gen. Genet.* **218**: 249-256.

Böhm, R., M. Sauter & A. Böck (1990). *Mol. Microbiol.* **4**: 231-243.

Bokrantz, M., M. Gutmann, C. Kortner, E. Kojro, F. Fahrenholz, F. Lauterbach & A. Kröger (1991) *Arch. Microbiol.* **156**: 119-128.

Boyd, D., B. Traxler & J. Beckwith (1993). *J. Bacteriol.* **175**: 553-556.

Brandis, A. & R.K. Thauer (1981). *J. Gen. Microbiol.* **126**: 249-252.

Brickman, E. & J. Beckwith (1975). *J. Mol. Biol.* **96**: 307-316.

Bruschi, M. & F. Guerlesquin (1988). *FEMS Microbiol. Rev.* **54**: 155-176.

Bruschi, M., P. Bertrand, C. More, G. Leroy, J. Bonicel, J. Haladjian, G. Chottard, W.B.R. Pollock & G. Voordouw (1992). *Biochemistry* **31**: 3281-3288.

Burbulys, D., K.A. Trach & J.A. Hoch (1991). *Cell* **64**: 545-552.

Calamia, J. & C. Manoil (1990). *Proc. Natl. Acad. Sci. USA* **87**: 4937-4941.

Cammack, R. & J.H. Weiner (1990). *Biochemistry* **29**: 8410-8416.

Davison, J., M. Heusterpreute, N. Chevalier, H.T. Vinh & F. Brunel (1987). *Gene* **51**: 275-280.

Deckers, H. & G. Voordouw (1993). *Antonie v. Leeuwenhoek* **65**: 1-6.

Degli Esposti, M. (1989). *Biochim. Biophys. Acta* **977**: 249-265.

Derman, A.I. & J. Beckwith (1991). *J. Bacteriol.* **173**: 7719-7722.

Derman, A.I. & J. Beckwith (1995). *J. Bacteriol.* **177**: 3764-3770.

Devereux, J., P. Haeberli & O. Smithies (1984). *Nucl. Acids Res.* **12**: 387-395.

Dodd, I.B. & J.B. Egan (1990). *Nucl. Acids Res.* **18**: 5019-5026.

Dougan, G. & D. Sherratt (1977). *Mol. Gen. Genet.* **151**: 151-160.

Graves, M.C., G.T. Mullenbach & J.C. Rabinowitz (1985). *Proc. Natl. Acad. Sci. USA* **82**: 1653-1657.

Hansen, T.A. (1993). p. 21-40 *In:* J.M Odom & R. Singleton, Jr. (ed.) *The sulfate-reducing bacteria: contemporary perspectives.* Springer-Verlag, New York.

Higuchi, Y., M. Kusunoki, Y. Matsuura, N. Yasuoka & M. Kakudo (1984). *J. Mol. Biol.* **172**: 109-139.

Hynes, M.F., J. Quandt, M.P. O'Connell & A. Pühler (1989). *Gene* **78**: 111-120.

Jankielewicz, A., R.A. Schmitz, O. Klimmek & A. Kröger (1994). *Arch. Microbiol.* **162**: 238-242.

Kyle, J. & R.F. Doolittle (1982). *J. Mol. Biol.* **157**: 105-132.

Kröger, A. & E. Winkler (1981). *Arch. Microbiol.* **129**: 100-104.

Laemmli, U.K. (1970). *Nature* **227**: 680-685.

Lemire, B.D., J.J. Robinson & J.H. Weiner (1982). *J. Bacteriol.* **152**: 1126-1131.

Li, P., J. Beckwith & H. Inouye (1988). *Proc. Natl. Acad. Sci. (USA)* **85**: 7685-7689.

Makino, K., H. Shinagawa, M. Amemura & A. Nakata (1986). *J. Mol. Biol.* **190**: 37-44.

Manoil, C. & J. Beckwith (1985). *Proc. Natl. Acad. Sci. USA* **82**: 8129-8133.

Manoil, C. & J. Beckwith (1986). *Science* **233**: 1403-1408.

Marmur, J. (1961). *J. Mol. Biol.* **3**: 208-218.

Menon, N.K., J. Robbins, H.D. Peck, Jr., C.Y. Chatelus, E.-S. Choi & A.E. Przybyla (1990). *J. Bacteriol.* **172**: 1969-1977.

Menon, N.K., J. Robbins, J.C. Wendt, K.T. Shanmugam & A.E Przybyla (1991). *J. Bacteriol.* **173**: 4851-4861.

Michaelis, S., H. Inouye, D. Oliver & J. Beckwith (1983). *J. Bacteriol.* **154**: 366-374.

Nivière, V., S.-L. Wong & G. Voordouw (1992). *J. Gen. Microbiol.* **138**: 2173-2183.

Odom, J.M. & H.D. Peck, Jr. (1981). *FEMS Microbiol. Lett.* **12**: 47-50.

Odom, J.M. & H.D. Peck, Jr. (1984). *Ann. Rev. Microbiol.* **38**: 551-592.

Odom, J.M. (1993). p. 189-210 *In:* J.M Odom & R. Singleton, Jr. (ed.) *The sulfate-reducing bacteria: contemporary perspectives.* Springer-Verlag, New York.

Pabo, C.O. & R.T. Sauer (1984). *Ann. Rev. Biochem.* **53**: 293-321.

Parkinson, J.S. & E.C. Kofoid (1992). *Ann. Rev. Genet.* **26**: 71-112.

Peck, H.D.,Jr. (1993). p. 41-76 *In:* J.M Odom & R. Singleton, Jr. (ed.) *The sulfate-reducing bacteria: contemporary perspectives.* Springer-Verlag, New York.

Pollock, W.B.R., M. Loutfi, M. Bruschi, B.J. Rapp-Giles, J.D. Wall & G. Voordouw (1991). *J. Bacteriol.* **173**: 220-226.

Pollock, W.B.R. (1992). Ph.D. Thesis, University of Calgary, Calgary.

Postgate, J.R. (1984). *The sulfate reducing bacteria,* 2nd ed. Cambridge University Press, Cambridge.

Radford, S.E., E.D. Laue, R.N. Perham, S.R. Martin & E. Appella (1989). *J. Biol. Chem.* **264**: 767-775.

Ronson, C.W., B.T. Nixon & F.M. Ausubel (1987). *Cell* **49**: 579-581.

Roof, S.K., J.D. Allard, K.P. Bertrand, K. Postle (1991). *J. Bacteriol.* **173**: 5554-5557.

Rossi, M., W.B.R. Pollock, M.W. Reij, R.G. Keon, R. Fu & G. Voordouw (1993). *J. Bacteriol.* **175**: 4699-4711.

Sambrook, J., E.F. Fritsch & T. Maniatis (1989). *Molecular cloning, a laboratory manual,* 2nd ed. Cold Spring Harbor Laboratory Press, Cold Spring Harbor, New York.

San Millan, J.L., D. Boyd, R. Dalbey, W. Wickner & J. Beckwith (1989). *J. Bacteriol.* **171**: 5536-5541.

Sawers, R.G., S.P. Ballantine & D.H. Boxer (1985). *J. Bacteriol.* **164**: 1324-1331.

Sawers, R.G. & D.H. Boxer (1986). *Eur. J. Biochem.* **156**: 265-275.

Schlensog, V. & A. Böck (1990). *Mol. Microbiol.* **4**: 1319-1327.

Schweizer, H.P. (1992). *Mol. Microbiol.* **6**: 1195-1204.

Simon, R., U. Priefer & A. Pühler (1983). *Bio/Technology* **1**: 784-791.

Staden, R. & A.D. McLaughlin (1982). *Nucl. Acids Res.* **10**: 141-156.

Staden, R. (1984). *Nucl. Acids Res.* **12**: 521-538.

Stock, J.B., A.M. Stock & J.M. Mottonen (1990). *Nature* **344**: 395-400.

Tabor, S. & C.C. Richardson (1984). *Proc. Natl. Acad. Sci. (USA)* **82**: 1074-1078.

Tabor, S. & C.C. Richardson (1987). *Proc. Natl. Acad. Sci. (USA)* **84**: 4767-4771.

Tabor, S. (1990). p. 16.2.1-16.2.11 *In:* F.M. Ausubel, R. Brent, R.E. Kingston, D.D. Moore, J.A. Smith & K. Struhl (ed.) *Current protocols in molecular biology.* Green Publishing Associates and Wiley & Sons Inc., New York.

Towbin, H., T. Staehelin & J. Gordon (1979). *Proc. Natl. Acad. Sci. (USA)* **76**: 4350-4354.

Trach, K., J.W. Chapman, P. Piggot, D. LeCoq & J.A. Hoch (1988). *J. Bacteriol.* **170**: 4194-4208.

Traore, A.S., C.E. Hatchikian, J.-P. Belaich & Jean Le Gall (1981). *J. Bacteriol.* **145**: 191-199.

Vieira, J. & J. Messing (1982). *Gene* **19**: 259-268.

von Heijne, G. (1992). *J. Mol. Biol.* **225**: 487-494.

Voordouw, G., J.E. Walker & S. Brenner (1985). *Eur. J. Biochem.* **148**: 509-514.

Voordouw, G. & S. Brenner (1985). *Eur. J. Biochem.* **148**: 515-520.

Voordouw, G., V. Nivière, F.G. Ferris, P.M. Fedorak & D.W.S. Westlake (1990). *Appl. Environ. Microbiol.* **56**: 3748-3754.

Voordouw, G. (1993). p. 88-130 *In:* J.M. Odom & R. Singleton, Jr. (ed.) *The sulfate reducing bacteria: contemporary perspectives.* Springer-Verlag, New York.

Voordouw, G. (1995). *Appl. Environ. Microbiol.* **61**: 2813-2819.

Weimer, P.J., M.J. van Kavelaar, C.B. Michel & T.M. Ng (1988). *Appl. Environ. Microbiol.* **54**: 386-396.

Weiner, J.H., R.A. Rothery, D. Sambasivarao & C.A. Trieber (1992). *Biochim. Biophys. Acta* **1102**: 1-18.

Weiner, J.H., G. Shaw, R.J. Turner & C.A. Trieber (1993). *J. Biol. Chem.* **268**: 3238-3244.

Winston, S.E., S.A. Fuller & J.G.R. Hurrell (1990). p. 11.3.4 *In:* F.M. Ausubel, R. Brent, R.E. Kingston, D.D. Moore, J.A. Smith & K. Struhl (ed.) *Current protocols in molecular biology.* Green Publishing Associates and Wiley & Sons Inc., New York.

Yagi, T. (1979). *Biochim. Biophys. Acta* **548**: 96-105.

Yanisch-Perron, C., J. Vieira & J. Messing (1985). *Gene* **33**: 103-119.